Dynamics Explorer Guest Investigator

Final Report for

NASA Research Grant NAGW-1547

Principal Investigator

J. J. Sojka

Utah State University

Center for Atmospheric and Space Sciences

Logan, UT 84322-4405

Reporting Period

April 1, 1990 to March 31, 1991

Table of Contents Page

1. RESULTS OF THE SECOND YEAR RESEARCH

The report prepared at the end of the first year of this NASA grant indicated work had begun on collecting an extensive data base of satellite particle, electric field, image, and plasma data. These data were to be used to determine correlations between the fields and the particle auroral boundaries. A data base of 8 days of excellent coverage from all instruments was completed. Table 1 lists the geomagnetic conditions associated with each of the selected data periods. This data set consists of 2 active days, 2 moderately active, and 4 geomagnetically rather quiet days. Auroral images were obtained from Dr. John Craven at the University of Iowa. A total of 944 images were converted from their raw form to auroral emissions in the geomagnetic coordinate system. This data set consisted of 313 UV images and 631 which were a combination of visible images mainly obtained using a 577 nm filter. Table 2 indicates how many UV image passes per study day were obtained as well as the total number UV images for each day. The intensity, oval size, and fine structure track well with the general Kp variations shown in Table 1. Indeed, they also track well with the Ae index during each day. As an example, on day 351 the first 15 hours are extremely quiet and the Ae index enhances to well over 500. During the quiet period the images from the first two passes show a faint oval whereas the images from the third pass during the enhanced geomagnetic activity are bright, structured, and show an expanded oval.

For each of the days listed in Table 1, both VEFI electric potential data and LAPI integrated particle energy fluxes were obtained. On the average between 8 and 11 passes of useful data per day were obtained. These data were displayed in a format such that either the statistical electric field model potential or the statistical precipitation energy flux could be superimposed. The *Heppner and Maynard* [1987] and *Hardy et al.* [1987] models were used for the electric potential and precipitation, respectively. In addition, the auroral image intensity along the Dynamics Explorer–2 (DE–2) satellite pass could be computed and plotted along with the LAPI precipitation data and *Hardy et al.* [1987] values.

An indication of the results of this study are obtained from the *Sojka et al.* [1991] (see attached pre-print) DE data and Time Dependent Ionospheric Model (TDIM) comparison. The equivalent LAPI and VEFI comparison with statistical models is given in Figures 3 and 4 of this attached pre-print. Figure 3 [*Sojka et al.*, 1991] compares the VEFI and Heppner and Maynard electric potential for 5 distinct orbits on day 326. Qualitatively the agreement is reasonable. Indeed, this set of VEFI data is in the top 5% of days with well behaved (systematic) variations in the set of all DE–2 passes [*J. Heppner* private communication, 1984]. Even so, the quantitative agreement is not good for each pass, i.e., for the first three passes the minimum negative potential from the model is at least 30 KV less than observed. When comparing the LAPI data with the *Hardy et al.* [1987] precipitation, Figure 4, the differences are even more extreme. The "topology" does not show good agreement. The model polar cap precipitation is significantly too high, the dawn and dusk ovals are too wide, and the maximum intensities are too large. Only the latter discrepancy can be adjusted by a rescaling of the absolute fluxes.

Unfortunately, the other 7 days of data extend this general tendency for the models to disagree strongly with the observations and for the variability of one pass to the next to be so large that they are different patterns. In summary, even from a visual comparison of the 8 days of data the statistical oval and electric potential morphologies do not look like the LAPI and VEFI morphologies on a pass-by-pass basis. Even adjusting the Hardy oval for each pass such that the three hourly Kp was used rather than the daily average from Table 1 did not produce significant improvement. The pass-to-pass differences were still larger than tweaking the statistical oval. In the electric field model both the IMF (B_y and B_z) and the Kp indices were adjusted, however, this did not produce a systematic improvement in model-data orbit-by-orbit comparisons. For most orbits the disagreement between model and data would, at its worst, exceed the value of the model potential itself.

Comparing VEFI and LAPI orbital morphology was similarly unfruitful. The zeroth order expectations of both the VEFI and LAPI data showing two cuts through a high

latitude auroral region per hemispheric pass is present. But for each auroral crossing the structure in the precipitation and convection show little systematic variation or correlation. Comparing with the images leads to further complications. The LAPI fine structure in each auroral crossing is typically contained within 4 to 6 pixels which were observed within ± 12 minutes of the LAPI data. This leads to a temporal and spatial mismatch that is not overcome. Basically, the variability is on time scales less than 12 minutes.

2. CONCLUSIONS AND RECOMMENDATIONS

The final objective of this study has been found to be unachievable with present day data for the following reasons:

- Present day auroral images do not have an adequate spatial nor temporal resolution.
- Electric field data acquired every orbit (90 - 100 minutes) are uncorrelated. Geomagnetic and solar wind variability is on time scales much shorter.
- Similarly, auroral precipitation is only weakly correlated from one pass to the next.

Consequently, both the observed electric field and precipitation is changing in what is mathematically a step wise sense which precludes determining either the time constants of the change or specifically which geomagnetic, solar wind, or other indices are driving or correlated with them. Although this conclusion may have been a reasonable guess prior to the study it was also expected that the combined DE data base being the most comprehensive to date might shed new light on the problem. Based upon this study, specific requirements can be imposed upon future data sets such that an improvement in our knowledge of the large scale magnetospheric electrodynamics can be made:

- Images need to have both enhanced spatial (~ 10 km) and temporal resolution (10's of seconds). The POLAR satellite will produce such a data base.
- These images need to be complete sequences spanning several DE–2 type orbit periods (hours).
- In situ particle and field measurements do not contribute significantly to this problem unless they can be made at multi-locations with repetition rates on the order of minutes.
- The (fine) structure observed in a single present-day pass does not contain information which can be correlated to activity indices or other indices. This is readily proven when a single pass is compared to a statistical model output for

the appropriate activity indices. The agreement is poor, the standard deviations and mean values are comparable.

- There is a need for more electric field-current measurements being acquired at the same time with repetition rates on the same time scales as images (10's of seconds). The Assimilate Mapping of Ionosphere Electrodynamics (AMIE) is a technique which combines various electrodynamic data sets into a simple global electric field and current distribution. However, to date, this technique is heavily data starved making its predictions statistically questionable.
- The data to answer this problem requires the deployment of many satellites. A constellation of 50 small electrodynamic satellites has been put forward by *Sojka* [1989] and *Sojka and Redd* [1990].

This requirement for many satellites described by *Sojka* [1989] and *Sojka and Redd* [1990] is a direct result of the research carried out under this grant.

REFERENCES

Hardy, D.A., M.S. Gussenhoven, R. Raistrick, and W.J. McNeil, Statistical and functional representations of the pattern of auroral energy flux, number flux, and conductivity, *J. Geophys. Res., 92*, 12,275-12,294, 1987.

Heppner, J.P., and N.C. Maynard, Empirical high-latitude electric field models, *J. Geophys. Res., 92*, 4467-4487, 1987.

Sojka, J.J., 2-DEF: A two dimensional electric field mission, Center for Atmospheric and Space Sciences, Utah State University, Report # 89-5-2, 1989.

Sojka, J.J., M. Bowline, R.W. Schunk, J.D. Craven, L.A. Frank, J. Sharber, J.D. Winningham, L. Brace, and J.P. Heppner, TDIM simulation compared with Dynamics Explorer ionospheric observations for 22 November 1981, *J. Geophys. Res.*, in press.

Sojka, J.J., and F.J. Redd, A small satellite constellation for "imaging" magnetospheric electrodynamics, *Adv. Space Res.*, submitted.

Table 1. Geomagnetic conditions

Day Number	Date	Average Kp	Designation
312	November 8, 1981	4	active
326	November 22, 1981	2+	moderately active
327	November 23, 1981	3+	active
331	November 27, 1981	1	quiet
333	November 29, 1981	1	quiet
351	December 17, 1981	1+	quiet
356	December 22, 1981	1−	quiet
365	December 31, 1981	3	moderately active

Table 2. UV image data base

Day Number	Number of Image Passes	Total Number of UV Images
312	3	41
326	2	28
327	3	50
331	2	33
333	1	17
351	3	54
356	2	41
365	3	49

APPENDIX 1

Papers Published

Sojka, J.J., M. Bowline, R.W. Schunk, J.D. Craven, L.A. Frank, J. Sharber, J.D. Winningham, L. Brace, and J.P. Heppner, TDIM simulation compared with Dynamics Explorer ionospheric observations for 22, November 1981, *J. Geophys. Res.*, in press.

Sojka, J.J., Ionospheric physics, *Rev. of Geophys., Supplement,* 1166-1186, 1991. (U.S. National Report to International Union of Geodesy and Geophysics 1987-1990).

Sojka, J.J., and F.J. Redd, A small satellite constellation for "imaging" magnetospheric electrodynamics, *Adv. Space Res.*, submitted.

Talks Given

Sojka, J.J., and F.J. Redd, A small satellite constellation for "imaging" magnetospheric electrodynamics, XXVII COSPAR, The Hague, The Netherlands, June, 1990.

Ionospheric Physics

J. J. Sojka

Reprinted from U.S. National Report to International Union of Geodesy and Geophysics 1987–1990

Published by American Geophysical Union

REVIEWS OF GEOPHYSICS, SUPPLEMENT, PAGES 1166-1186, APRIL 1991
U.S. NATIONAL REPORT TO INTERNATIONAL UNION OF GEODESY AND GEOPHYSICS 1987-1990

Ionospheric Physics

J. J. SOJKA

Center for Atmospheric and Space Sciences, Utah State University Logan, Utah

1. INTRODUCTION

The author has taken a parochial view of the subject matter under the title of ionospheric physics. Physics is used as the key to separating this section of the aeronomy review from the other aeronomy reports. Specifically, work categorized as chemistry, optical emissions, and thermosphere will not be reviewed in this section. However, coupling to the thermosphere and more specifically to the magnetosphere is considered. A brief section is also included on active experiments which is a productive area in plasma physics and also to some extent in ionospheric physics, but one that has fallen on hard times with regard to the U.S. funding agencies. To many, the ionosphere and its physics is regarded as a mature applications science or perhaps even a technology. This is far from the truth. The original wave of zeroth order exploratory experiments and theories have long since gone, but we still do not have predictive models (theories) that are worthy of being called technological tools. There is considerable current interest in developing a capability to predict the morphology of ionospheric parameters on a global scale. Some shortcomings for achieving this goal are summarized in Section 4, the conclusion; they define, in part, the future research goals of the ionospheric physics community. Section 2 divides ionospheric physics according to the community's normal regional classification, i.e. equatorial, mid-latitude, auroral, and polar ionosphere. In addition, the mid-latitude is extended upwards to include the cold plasmaspheric population, and the polar region is also extended upwards to include the polar wind. To date, this polar wind population has still not been fully surveyed. Not all ionospheric physics is naturally restricted to a regional discussion and, therefore, in Section 3 the topics of ionospheric electrodynamic inputs, ionospheric irregularities and waves, active experiments, forecast modeling, and coupling to other regions are reviewed, but material already discussed in Section 2 is not repeated.

A measure of the balance of research in ionospheric physics is obtained from the distribution of experimental, analytical, and theoretical publications that have appeared during this reporting period. Of course, the author has applied subjective criteria in classifying papers according to these three categories. However, the results are still representative of the balance in the U.S. ionospheric community. Figure 1 shows this distribution not only by research category but also by the four regional areas identified in Section 2. The data used to create Figure 1 are taken from the Journal of Geophysics Research and Geophysics Research Letters in the reporting period up to August, 1990, including a total of 172 papers by U.S. authors (at least one U.S. author was the criterion for inclusion in this review). As expected, auroral physics dominates the research effort because it includes the most diverse collection of dynamic and exotic effects, and it is also in this region that coupling with both the thermosphere and magnetosphere is most prominent. Currently, the polar ionosphere is receiving renewed attention especially in its coupling to the open magnetosphere/solar wind for northward IMF* conditions.Several ionospheric physics review articles have appeared since the last IUGG report; papers by Heelis [1987], Killeen [1987], and Inan [1987] are the most relevant to this review. Fraser-Smith [1987] reviewed the magnetic field topology in the ionosphere while Gorney [1990] discussed the solar cycle effects on the near earth environment. Measuring wavelength in space plasmas was considered by LaBelle and Kintner [1989] and high latitude F region plasma irregularities were reviewed by Tsunoda [1988]. LaBelle [1989] reviewed studies of auroral radio noise during the past twenty years. A series of review articles described the contribution of the first five years of the Dynamics Explorer (DE) program, of which the most relevant to this review are those by Hoffman [1988], Heelis [1988], and Burch [1988]. Demars and Schunk [1987] reviewed temperature anisotropies in the terrestrial ionosphere, Schunk [1988] reviewed the theory and numerical implementation of ionospheric models, and Sojka [1989] reviewed the status of global scale, physical models of the ionosphere.

2.1. EQUATORIAL IONOSPHERE

Research in this region focused on the observation and the analysis of plasma density, composition and drift, equatorial bubbles, and instabilities. Further analysis of the CONDOR experiments on E region instabilities was carried out. Modeling and theory focused on large scale equatorial plasma and instability studies. The equatorial F-layer, especially in the night sector showed large scale structure, i.e., the equatorial anomaly. Our understanding of these structures is qualitatively good but quantitatively poor. These structures arise from a combination of **E** x **B** and neutral wind induced drifts. Much of the work focuses on separating these drift effects and quantifying them. Eastward electric field data from Dynamics Explorer (DE)-2 (Aggson et al., 1987, Maynard et al., 1988, and Coley and Heelis, 1989) together with incoherent scatter radar drift data from Jicamarca (Pingree and Fejer, 1987 and Fejer et al., 1989) were used to observe the equatorial plasma drifts. These analyses show a high degree of compatability and allude to the strong local structure present, especially in the evening post sunset region. Fejer et al., [1990] showed that during disturbed storm periods equatorward penetration of high latitude electric fields is preferentially in the zonal component. Night enhancements of 630 nm

Paper number 91RG00727.
8755-1209/91/91RG00727 $15.00

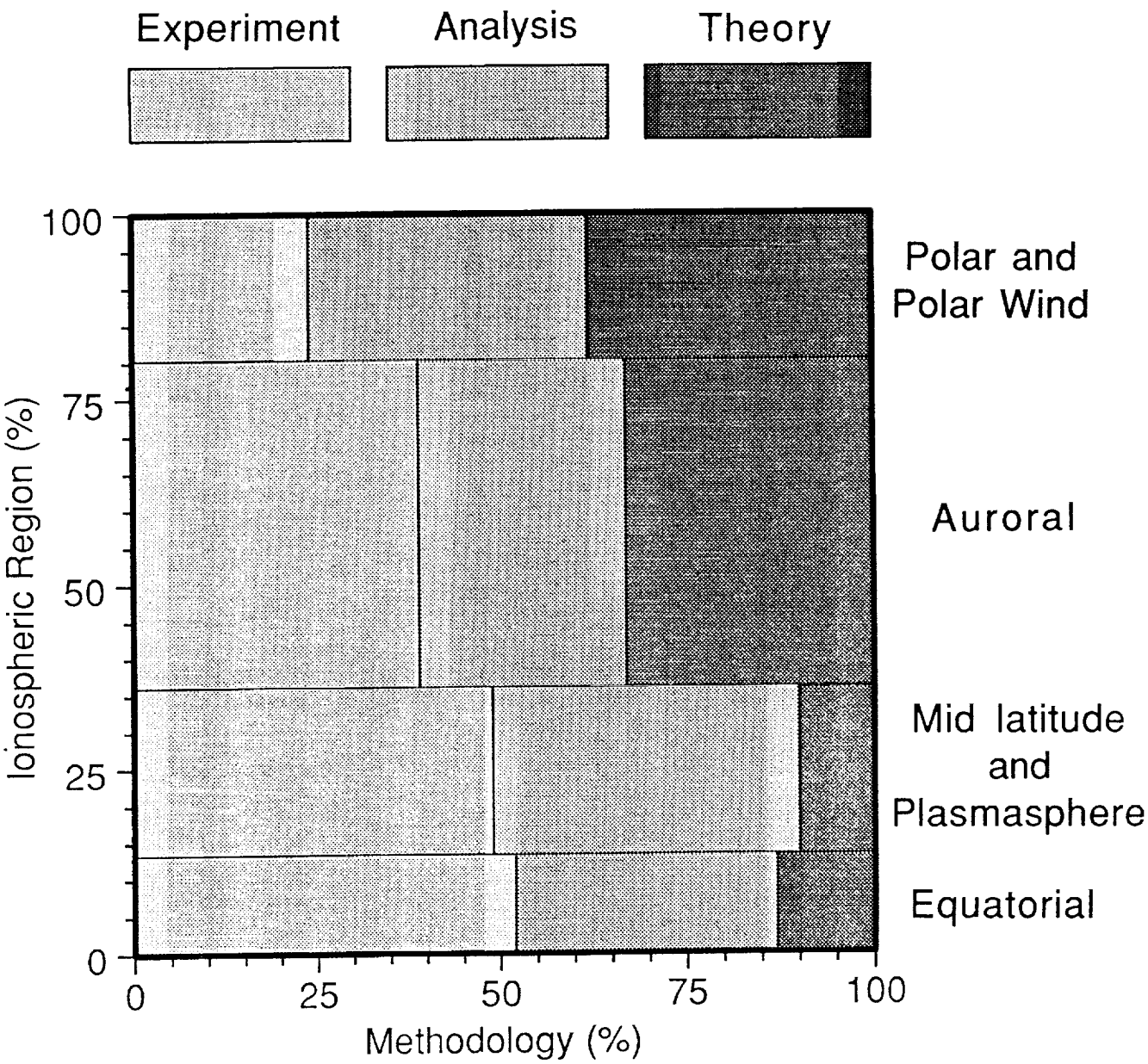

Fig. 1. Relative distribution of ionospheric physics publications for JGR and GRL in this reporting period as a function of research methodology and ionospheric latitudinal region.

emission observed by the AE-E satellite led Fesen and Abreu [1987] to conclude that the local time distribution of plasma **E** x **B** drift needed to be offset by an hour from the normally adopted convection pattern. During the main phase of strong storms Sahai et al., [1988] observed 391 and 486 nm emissions and inferred the presence of energetic particle precipitation and used the 630 nm emissions to follow the F-layer vertical motions during storm periods. Campbell and Schiffmacher [1988] analyzed magnetometer data for 1965 to obtain hemispheric asymmetries, seasonal, and kp dependence of the Sq current system.

Bubbles in the equatorial plasma were studied by rocket experiments which were able to create them chemically [Klobuchar and Abdu, 1989] and Rohrbaugh et al., [1989] were able to track them optically along magnetic field lines from Hawaii. The instabilities present in the equatorial plasma were remotely sensed by radar techniques: a 50 MHz radar interferometer [Kudeki and Farley, 1989], a 250 MHz signal from geosynchronous satellites [Bhattacharyya et al., 1989], and a combination of VHF and HF radars [Kudeki et al., 1987]. The latter research was in conjunction with the CONDOR project in which rocket instruments were flown through the equatorial E region. In situ data from this project led to direct observation of the plasma structure associated with plasma instabilities [Pfaff et al., 1987 a,b]. These papers focused on the analysis of gradient drift and two stream waves. Ronchi et al., [1989] carried out a linear global eigenmode analysis of the gradient drift instability. The effect of small scale turbulence (<100m) on irregularity models of the gradient drift instability of kilometric scale was developed by Ronchi et al., [1990]. Maruyama [1988] developed a diagnostic model of linear growth rates for the gravitational Rayleigh-Taylor instability. These models allow for the effects of **E** x **B** and wind induced drifts and, hence, have application to equatorial

spread F and equatorial bubble phenomena. The generation of gravity waves by a solar eclipse was observed using TEC measurements and was found to be limited to observing stations within 500 km of the eclipse path [Singh et al., 1989]. Klobuchar and Lee [1989] observed amplitude variations in VHF signals as a precursor to onset of strong equatorial scintillations, although they found no modulation of the TEC measurements.

Satellite composition measurements were used to study the equatorial plasma. Grebowsky and Reese [1989] used AE-E ion spectrometer measurements of Fe^+ to study the diurnal and seasonal equatorial F region distribution. Their analysis found trends which were not entirely consistent with earlier theoretical studies. Heelis et al., [1990] used DE-2 plasma data to study the He^+ distribution with special emphasis on seasonal trends and a comparison with mid-latitude data. The response of the equatorial ionosphere to neutral atmosphere perturbations induced by magnetic storms was modeled by Fesen et al., [1989]. Separate ionosphere and neutral atmosphere (TGCM) modeling was carried out to simulate the March 22, 1979 storm; agreement between plasma calculations and observations was limited to the 140° W sector. Sojka and Schunk [1989] carried out a study of the seasonal dependence of the global ionosphere. They found significant seasonal (and hemispherical) differences in the Appleton anomaly and attributed these to asymmetries in the neutral atmosphere. A fully analytic, low and middle latitude ionosphere model was developed by Anderson et al., [1989]. This model has seasonal and solar cycle dependence and reproduces results of earlier semi-empirical models.

2.2. MID-LATITUDE IONOSPHERE AND PLASMASPHERE

A wide range of experimental, theoretical, and analytical research techniques has been used in mid-latitude ionospheric physics. Although these techniques are not new, collaboration in coordinated campaigns has resulted in significant progress being made in this area. The upward extension of the mid-latitude ionosphere into the plasmasphere as well as downward coupling from the magnetosphere in the form of stable auroral red (SAR) arcs has similarly benefited from this coordinated research approach. The extension of the F region mid-latitude trough into sunlight was extensively studied by Whalen [1987, 1989]. He showed that this feature was spatially well-defined and dependent, both on longitude and magnetic activity. Sojka et al., [1990] showed that these empirical relationships were present in their time dependent ionospheric model. Heelis et al., [1990] using DE-2 plasma composition data, showed that at 900 km He^+ is the dominant ion in the mid-latitude night sector and argued why this He^+ dominance was restricted to mid-latitudes. The presence of Ca^+, its altitude distribution, and relationship to a meteor shower [Ursids, (December)] was studied by Torr et al., [1990]. They observed a resonance fluorescence emission from Ca^+, inverted the surface brightness profile, and produced volume emission rate profiles. Emission peaks were present in both the E and F region during the shower. Rasmussen et al., [1988] compared ionospheric densities and electron temperatures from incoherent scatter radar observations (Chatanika, Millstone Hill) from a MITHRAS study with the TDIM. They found that although the densities throughout the F region were in agreement, the electron temperature interpretation was ambiguous. The mid-latitude F region density and height were studied using data from 41 ionosonde stations from a SUNDIAL campaign and fitted with TDIM simulations by adjusting the neutral wind [Sica et al., 1990]. This study showed that the topside O^+ flux was a significant unknown parameter, preventing a unique wind solution from being obtained. The solar cycle dependence of the neutral wind at both Boulder and Wallops Island, USA, was deduced from ionosonde data by Buonsanto [1990]. Sojka et al., [1988] compared the "quiet day" diurnal, seasonal, and solar cycle variations of F_0f_2 at Argentine Islands with the TDIM and obtained very good agreement. Berkey and Stonehocker [1989] compared different methods of true height analysis of ionosonde data. The effect of conjugate ionospheric photoelectrons upon the net ionization rates of O^+ and N_2^+ was modeled as a function of altitude by Richards and Torr [1988]. They found that these ionization rates were a function of altitude which is complicated by the presence of the conjugate photoelectrons down to around 250 km. Sojka and Schunk [1989] using the TDIM showed that the hemispherical difference in the mid-latitude seasonal anomaly was associated mainly with the hemispheric difference in the neutral atmosphere. Detailed longitudinal dependencies and absolute ratios of the seasonal anomaly were, however, only qualitatively modeled. Anderson et al., [1989] developed a fully analytic low mid-latitude ionospheric model.

The dynamics of the mid-latitude ionosphere, especially during storm periods, is driven by enhanced electric fields, neutral drifts, and composition changes. Fejer et al., [1990] using incoherent scatter radar data from the January, 1984 GISMOS campaign, studied the penetration of high latitude electric fields through the mid-latitude region and showed that there were differences between the observation and the theory. Burnside et al., [1987] improved the Arecibo plasma drift measuring technique and Berkey et al., [1990] analyzed the solar cycle dependence of the plasma drifts at Arecibo and found the most marked N_mf_2 variability in the night sector. Maynard et al., [1988] using DE-2 electric field observations, computed average meridional electric fields at mid-latitudes. Although various dependencies were found, no consistent magnetic activity trend was found in these averaged data. The effects of major storms on the ionosphere were studied in several different ways; Forbes et al., [1988] used a harmonic analysis of F region data from a latitudinal chain of ionosondes to show ionospheric storm effects; Hajkowicz and Hunsucker [1987] used the periodic variation of the F-layer's virtual height in both the northern and southern hemisphere to locate the source of TID's at the foot of the energetic particle precipitation belts; Richards et al., [1989] using Millstone Hill ETS data, found that vibrationally excited N_2 did not account for the ionospheric negative storm phase and that during the storms, MSIS 86 densities were not reliable; while Yeh and Foster [1990] observed exceptionally large O^+ outflows in the mid-latitude ionosphere above Millstone Hill during a large storm. Coherent-array HF Doppler techniques were developed to monitor TID's [Adams et al., 1988; Jacobson and Carlos, 1989 a,b]. Storm effects also manifest themselves in the thermosphere. The use of ionospheric observations to deduce neutral atmospheric parameters at Arecibo, was studied by Burnside et al., [1988] who showed the difficulty in obtaining agreement with MSIS [Richards et al., 1989 and Oliver, 1990]. From Millstone Hill,

Foster and Aarons [1988] observed strong, 300m/s, westward convection in the morning sector as a region of storm enhanced sunward convection retreated poleward. These observed westward drifts were equatorward of the magnetospheric shielding layer and were driven by the storm enhanced neutral winds modeled by Spiro et al., [1988]. Hagan [1988] studied the effect of the February, 1986 storm on the thermosphere while Forbes and Roble [1990] investigated the F region storm effects on the thermosphere (TGCM) as a precursor to a fully self-consistent ionosphere-thermosphere study. Williams et al., [1987] discussed coupling of the D and E region with the middle atmosphere. The D and E region incoherent scattering observations were compared with theory by Ganguly and Coco [1987].

Rasmussen et al., [1988] developed a combined conductivity and E region bottomside F-layer (85-220 km) model and showed their E region model densities to be within 50% of those observed at Chatanika and Arecibo incoherent scatter radar observations. They also found that at night the F_1 densities can contribute as much as 80% to the height integrated Pedersen conductivity. Cole [1990] studied the electric currents flowing in the ionospheric E region and developed new expressions for the components of heat dissipation and conductivity associated with the ionospheric current drivers. He also derived a new diffusion equation for magnetic induction in E region like plasma regions. Buonsanto [1990] developed an E-F_1 daytime photochemical equilibrium model and compared it with extensive mid-latitude data sets. He concluded that to get agreement with observations, the EUV fluxes needed to be increased by 25-30% and that at equinox MSIS 86 neutral densities needed to be decreased by about 25%. In winter, this neutral density decrease would have to be even larger. These shortcomings in the MSIS model were consistent with the Arecibo analysis of Burnside et al., [1988]. St-Maurice et al., [1989] analyzed coherent echoes at 44 MHz from the Millstone Hill radar. They observed these echoes in the 105 to 115 km region north of the radar where the viewing geometry was suitable for coherent scatter. At Arecibo, Djuth and Gonzales [1988] used the 430 MHz radar during high-power, high frequency experiments to study the growth of Langmuir waves. The conversion of HF into Langmuir waves was put forward by the authors as a promising mechanism for the production of Langmuir waves in sporadic E. Riggin and Kadish [1989] modeled the non-local growth rate of gradient drift plasma waves and compared those with local growth rates of kilometer-scale waves observed in the vicinity of mid-latitude sporadic E layers. However, they found that the non-local effects alone do not explain the dominance of the kilometer-scale waves. Fukao et al., [1988] observed 1m small-scale field-aligned irregularities in the mid-latitude F region using the MU (VHF) radar. Their results showed that the irregularities were, on occasions, quasi-period on both space (50 km) and time (12 minutes) scales. Rodger and Aarons [1988] compared conjugate occurrence frequency of irregularities and deduced both seasonal and storm correlations. Djuth et al., [1987] observed enhanced ion-acoustic waves (1m wavelengths) with a 138.8 MHz backscatter radar at Arecibo during the high-power, high frequency F region modification experiments. Hansen and Henley [1988] modeled the effect of isotropic turbulence in a background F region plasma into which a barium release was made. They found that the turbulence enhanced the diffusion coefficient for the release and, hence, could explain the predominance of large length scale turbulence observed during such releases.

Slater et al., [1987] found enhanced 10 eV electron precipitation (DE-2 data) in conjunction with 23 instances of SAR arcs observed by ground based photometers. The electron energy fluxes were found to be sufficient to produce the 630 nm SAR emission rates. Kozyra et al., [1987] using both DE-1 and DE-2 correlated ring current heavy ion fluxes at 17 keV with SAR arc electron temperature enhancements. Such energetic heavy ions (O^+) provide the electron heating (10 eV electrons) needed for the SAR arc through Coulomb collisions. Mendillo et al., [1989] studied three distinct sub-auroral 630 nm emission features, detached arcs, ripples in the diffuse aurora, and patches. DMSP satellite and Millstone Hill radar data were used to infer the sources of these emissions. The ripples in the diffuse aurora appear to be driven by enhanced ion heating due to enhanced plasma convection while the arcs (SAR) were associated with F region density enhancements and ion precipitation, and the patches appear to be associated only with enhanced radar returns from the E region. Okano and Kim [1987] used photometric triangulation to infer the SAR arc emission height to be 370-460 km on the 26/27 September, 1979. This height rapidly decreased as the SAR arc brightened in response to substorms. The relative effects of the ionosphere-thermosphere and the magnetosphere on SAR arc formation was studied by Kozyra et al., [1990] as a function of season and solar cycle. The seasonal asymmetries, especially around solstice, can best be explained by the ionospheric-thermospheric asymmetries. However, the solar cycle dependence can best be explained by a reduction in magnetospheric heat flux from solar maximum to solar minimum which is attributed to the compositional change in the magnetospheric plasma.

The strong interdependence of the plasmasphere and the mid-latitude ionosphere justifies regarding the plasmasphere in the context of ionospheric physics. Brace et al., [1988] used both DE-2 F region and DE-1 plasmasphere electron temperatures to correlate latitudinal boundaries in these regions. In the 2200 to 1300 LT sector (i.e., midnight, morning, and noon), the T_e signatures are essentially identical. Outside this sector, the plasmasphere bulge complicates the correlation since no similar feature is found in the ionosphere. In the region of electron heating at the outer plasmasphere, Roberts et al., [1987] found enhanced heavy ion [O^+, O^{++}, N^+] densities. The latitude of the heavy ion enhancements tracked the magnetic activity variation (Dst) and was associated with an ionospheric heavy ion outflow. Topside H^+ fluxes were not found to follow the same diurnal variation as the O^+ fluxes at Arecibo, but did show flows during magnetic storm disturbances [Tepley and Kerr, 1989]. At higher altitudes in the plasmasphere, Menietti et al., [1988] studied the ion flow morphology using DE-1 data. Horwitz et al., [1990] used DE-1 and 2 composition data and the FLIP model to compare the composition and density of the F region and the plasmasphere. The O^+ latitudinal variation in the plasmasphere correlated with that of O^+ in the F region, but not with the light ion H^+. The He^+/H^+ ratio was greater than unity in the topside ionosphere, but was around 0.2 in the plasmasphere. When the FLIP model allowed for fractional trapping of ionospheric photoelectrons, the results of

calculations were in good agreement with the observations. Horwitz et al., [1990] used the RIMS database to characterize both the plasmasphere's density structure and boundary locations. Singh and Torr [1990] used a hydrodynamic model to study the effect of ion temperature anisotropies on interhemispheric plasma transport. Rasmussen and Schunk [1990] developed a three-dimensional time dependent, non -linear hydrodynamic model of the plasmasphere which included cross-L-shell drifts. The initial solar minimum study of equatorial densities gave results within a factor of 2 of the average whistler and satellite density observations. The mid -latitude ionosphere is at the feet of the closed magnetic flux tubes which duct VLF signals, and this same magnetic field geometry supports the ring current wave-induced precipitation events; both the ducting of the VLF signals and the wave -induced precipitation were the topic of several studies [Neubert et al., 1987; Carpenter et al., 1988; Carpenter and Orville, 1989; Burgess and Inan, 1990; Jarvis et al., 1990].

2.3. AURORAL IONOSPHERE

The auroral ionosphere contains a diverse collection of phenomena; very few of these can be understood in isolation. No clear distinction between magnetospheric and ionospheric phenomena exists here. Dynamics are present both spatially and temporally over a wide range of scales. Work in this field continues to be prolific and advances often appear to further complicate rather than resolve problems. In the following paragraphs the research is reviewed by forcing a subjective ordering, but subsections are not defined as this would be a futile categorization.

Both theoretical and empirical research has found the auroral ionosphere abound in small-scale irregularities and waves. The classification and subsequent understanding of instabilities has led to a continuing series of studies. In turn, our knowledge of the plasma structuring mechanisms has advanced significantly. Observations in the F region by Ruohoniemi et al., [1987] using HF coherent scatter and incoherent scatter radars from Goose Bay and Sondrestrom Fjord, respectively, showed that small-scale (13.9m) field aligned irregularities drift at the ambient plasma drift speed. Using the same HF radar, Ruohoniemi et al., [1988] observed similar coherent backscatter from decameter scale plasma density irregularities for periods of about 1 hour in the evening sector at sub-auroral latitudes. Foster et al., [1988] found that certain Millstone Hill radar spectra which were typically regarded as "hard-target" backscatter were also consistent with intense radar returns associated with topside unstable plasma regions of current driven ion acoustic modes. Using rocket data, Earle et al., [1989] found that in the presence of large velocity shears in the F region there were both turbulence and electrostatic waves and concluded that the velocity shears were associated with field aligned currents which drove the electrostatic ion cyclotron waves. Theoretical work on the F region also covered several topics. Chaturvedi and Huba [1987] looked at the interchange instability associated with plasma blobs (300-600km) and found that it could generate the scintillation causing irregularities (1.1 km wavelength) associated with the blobs. Cornwall [1988] found exact solutions for the Liouville equation of an adiabatic auroral arc. These solutions gave stability limits for processes such as the Kelvin-Helmholtz instability. Basu and Coppi [1988, 1989] developed a theory of collisional electrostatic modes driven unstable by sheared field aligned ion flow velocities and showed that this theory could predict the observed [Basu et al., 1988] fluctuations from several meters to a kilometer. However, Ganguli et al., [1989] argued that the transverse velocity shear would readily stabilize the above unstable modes. Nishikawa et al., [1990] modeled electrostatic turbulence due to both the transverse and parallel sheared flows. The effect of ion-ion and ion-neutral collisions on quasi-linear ion heating by the current-driven ion cyclotron instability was studied by Satyanarayana et al., [1989]. In the lower F region (200-300km), they found that the collisions isotropize the temperature distribution while at higher altitudes (600km) anisotropies can be sustained even with the collisions.

Experimentally, Noble et al., [1987] studied E region irregularities of 1 to 7m using the HF ionospheric heater facility near Tromso in conjunction with backscatter radars. Their results indicated that the E region irregularities were associated with instabilities at the upper hybrid resonance level rather than the reflection level. Valladares et al., [1988] used the Sondrestrom Fjord incoherent scatter radar to observe enhanced plasma lines from the topside of the particle produced E-layer. Villain et al., [1990] observed decameter irregularities of 10-20m jointly with the Goose Bay and Schefferville HF radars. They found evidence of two irregularity layers in the E region which are related to the action of the gradient drift and ion acoustic instability mechanisms. The Farley-Buneman instability was theoretically studied by Chaturvedi et al., [1987] and Machida and Goertz [1988]. Chaturvedi et al considered the effect of a parallel current on two-stream plasma instabilities and found that it modified the threshold for the onset of the Farley-Buneman instability, while Machida and Goertz studied the nonlinear saturation of the Farley-Buneman instability using a collisional 2.5 dimensional electrostatic particle simulation and found that the dominant mechanism for electron heating was an enhanced effective collision frequency rather than heating from the parallel electric field component of the waves. Kuo and Lee [1988] found that E region irregularities greater than 13m could be produced through a thermal instability causing filamentation of the auroral electrojet current. Farley and Providakes [1989] reconsidered the validity of the isothermal assumption in the theory of unstable ionospheric two-stream waves. They found that although the electrons are adiabatic, the ions are not. This leads to a 20 to 40% difference in modeling the wave velocities with the newer calculations being in better agreement with the EISCAT and CUPRI observations. Satyanarayana et al., [1987] studied theoretically the effect of Coulomb collisions and parallel electrodynamics on the transverse Kelvin-Helmholtz instability, while Ganguli and Palmadesso [1988] studied the effect of parallel currents and transverse electric fields on electrostatic ion instabilities.

Using the EISCAT incoherent scatter radar, Lockwood et al., [1987] observed bursts of intense poleward ion flows in the dayside auroral region. When the ion drift velocity exceeded the neutral thermal speed, they observed non-Maxwellian ion velocity distributions. Senior et al., [1987] observed both the E and F region density in the evening sector auroral oval using the Chatanika incoherent scatter radar data and found that the auroral E region extended 2° further

equatorward than the F region. Using both DE-2 and NOAA-6 particle data, they showed that the extended E-layer was formed by proton precipitation in contrast to the higher latitude E-F layers which were formed mainly by electron precipitation. In the high latitude dawn sector, Robinson et al., [1988] found discrete arcs in diffuse auroral regions. The observed (Sonderstrom Fjord radar) electron density of the arcs peaked at 180km while the diffuse auroral electron density peaked at 115 km. Using both DMSP and HILAT satellites, they showed that the discrete arcs were associated with enhanced fluxes of low energy electrons. Kondo et al., [1990] statistically analyzed upflowing ion beam and conic distributions observed on DE-1 and found them to be mostly associated with auroral field lines, although there was not a strong correlation with the direction of the field aligned currents. They also found that O^+ was accelerated more efficiently at higher levels of magnetic activity (Kp). On a global scale, Sojka and Schunk [1989] modeled the high latitude ionosphere using their TDIM model and showed the strong seasonal and UT control of the auroral ionosphere. Sojka et al., [1989] carried out a TDIM auroral substorm simulation using both the DE-1 and DE-2 data to define the auroral dynamics. The DE-1 images defined the global scale precipitation dynamics for the substorm. Their simulation indicated the need for a storm representation of the convection electric field.

Schunk et al., [1987] used the TDIM model and the electron energy equation to study the effect of ionospheric return currents on the electron temperature. The uncertainty of the magnitude and direction of the magnetospheric heat flux was shown to be a major problem. Lilensten et al., [1990] used both Viking and EISCAT data to solve the electron energy equation along an auroral field line which enabled them to deduce the topside heat flux. Chiu et al., [1988] used a Monte Carlo simulation of wave particle ion heating in the auroral topside ionosphere to study the efficiency of the topside as a provider of magnetospheric plasma. They found it was very sensitive to charge exchange collisions and downward parallel electric potential drops. In addition, they predicted the presence of a heated (<10 eV) neutral population in the topside ionosphere.

The auroral electron density profile is dependent upon the spectral shape of the incident precipitating particles, and the auroral emission is dependent upon the photochemistry of the auroral ionosphere. Jones et al., [1987] used electron density profiles measured by a radar to deduce the average energy of the incoming electrons and then compared this to the I(630.0) /I(427.8) and I(844.6)/I(427.8) optical emission ratios (see also Niciejewski et al., [1989]). Rees et al., [1988] deduced auroral energy deposition rates, characteristic electron energy, and ionospheric parameters from DE-1 auroral images at three wavelengths. The ionospheric conductance was deduced from the DE-1 auroral images and was checked against the conductance inferred from Chatanika incoherent scatter radar data [Robinson et al., 1989]. All sky television at Syowa station and particle data from the DMSP-F6 satellite were used by Ono et al., [1989] to analyze the dusk auroral emissions caused by protons and electrons. Theoretical work on the ratio of auroral emissions to obtain the characteristic energy of the electron spectrum was done by Rees and Lummerzheim [1989] who found the I(337.1)/I(427.8) ratio to be better than the I(630.0)/I(427.8) ratio. Richards and Torr [1990] modeled the 337.1nm emission rate dependence upon the characteristic energy of the auroral electrons. Morrill and Benesch [1990] studied how "preconditioning" the N_2 gas affects the production of excited N_2 vibrational distributions and subsequently, the N_2 band intensities observed in the aurora. Enhanced soft auroral precipitation (<1keV) was observed by rocket borne instrumentation in the morning sector auroral zone in conjunction with electron density enhancements [LaBelle et al., 1989]. These enhanced densities were modeled and were found to be produced by the soft precipitation. Basu et al., [1987] compared a linear transport theory model of auroral ion (proton) precipitation with Chatanika radar electron densities and the NOAA-6 proton precipitation data and found good agreement. Hardy et al., [1989] binned the auroral ion precipitation measured by DMSP-F6 and F7 satellites as a function of Kp to produce a statistical ion precipitation model. The dependence of ionospheric conductivity calculations upon the flux and the energy of the precipitating electron spectrum was used by Robinson et al., [1987] to highlight the difference between the characteristic energy of a Maxwellian distribution versus the average energy of an auroral spectrum. Fuller-Rowell and Evans [1987] produced a model of the height integrated Pedersen and Hall conductivities from TIROS-NOAA satellite data, while Hardy et al., [1987] used DMSP data to model the pattern of ionospheric conductivity as well as auroral energy and number flux. Foster et al., [1989] combined the Fuller-Rowell and Evans [1987] conductivity model with Millstone Hill convection patterns to deduce auroral ionospheric currents. Robinson et al., [1989] developed a procedure for the inversion of auroral Bremsstrahlung x-ray spectra to obtain electron deposition information, while Ahn et al., [1989] used such a technique to deduce auroral conductivities which they combined with ground based magnetometer data to infer global scale heating rates. Kamide et al., [1989] used ground magnetometer data together with DE-1 and 2 observations to deduce ionospheric electromagnetic quantities.

Jet stream wind models were shown to produce electric fields parallel to the magnetic field with current closure in the F region [Nakada, 1987]. Additionally, Nakada [1989], using an oscillatory electrical circuit, showed that the jet stream could cause oscillations in the Pc-1 to Pc-3 range which is in accordance with observations. Poulsen et al., [1990] developed a three-dimensional night time D region model to study the effect of localized perturbations upon sub-ionospheric VLF propagation.

The cleft/cusp region has received attention due to its key location in relation to plasma flow into the polar cap as well as mapping FTE signatures. Sandholt et al., [1989] used HILAT plasma data and ground observations of polar cusp auroras to deduce the electrodynamics of the cusp. Using ground-based search coil magnetometer, riometer, photometer and ELF-VLF receiver data from South Pole and McMurdo stations, Engebretson et al., [1990] looked for Pc-3 pulsation signatures in the ionosphere. They found low energy precipitating magnetosheath-like electrons in the cleft which were, at times, modulated with frequencies similar to those of upstream waves. Wolfe et al., [1990] used conjugate stations at Igaluit and South Pole to study Pc-3 pulsations near the cusp. Very few conjugate and simultaneous observations of Pc-3 were made. The authors concluded that upstream ion cyclotron waves were the source of the Pc-3 events. Greenwald et al., [1990] observed simultaneous conjugate dayside convection and noted rapid response to changing IMF-By conditions. Yeh et al., [1990], using the Millstone Hill

incoherent scatter radar, observed the dayside cusp extending as low as 60° invariant latitude during the large February 8-9, 1986 storm.

The FTE electrodynamic signatures are associated with the cusp region. Lockwood et al., [1988] and Smith and Lockwood [1990] used the EISCAT radar to observe the plasma flow in the cusp and inferred convection signatures consistent with a simple twin-vortex FTE model. Strong upward plasma flows were observed by AMPTE-UKS in these events [Smith and Lockwood, 1990]. Saflekos et al., [1990] indirectly observed evidence of reconnected flux tubes which they interpreted to be extensions of FTE's found near the magnetopause. The FTE signatures were studied theoretically by Zhu and Kan [1989]; the ground magnetic signature was studied by Wei and Lee [1990]; the ground magnetic signature for a moving elongated plasma cloud was modeled by Crooker and Siscoe [1990]; and the convection footprint in the ionosphere was studied by Crooker [1990]. It is in the ionosphere that high resolution two-dimensional analysis of the FTE can be made, and several studies have focused on the expected and observed FTE ionospheric signature [McHenry and Clauer, 1987; Bering et al., 1988; Kan 1988; Basinska et al., 1989; Lockwood and Smith 1989].

Brüning et al., [1990] and Potemra et al., [1990] used Viking satellite data to study dynamic discrete auroral structures in the 1400 MLT time sector. Bruning et al., considered the current systems and parallel potential drops and found evidence for a saturation current in intense postnoon aurora, while Potemra et al., studied the temporal variation of "bead" or "pearl" auroral forms from the UV images. Using particle distributions, waves, and dc electric and magnetic fields measured from two sounding rockets, McFadden et al., [1990] determined the electrodynamics of a thin (10 km) auroral arc. How the neutralization of the auroral arc upward current depends on arc thickness was theoretically studied by Nakamura et al., [1989] and how the upward currents are distributed across the arc was theoretically studied by Greenspan [1989]. Porter et al., [1987] developed a computationally fast electron transport deposition code using a Neuman iteration method. Reiff et al., [1988] used simultaneous high altitude (DE-1) and low altitude (DE-2) satellite data to observe indirectly the auroral parallel potential drop, while Kan and Cao [1988] considered the effect of an auroral parallel potential drop on magnetosphere-ionosphere coupling. Observations were also made to extend our empirical understanding of the ionospheric role in generating auroral signatures [Evans et al., 1987; Rosenberg et al., 1987; Imhof et al., 1988; Miah 1989]. Sandahl et al., [1990] studied the correlation of auroral precipitation (Viking UV images) and convection (EISCAT) in the midnight auroral region. During the substorm breakup when the auroral poleward boundary expands poleward, Robinson et al., [1990] found that this motion did not correlate with the variation in the local convection electric fields. Boehm et al., [1990] used high resolution sounding rocket observations to infer the presence of shear Alfven waves with amplitudes > 100 mV/m in the auroral zone. The auroral zone plasma convection was modeled empirically by Holt et al., [1987]. They used Millstone Hill radar observations and compared their model with earlier results; however, in the average model discrete features like the Harang discontinuity are lost. Sica et al., [1988] modeled theoretically the high latitude ionosphere to find conditions under which large field aligned ion drifts could be maintained.

Temporal storm and substorm features associated with the auroral zone ionosphere were also studied. Gledhill et al., [1987] used data from Sanae, Antarctica to study the electrodynamics of the substorm and found that the magnetometer D component gave a positive spike instead of the normal negative spike. Robinson and Vondrak [1990] deduced the electrodynamic properties of auroral surges using Chatanika and DE-1 and 2 data. Similarly, Lyons et al., [1990], used Viking satellite, magnetometer, and radar data to study auroral surges in the vicinity of the Harang discontinuity. Pangia et al., [1990] correlated Pc-5 magnetic pulsations with substorm onset using Goes-2 and 3 geostationary data in conjunction with ground magnetometer data. The AMIE technique was used by Knipp et al., [1989] to deduce the electrodynamic patterns during the ETS disturbed day of September 19, 1984. Strong eastward convection in the midnight sector of the auroral oval during the first large substorm was found to be associated with a marked westward rotation of the two-cell convection pattern. Zhu and Kan [1990] considered theoretically the effect of ionospheric recombination time scales on auroral substorm signatures. Their model produced discrete aurora along the poleward boundary of the diffuse aurora in the evening-midnight sector. Stern [1990] analyzed qualitatively the auroral substorm using a one-dimensional model. The critical dependence of Region II field aligned currents upon ionospheric conductivity gradients was highlighted by Kan [1987] and Cheng et al., [1987].

Finally, a few auroral papers that do not fit into the above topic catagorization by paragraphs. Hones et al., [1989] used DE-1 auroral images and found that for about one third of the time, when IMF Bz was northwards, the auroral oval was configured like a "horse collar". This pattern often evolved into a theta-like auroral pattern. Robinson et al., [1989] studied the plasma and field properties of auroral suprathermal electron bursts and found that the bursts, typically < 1keV were strongly correlated with enhancements in the ac electric field at frequencies below 1kHz. This led the authors to suggest that the electrons were heated via interaction with ion cyclotron waves. Hultqvist et al., [1988] using Viking data, observed both energetic electrons and ions of similar energy moving upward along magnetic field lines and concluded that these field aligned fluxes were associated with strong broadband low-frequency turbulence and a downward current. They inferred that the waves accelerated the electrons (a resonance effect), but that the ions "see" it only as a wave field (no significant heat extraction). Calvert and Hashimoto [1990] studied magnetoionic modes and the propagation properties of auroral radio emissions using the DE-1 radio spectrograms and then ray traced their propagation behavior. They found that all four modes which could propagate were present in the data and all were associated with specific regions in the auroral zone. Sá [1990] observed VLF emissions triggered by discrete waves transmitted from Siple Station and received at Lake Mistissini, Quebec. Killeen et al., [1988] used DE-1 and 2 data of the auroral and polar ionosphere to study the relationship between the auroral morphology and the high latitude thermospheric dynamics.

2.4. POLAR IONOSPHERE AND POLAR WIND

During the 80's it was realized empirically that the magnetosphere under IMF Bz northward conditions was

different from that under Bz southward conditions. Nowhere was this more clearly manifested than in the polar cap ionosphere. Similarly, the re-evaluation of the origin of the magnetospheric plasma, i.e., solar or terrestrial, has led to new work on the heavy ion polar wind, its transport, and its energization. Again, the high latitude ionosphere is a key region for this work.

Our understanding of the high latitude convection under southward IMF conditions is complex, but well developed. Moses et al., [1987] considered southward IMF conditions and studied the plasma flow into the polar cap and its By dependence. Using DE-2 drift data, Moses et al., [1988] deduced that for about one third of the data multiple flow entry regions existed. Friis-Christensen et al., [1988] observed traveling convection vortices in the polar cleft region using a magnetometer network. However, these traveling vortices were inconsistent with present-day FTE current-closure models. Hairston and Heelis [1990] developed an empirical convection model for southward IMF conditions based upon DE-2 plasma drift data. Rich and Maynard [1989] developed analytical functions to represent the electric fields of Heppner and Maynard [1987]. An alternative procedure for deducing the electrodynamics in the high latitude ionosphere self consistently was developed by Richmond and Kamide [1988] and Richmond et al., [1990]. By combining conductivity, current, and electric field data, they produced the equivalent global current and electric field patterns which best satisfied a generalized Ohms law. At present this AMIE technique is limited by the sparsity of input data. Ahn et al., [1989] showed that the ionospheric conductivity dependence upon both the cross-polar cap potential difference and the global Joule heating rate were reasonably modeled by present day statistical models.

Density structures in both the E and F region were the topic of several studies. Such density features are more readily observed and tracked than their electrodynamic source parameters. Schunk and Sojka [1987] used the TDIM to compare the lifetimes of F region plasma density structures and found that in darkness the ratio of enhanced density to the background density remained constant for many 10's of hours. In fact, it is only by transport that these regions convect into regions of solar illumination or auroral precipitation and hence, enhanced ionization that the structures disappear. Sojka and Schunk [1987] similarly showed that in a dark polar cap in the presence of sustained multi-cell convection, regions of low density could be maintained because plasma transport would not take the flux tubes into regions of solar illumination or auroral precipitation and hence, enhanced ionization. Maynard et al., [1990] used DE-2 plasma data to search for those density signatures which were predicted to occur for Bz northward conditions. The location of the polar cap depletion regions was predicted to be a strong function of the IMF By component. Tulunay and Grebowsky [1987] compared winter electron density signatures in the topside ionosphere for the northern and southern polar regions using Ariel plasma data. They found systematic differences, with the southern hemisphere having the lowest densities. Hoegy and Benson [1988] compared plasma data from the ISIS and DE-2 satellites to study the extent and convection control of high latitude plasma features. Under dynamic conditions when the polar cap electric field was highly structured, the plasma density depended heavily upon this structure. Sojka and Schunk [1988] modeled the polar cap F region with the TDIM for these conditions and found that significant density depletions were present in the regions of strong electric fields even if these enhanced fields were quite local. Heelis and Vickrey [1990] showed that plasma structures created in the F region produce plasma images in the E region through field aligned electrostatics. They showed how the scaling depended on the altitude of the source structure.

Basu et al., [1990] used plasma and electrodynamic observations from DE-2 to study plasma instabilities formed at the edges of ionospheric patches. They contrasted the gradient drift with the velocity shear process, which is usually found in association with auroral zone density blobs. Dawn-dusk versus noon-midnight asymmetries were observed for the instabilities associated with the patches. Weber et al., [1989] found instability asymmetries across a polar cap sun aligned arc. They inferred that on the dusk side the interchange process was present, while on the dawn side it was the velocity shear instability. The effect of density irregularities was studied by James et al., [1990] using radio wave reception on DE-1 as the satellite crossed the plasma heater facility at Tromso. The irregularities caused both spectral broadening and long delays in the signals. Satyanarayana et al., [1987] analyzed the effects of Coulomb collisions and electron parallel dynamics on the transverse Kelvin-Helmholtz instability with the high latitude ionospheric plasma in mind. The parallel dynamics were found to simulate "buoyancy" in their analysis and to stabilize the instability. The effect of plasma turbulence in the D region associated with water cluster ions was analyzed by Kelly et al., [1987]. Based on 50 MHz radar backscatter measurements, they predicted how the EISCAT facility should be able to verify the water cluster ion theory.

Above the polar ionosphere is a region containing ionospheric and magnetospheric plasma, the ionospheric plasma component being the polar wind. The outflow of plasma is controlled by various magnetospheric, ionospheric, and solar processes. Gombosi and Killeen [1987] considered how thermospheric dynamics, driven by heating, modified the polar wind flow. Barakat and Schunk [1987] modeled the solar cycle, seasonal, and magnetic activity dependence of this outflow. Ganguli et al., [1987] and Demars and Schunk [1989] developed 16 moment transport models of the polar wind. Gombosi and Schunk [1988] compared hydrodynamic and collisionless polar wind formulations for plasma expansion. Singh et al., [1989] studied enhanced O^+ outflows caused by high altitude plasma cavities, and Gombosi and Nagy [1989] considered the effects of return currents on the polar wind outflow. Cannata and Gombosi [1989] contrasted the composition of the polar wind between solar minimum and solar maximum. In their study, the solar cycle dependence was introduced as an underlying thermospheric dependence. This compositional dependence was found to be consistent with a vast body of satellite plasma composition data analyzed by Grebowsky et al., [1990]. Grebowsky et al., considered the altitude dependence of plasma composition in the noon $\pm$ 3 hours sector of the polar cap for different seasonal, solar cycle, and magnetic activity conditions. Using DE-1 composition data, Chen et al., [1990] obtained the distribution of O^+, H^+, and He^+ in upward flowing beams in the polar cap. The horizontal transport of such beams leads to the effect called the cleft ion fountain. Using a three-dimensional particle code, Delcourt et al., [1989b] showed that under storm conditions, polar wind protons became a source for ion precipitation.

Horwitz [1987] showed that in describing this process, two-dimensional kinetic models produced different results from simpler one-dimensional kinetic models. Schunk and Sojka [1989] developed a fully three-dimensional time dependent model of the F region and polar wind. In this model, the polar wind was coupled to the ionospheric plasma and the polar wind was driven by temporal and spatial changes in the ionosphere. With such changes, transient large scale ion upflows and downflows occurred in the polar wind. Swift [1990] developed a one-dimensional fluid model to describe the ionosphere-polar wind from 100km to many Re. Using this model, he simulated changing magnetospheric flux tube boundary conditions, i.e., open and closed field lines. Wilson et al., [1990] developed a new kinetic polar plasma outflow model.

Although ion composition measurements of the energized ionospheric ions as they flow into the magnetosphere are available, systematic observations of the thermal polar wind still need to be made. Sagawa et al., [1987] used DE-1 ion data to study the flow of O^+ and H^+ at L< 6 and found it to be bi-directional along the field lines, implying an ionospheric source, while Collin et al., [1988] used the same satellite data set to map the morphology of the He^+ ionospheric outflows. Fuselier et al., [1989] observed two distinct O^+ populations in the dayside low latitude boundary layer with the AMPTE/charge composition Explorer. These two populations were a convected O^+ population from the outer magnetosphere and an injected O^+ population from the high latitude ionosphere.

The question of whether the solar wind or the ionosphere is the principal source of magnetospheric plasma has been extensively investigated during the past decade. More recently, the idea of the ionosphere as the primary source has gained respect and has been quantified by a variety of studies, although, even today, only a few isolated observations of the thermal polar wind have been made. The research focuses on the suprathermal and energetic ion species that are clearly of ionospheric origin, on how they are heated and subsequently transported into the magnetosphere. Based upon ion composition measurements in the topside ionosphere-magnetosphere, Chappell et al., [1987] demonstrated that the ionosphere is a plausible source for all the plasma in the magnetosphere. The adiabatic motion of these ions into the magnetosphere was studied with a three-dimensional model up to a distance of 17 Re by Delcourt et al., [1989a]. In the absence of direct measurements of the thermal polar wind, identifying the location and nature of the cold plasma heating mechanisms is extremely difficult. Tsunoda et al., [1989] empirically correlated the ion fountain with the cusp while Collin et al., [1987] found a strong solar cycle dependence in the energized ion outflows. Both these results indicated that the initial ion heating occurred in the ionosphere. The ion heating mechanism is still unknown although wave particle mechanisms have been studied [Winglee et al., 1987; Bergman et al., 1988; Johnson et al., 1989; Winglee et al., 1989; Crew et al., 1990; Schriver et al., 1990].

The stability of these outflowing beams is of concern as they are highly non-Maxwellian and anisotropic. Barakat and Schunk [1987] considered the ion parallel to perpendicular temperature anisotropy as well as the ion to electron temperature ratio in the excitation of electrostatic waves. They found that the polar wind was very stable to such wave excitation and defined the temperature characteristics of this region of stability. The effect of convecting H^+ beams on the stability of the polar wind was studied by Barakat and Schunk [1989]. Their analysis showed that the plasma was destabilized for relative drift energies of 1 eV and that for large electron temperatures the parallel propagating ion/ion plasma-acoustic instability was triggered first, while for lower values of Te the obliquely propagating ion/ion cyclotron instability was triggered first.

Under northward IMF conditions the polar region becomes aurorally active with the presence of sun aligned arcs. Associated with these arcs are field aligned electrodynamic systems which close in the ionosphere. Several studies of complementary observations were carried out to deduce both the electrodynamics and the sun aligned arc dynamics. Robinson et al., [1987] combined Sondrestrom Fjord radar data and all sky images of a sun aligned arc to study its westward drift and transition into the midnight sector of the oval. Carlson et al., [1988] used all sky images combined with DE-2 data and found that the arc electrodynamics were consistent with an electric field negative divergence model. Mende et al., [1988] used all sky imaging TV, the Sondrestrom Fjord radar, and DMSP data to follow a group of sun aligned arcs which, in this case, were drifting toward dawn from the midnight sector. They found the plasma drift inside the arc was mainly anti-sunward, which was also found by Robinson et al., [1987], and that both sunward and anti-sunward drift was found outside the arcs. Weber et al., [1989] launched a rocket from Sondrestrom Fjord which crossed a sun aligned arc and made electrodynamic and plasma measurements. These measurements were supported by aircraft all sky camera data. This arc was drifting toward dusk at a speed consistent with the overall electric field, however, inside the arc the plasma was convecting sunward. Inside the arc, the F region plasma showed a slight decrease from that outside the arc. Zanetti et al., [1990] used Viking magnetic and electric field data with auroral images to study the polar region for northward IMF conditions. They tested the two hypotheses for the generation of polar aurora; namely, converging electric fields and bifurcation of the magnetotail with plasma convection and found that the converging electric field hypothesis ($\nabla \cdot E < 0$) adequately explained the polar cap aurora. During the major magnetic storm on February 7, 1986, the IMF Bz component turned northward for several hours and during this time an NBZ current system developed in the summer polar cap while an irregular pattern of field aligned currents developed in the winter hemisphere [Rich et al., 1990]. Polar cap arcs were observed but were not correlated with the location of the large scale field aligned currents. Chiu [1989] proposed that the sun aligned arcs were driven by a negative divergence of the electric fields, a velocity shear. In this model each velocity shear structure in the ionosphere drove a pair of field aligned currents, with the upward currents associated with the downward acceleration of polar rain electrons.

3.1. IONOSPHERIC ELECTRODYNAMIC INPUTS

A large fraction of magnetospheric electrodynamics links with the ionosphere where it can be studied in depth. A major part of the ionospheres ionization and energy come from the magnetospheric electrodynamic systems. For a complete analysis of the ionosphere, it is necessary to understand how

magnetospheric electrodynamics maps into the ionosphere; such a description is as yet not available. However, the last four years have seen significant advances in this area of research. Statistical magnetospheric convection models now include an IMF dependence, although there is no agreement on the convection pattern resulting from a Northward IMF (Heppner and Maynard 1987, Crooker 1988, Moses et al., 1988, 1989, Lu et al., 1989). Advancements have also been made in describing current/convection/conductivity dependence upon the IMF orientation [Min-Yun et al., 1987, Rasmussen and Schunk 1987, 1988]. Rich and Gussenhoven [1987] and Hoffman et al., [1988] observed that Region 1 and 2 current systems were virtually absent under very quiet geomagnetic conditions. This quiet case situation does not appear in present day models. Also, the statistical convection, current, and conductivity models do not reproduce the specific day-to-day variability observed in the ionosphere. Richmond et al., [1988] applied the AMIE procedure to infer the high latitude electric fields and currents during a specific study period. The use of global scale auroral images to infer the instantaneous conductivity distribution has been extensively developed [Marklund et al., 1987, 1988, Ahn et al., 1989, Rees et al., 1988].

Local time dependencies in the colocation of conductivity and convection boundaries and the subsequent effect this has on Joule heating was pointed out by Kamide and Richmond [1987], and to some extent were quantified by Foster [1987], while Heelis and Coley [1988] derived both global and local Joule heating rates based on in situ DE-2 observations. Coordinated observations of multiple parameters associated with the magnetospheric inputs to the ionosphere in the cusp-polar cap region were made by Basinska et al., [1987], Baker et al., [1989], and Niciejewski et al., [1989]. These studies indicate why the phenomena associated with fine structure need comprehensive multiparameter observation to constrain the physical interpretation. The latter is an example of how the CEDAR cooperative programs can be utilized to maximize constraints on the physical interpretation of ionospheric observations.

Earle and Kelley [1987], using incoherent scatter radar data, carried out a spectral analysis of ionospheric electric fields at high latitudes and their penetration to the equator. They found a peak penetration to low latitudes for fluctuations in the 3-5 hour period range and noted that the zonal electric field components penetrated with little or no attenuation. Richmond and Roble [1987] used the NCAR TGCM to study the electrodynamic effects associated with thermospheric winds and reproduced the general pattern of the Sq current system. Aggson et al., [1987] and Ganguly et al., [1987] empirically studied the equatorial ionospheric convection using DE-2 data and Arecibo observations, respectively. The use of coherent HF radars to map the plasma convection in the F region was discussed by Ruohoniemi et al., [1989]. Optically tracking F region cavities generated by high power ionospheric heaters to deduce plasma convection was demonstrated by Bernhardt et al., [1989].

Extensive conjugate observations using satellites in both polar regions have quantified the extent to which polar cap arcs and the cusp are conjugate [Mizera et al., 1987; Candidi and Meng 1988; Carbary and Meng 1988]. Newell and Meng [1988] reported the observation of an ion polar rain event which was significantly larger than any previously reported, while Sergeev et al., [1990] found transient plasma injection events which were not linked with substorms.

The role played by the ionosphere in the transmission of VLF signals, whistlers, and lightning continues to be a topic where progress is being made. Inan et al., [1989] quantitatively verified the predictions of lightning-induced electron precipitation (LEP) by observing the gyroresonant whistler particle interaction on an L=2.24 field line along with a burst of precipitation. A longitudinal dependence of electron precipitation at L=4 associated with the south Atlantic anomaly was observed by Bering et al., [1988]. Neubert et al., [1987] proposed the resonance of coherent whistler mode waves with energetic electrons in the topside ionosphere as a source of Fast Trimpi events. The modification of sub-ionospheric VLF signals by LEP ionization changes in the D region was observed and statistically modeled [Carpenter and Inan 1987, Inan and Carpenter 1987, Inan et al., 1988]. Baginski et al., [1988] used a model of the lightning return stroke to show that it can be a major component of the transient field and energy coupled to the ionosphere. The role of mid-latitude precipitation in modifying the geoelectric field was studied by Sheldon et al., [1988] who found that the precipitation produces a diurnal modulation of the geoelectric field.

3.2. PLASMA WAVES AND IRREGULARITIES

The ionosphere, apart from having a diverse collection of particle species, harbors a zoo of naturally present wave-particle processes. Many of the research topics already reviewed have covered some of these processes. However, other studies have been conducted which are of a more general plasma physics nature, or which do not readily fit within the constraints of the previous sections. These are reviewed in this section. Much of this work involves solving non-linear systems of equations whose boundary conditions are not well understood; nonetheless, significant progress has been made on several of these wave-particle problems.

Maggs [1989] considered the nonlinear spatial evolution of an auroral electron beam and of beam generated electrostatic whistler noise as the beam propagates into the atmosphere and found that the wave intensities were sufficient to modify the ionospheric density profile. Seyler [1988] considered the three-dimensional nonlinear evolution of kinetic Alfven waves due to shear flow and collisionless tearing instability under boundary conditions similar to those of a discrete auroral breakup arc. Mode conversion to fast magnetosonic waves by anisotropic ionospheric currents from shear incident Alfven waves was modeled by Fujita and Tamao [1988] and Fujita [1988]. They considered the dispersion characteristics, loss mechanisms, and the ground magnetic signature of this mode conversion mechanism. The heating of ions in a multicomponent plasma was found to occur even when the electron drift speed was too small to excite the lower hybrid instability. In this case, Ashour-Abdalla et al., [1987] found that an ion-ion hybrid mode became unstable and heating of both the light (bulk heating) and heavy (tail heating) ions occurred [Schriver and Ashour-Abdalla 1988]. Suscynsky et al., [1989] carried out a laboratory two-ion plasma experiment to generate EIC waves. They used K^+ for the light ion and Cs^+ for the heavy ion and found that the EIC wave frequencies depended on the density ratio of the ions. Benson and Wong [1987] used ISIS-1 observations to show that the cyclotron maser instability generates most of the auroral radio

emissions, and they predicted the characteristics of these radio emissions for ground observations. A ground-based search for these auroral radio emissions found them to occur within ± 30 minutes of magnetic midnight but that they were poorly correlated with geomagnetic activity [Benson et al., 1988a]. Using DE-1 data, Benson et al., [1988b] found ordinary mode AKR fine structure; however, the present day theories used to describe the intense right-hand extraordinary mode AKR do not generate this left-hand ordinary mode/AKR. Keskinen et al., [1988] considered the non-linear evolution of the Kelvin-Helmholtz instability caused by velocity-sheared plasma flows. Specifically, they studied the role of ion-neutral collisions and compared their results with DE observations.

Plasma wave interactions were the topic of several studies; De Groot and Mizuno [1989] considered the effect of the ion acoustic decay instability on microwave-plasma interactions. Yu et al., [1987] showed that in an ionospheric plasma a large amplitude electromagnetic wave can parametrically excite low-frequency electrostatic modified electron acoustic waves; Vampola [1987]; Gail et al., [1990]; Gail and Inan [1990]; Datlow and Imhof [1990]; Rosenberg et al., [1990] and others identified in Section 2.3 considered the role of VLF waves in the precipitation of ring current particles; Groves et al., [1988] observed intense hiss from an auroral rocket flight and compared their observations favorably with the predictions of a convective beam amplification hiss model. A variety of plasma wave phenomena can be generated using the HF sounders and heating facilities; Osherovich [1987] discussed the physics of the diffuse plasma resonances as stimulated by HF sounders; the resonant absorption of HF waves by the electrons to produce a "bump in the tail" distribution was studied by Shoucri et al., [1987] and Villalon [1989]; while Hansen et al., [1989] refined the calculations of how deep the associated electron density depletions (cavities) can become. Swartz et al., [1988] discovered that the interpretation of topside incoherent scatter echoes can be heavily aliased if velocity shears are present in the plasma. This effect tends to reduce the apparent electron temperature while enhancing the ion temperature, even to the extent of wrongly deducing that Te < Ti. Lockwood et al., [1988] and Providakes et al., [1988] considered the role of plasma temperature in the F and E regions, respectively, in wave plasma interaction using ground-based sounding techniques.

Basu et al., [1987] used an HF heater facility to study the growth and decay rates of ionospheric scintillations associated with 750m scale irregularities. Villain et al., [1987] used another HF radar to study E region decametric irregularities produced by oblique electron streaming. The HF heater facility was also used to produce field aligned irregularities which had spread F echoes associated with them; in this case, a thermal instability generated the density irregularities [Kuo and Djuth, 1988]. Bell and Ngo [1990] showed that electrostatic lower hybrid waves are excited by whistler mode waves scattering from field aligned plasma density irregularities. A generalized Rayleigh-Taylor instability model was used to study the collisional interchange instability associated with equatorial irregularities and the results were successfully compared with observations [Zargham and Seyler 1987; Kelley et al., 1987]. Zargham and Seyler [1989] included ion inertia and ion-neutral collisions in a two-dimensional fluid model of ionospheric interchange instability. Using this model, they computed the density structure power-spectra for several forms of plasma irregularities: rising plasma bubbles, unstable plasma strata, and driven plasma irregularities. Lee et al., [1989] modeled the effect of both rod-like and sheet-like ionospheric irregularities on Faraday polarization fluctuations. They found that the sheet-like irregularities had the most severe effect on radio waves; such irregularities being found in both the equatorial anomaly and auroral regions. The fading of HF waves returned from the F region when the receiver is close to the transmitter was studied by Booker and Tao [1987]. Franke and Liu [1987] used fading of saturated VHF amplitude scintillations to deduce the characteristics of equatorial plasma bubbles.

Lakhina et al., [1990] considered the stability criterion of the ballooning mode instability at the plasmapause; Hollweg [1990] studied the resonance absorption of propagating fast waves in a plasma density gradient; while Sentman [1989, 1990] studied the polarization and mode splitting in Schumann resonance excitation as well as the resonance phenomena in a two-scale-height ionosphere. Liao et al., [1989] proposed the parametric instability excited by lightning-induced whistler waves as a cause of explosive spread F.

3.3. ACTIVE EXPERIMENTS

The ionosphere is a readily accessible "unbounded" plasma suitable for basic plasma physics research. Some of this research also highlights certain ionospheric physics problems. This section focuses upon this subset of research.

Two major high power HF heater facilities at Arecibo, Puerto Rico and at Tromso, Norway have been used extensively to modify the upper atmosphere. The heating of ionospheric plasma, specifically the electrons, was reported by Fejer and Sulzer [1987], Bernhardt and Duncan [1987], Djuth et al., [1987b] and Inan [1990], while Shoucri et al., [1987] described how the electron distribution function was modified by the HF waves through a resonant electrostatic field interaction. Newman et al., [1988] pointed out that under certain solar/seasonal conditions the apparent anomalous heating was due to very low electron cooling rates. Osherovich [1987, 1989] developed theoretical descriptions of the stimulated diffuse plasma resonances observed during HF heating experiments. Chaturvedi et al., [1987] described the production and control of ion-cyclotron instabilities at high latitudes using high power radio waves. Hansen et al., [1989] studied theoretically the lifetime of density depletions created by the heating experiments, while Bernhardt et al., [1989a] showed how these density depletions could be used as a tracer for ionospheric convection and also how the associated optical signatures could be observed and tracked [Bernhard et al., 1989b]. Associated with these density gradients are waves and irregularities; Bernhardt [1988] showed how the **E x B** gradient drift instability produced irregularities on the upwind edge of a density depletion. Using the HF heater to create density depletions, Basu et al., [1987] was able to observe the e-folding growth and decay rates of F region irregularities of the 750m scale size while Noble et al., [1987] made a similar study of the 1 to 7m E region irregularities. The mechanism by which the HF experiments are able to stimulate enhanced plasma line emission and the "overshoot" aspects are still unknown. Observations of the enhanced plasma line and the "overshoot" were made by Djuth et al., [1987a] and Djuth and Gonzales [1988], and the role of Langmuir waves in the overshoot process was studied theoretically by Kuo et al., [1987]; however, Sulzer et al., [1989] showed that significant aspects of the phenomena still remain unexplained.

The artificial generation of F region bubble irregularities was reported by Klobuchar and Abdu (1989). Rockets were launched into the bottomside F-layer from Natal, Brazil as part of the BIME program. These payloads released H_2O and CO_2 to create plasma depletions. The subsequent motion of the depletions and evolution of plasma irregularities provided a good test of equatorial bubble irregularity theories.

In-situ generation of whistler mode waves by an electron beam generator and a remote wave detector on board the space shuttle was the focus of both observational and theoretical reports. On both the space shuttle STS-3 and SpaceLab-2 flights the electron generator (FPEG) and a plasma monitor (PDP), respectively produced and observed enhanced VLF emissions [Farrell et al., 1988; Frank et al., 1989; Reeves et al., 1988, 1990]. Goerke et al., [1990] observed VLF emissions generated by an electron beam gun on a Nike Black Brant V sounding rocket; similarly, Winglee and Kellogg [1990] reported electromagnetic wave emissions generated by beams, and Olsen et al., [1990] studied plasma waves generated by ion beams on the SCATHA satellite. The role of coherent Cerenkov radiation driven by bunching of the electron beam was developed theoretically by Farrell et al., [1989] and Pickett et al., [1989]. Nishikawa et al., [1989] modeled the whistler mode excitation using a three-dimensional partially magnetostatic code and subsequently identified the beam instability responsible for the excitation. In a theoretical study, Okuda and Ashour-Abdalla [1988] showed that suprathermal electron beams could also drive ion-acoustic waves in the ionosphere which, in turn, leads to ion heating. Water dumps from the space shuttle that produce a host of plasma irregularities in the few Hz to KHz range were studied by Pickett et al., [1989], who considered both ion-plasma and Ott-Farley instabilities as sources of plasma density irregularities.

In addition to these active experiments in ionospheric physics, several other categories of ionospheric modification such as beams in the ionosphere, chemicals in the ionosphere, and ionosphere-vehicle interactions were reported. As these studies apply primarily to plasma physics, only a categorization and references are given below. Various aspects of the plasma vehicle interaction, i.e., wake, charging, sheath, were studied (Lai et al., [1987]; Samir et al., [1987]; Okuda and Berchem [1988]; Singh and Kwang [1988]; Hastings and Blandino [1989]; Katz et al.,[1989]; Kaufman et al., [1989]; Ma and Schunk [1989]; Murphy and Katz [1989]; Murphy et al., [1989]; Myers et al., [1989]; Samir et al., [1989]; Senbetu and Henley [1989]; Tribble et al., [1989] Kellogg et al., [1990]; Neubert et al., [1990a,b]; Svenses et al., [1990]). Chemical releases leading to plasma modifications and neutral clouds were reported by Bernhardt [1987]; Bernhardt et al., [1987]; Grebowsky et al., [1987a,b]; Hunton et al., [1987]; Lai et al., [1988]; Eccles et al., [1989]; Lai and Murad [1989]; Paterson and Frank [1989]; Elgin et al., [1990]; Gilchrist et al., [1990]; Jacobson et al., [1987]; Ma and Schunk [1990]; Pike et al., [1990]. The physics of beams in ionospheric plasmas was extensively reported upon (Cai et al., [1987]; Chung [1987]; Harker and Banks [1987]; Parish et al., [1987]; Pritchett and Winglee [1987]; Banks and Raitt [1988]; Hudson and Roth [1988]; Pollock et al., [1988]; Reeves et al., [1988]; Abe et al., [1988]; Erlandson et al., [1989]; Frank et al., [1989]; Heppner et al., [1989]; Neubert and Harker [1988]; Stenzel and Urrutia [1989]; Hallinan et al., [1990]; Mandell et al., [1990]; Pritchett [1990]; Scales and Kintner [1990 a,b]; Winglee [1990]). Additional HF plasma heating results were described by Isham et al., [1987]; Fejer et al., [1989]; Kuo and Lee [1989]; Thide et al., [1989]; Kuo and Lee [1990]; Milikh [1990]. The critical velocity ionization phenomenon was studied by Lai et al., [1990 a,b]; McNeil et al., [1990]; Person et al., [1990]; Stenbaek-Nielsen et al., [1990] and others already listed above.

3.4. IONOSPHERIC FORECASTING

Since ionospheric physics is regarded by many as a mature research field, one measure of its maturity is the quality of the community's modeling and forecasting ability. The primary parameters to be modeled and predicted are the plasma density, its temperature and composition, and the waves generated in the presence of anisotropic plasma distributions. Models exist for each of the regions described in Section 2; however, most of these models are limited, either inherently by physical assumptions or by inadequately defined boundary conditions. In this quadrennium, improvements in modeling have occurred in several areas. These are discussed in the following paragraphs.

The RIMS instrument on the DE-1 satellite produced measurements that led to new insights into the plasmasphere's exotic, but normal status. The role of minor ions, their solar cycle, and storm dependencies have been incorporated into recent models of the plasmasphere [Chandler et al., 1987, Newberry et al., 1989]. The question of where refilling begins along a plasmaspheric flux tube was addressed by Rasmussen and Schunk [1988] using a new multistream hydrodynamic model. They confirmed earlier findings that it is at the equator that refilling begins, but showed that in the initial refilling period (4 hours) the flow characteristics were substantially different from those previously reported. Another example showing the limitations of present day models is associated with electron temperature modeling and global scale coupling. Brace et al., [1988] used both DE-1 and DE-2 plasma measurements to correlate the location of plasmaspheric and ionospheric enhanced electron temperatures and found that in the evening bulge region they were not correlated. This bulge region is very dependent upon magnetic activity, and, therefore, this discrepancy is readily explained in a qualitative way. Present day models do not reproduce the dynamics of such ionospheric plasmaspheric temperature structures.

Even greater difficulty is encountered in describing and modeling observations at higher latitudes. Persoon et al., [1988] found that in the topside ionosphere (polar and auroral flux tubes) marked plasma depletions and structuring exist. In such regions, the cold plasma is susceptible to acceleration by a wide range of auroral processes which are not included in present day models, e.g., Demars and Schunk [1987], Schunk and Sojka [1987, 1989]. Even when auroral systems are included, i.e., return currents as by Schunk et al., [1987], the work is still of a parametric nature. It is difficult to include micro scale phenomena in large scale models. St. Maurice [1987] outlined how, in the case of E region electron heating in plasma irregularities, the micro scale heating rate could be parameterized on a larger scale. Rasmussen et al., [1988] and Richards et al., [1989] showed the difficulty of using present day models and extensive observations to describe case studies in the sub-auroral/mid-latitude F region. In both case studies, significant, unexplained differences remain, although extensive validation of the model inputs was carried out.

Buonsanto [1989] compared Millstone Hill incoherent scatter radar data with the International Reference Ionosphere (IRI) model for different solar, seasonal, and diurnal conditions. The topside densities were significantly larger in the model while the observed T_e variability was not present in the IRI model. The observed T_i diurnal variation was present in the model but with a small amplitude. Sica et al., [1990] used extensive data sets from many locations to test the TDIM mid -latitude model. A similar test was carried out by Sojka et al., [1988] using a single station data base over an entire solar cycle. In both these cases, since the inputs were not adequately constrained, agreement could be obtained in several ways. Often the inputs are still inadequately understood as is the case for the cleft plasma heating source. Fontheim et al., [1987] showed that elevated electron temperatures (up to 10,000° K) were independent of solar EUV, but were coupled to precipitation and, hence, concluded that particle heating was the source mechanism. However, to include such a mechanism in present day ionospheric models requires much improved knowledge or parameterization of magnetospheric cleft precipitation.

On a global scale only climatological ionospheric modeling is possible at present. Several studies were conducted and models developed to improve our global scale climatological knowledge. Roble et al., [1987] carried out a global mean coupled ionosphere-thermosphere study; Anderson et al., [1989] developed a fully analytic mid- and low - latitude model, while Sojka and Schunk [1989] contrasted F region seasonal global effects. In each case, although new capability was achieved, forecasting capability was only at a climatological level. To extend our capability beyond this climatological status, dynamics associated with the regions coupled to the ionosphere, namely, the magnetosphere and thermosphere, are needed. Knipp et al., [1989] used extensive data sets and the AMIE technique to produce storm dependent electrodynamic patterns for a specific study period. Sojka et al., [1989] used DE-1 auroral images to define auroral dynamics for an ionospheric simulation. Since the associated electrodynamics were not available, a "parametric" study resulted rather than an actual ionospheric simulation.

The accuracy of our ionospheric physics models is still far from being predictive. At best, climatological predictive modeling is possible for certain phenomena, however, these are mostly of a semi-empirical nature [Schunk and Sojka, 1988]. At the present time, complete understanding of the phases and morphology of an ionospheric storm illude us. Part of the reason for this is the lack of understanding of how inputs to the ionosphere behave (magnetospheric and thermospheric dynamics), the difficulty of including small -scale size variability in global scale simulations, and of understanding how certain processes operate (auroral plasma heating, irregularities, return currents, etc.). All of this can be summarized by the need to include ionospheric weather rather than only deal with climatological trends. During this quadrennial period, preliminary studies have examined the spatial and temporal effects of ionospheric weather on climatological models. These studies have also highlighted the inability to tweak climatological model inputs (statistical models for auroral precipitation, plasma convection and neutral atmosphere) to give weather. Rich and Maynard [1989] carried out a critique of statistical representations of the electrodynamic input to the ionosphere and raised some of these issues.

3.5. COUPLING THE IONOSPHERE WITH OTHER REGIONS

Both theoretically and experimentally the community continues to make progress in coupling other regions to the ionosphere. The characteristics of hydromagnetic waves in the magnetospheric cavity are, to a large extent, determined by the ionosphere. Crowley et al., [1987] observed Pc-5 pulsations using ground based magnetometers and EISCAT and were able to deduce that the Pc-5 damping was controlled by the damping of the cavity mode rather than the energy dissipation from the resonance field line. Lysak [1988] showed theoretically how bursts of irregular pulsations (PiB) were associated with a resonant cavity in the topside ionosphere where the density decreased exponentially with height, and Kivelson and Southwood [1988] reconsidered the role of the ionosphere in the theory of hydromagnetic surface waves in the magnetosphere. The ionosphere is also a key element in auroral dynamics and arc formation. Lotko et al., [1987] introduced the ionosphere into a two-dimensional model of perpendicular flow dynamics in boundary layers in the magnetospheric equatorial plane coupled with the ionosphere and found that the ionosphere controlled the disturbances at different scale sizes. Kan et al., [1988] found that the co-location of the magnetospheric convection reversal with a conductance gradient in diffuse aurora determined the stability and onset of substorms. Zhu and Kan [1987] showed that the dynamics of westward traveling surges in a coupled magnetospheric-ionospheric system was controlled by the recombination rate in the auroral ionosphere. Mapping electric fields from the ionosphere into the magnetosphere during disturbed times in the vicinity of westward traveling surges was studied by Kaufmann and Larson [1989]. Chiu [1989] argued that the magnetospheric convection velocity shears in the ionosphere drove and supported polar cap auroral arcs without the need to bifurcate the magnetospheric topology with adjacent open and closed field lines. Coupling the polar wind from the magnetosphere to the polar ionosphere was accomplished theoretically by Schunk and Sojka [1989] with a three-dimensional time dependent model. This model enabled ionospheric topside boundary conditions to be replaced with more realistic physical processes in the high altitude polar magnetosphere.

Solar x-ray fluxes can lead to photoelectrons in the ionosphere at energies higher than those associated with the solar EUV spectrum and, hence, provide the magnetosphere with an additional electron source [Winningham et al., 1989]. Transient lightning pulses transmit energy into the ionosphere and magnetosphere; Baginski et al., [1988] self consistently coupled these transient pulses with the ionosphere and showed that significantly more energy than previously expected was directed to the ionosphere. Inan and Carpenter [1987] showed how lightning induced electron precipitation caused modification of the D region conductivity which, in turn, modified the ionosphere's role in VLF transmission. The modification of the D region by relativistic electrons associated with high speed solar wind streams was inferred by Baker et al., [1987].

Coupling of the ionosphere and thermosphere has progressed significantly. Roble et al., [1988] has developed a self-consistent thermosphere-ionosphere model (TIGCM) which combines the physical processes of each. Work continues in deducing self consistent ionospheric and

thermospheric parameters from the analysis of incoherent scatter radar data [Burnside et al., 1988]. Johnson and Luhmann [1988] were able to infer from the lack of geomagnetic control of upper mesopheric neutral winds that magnetospheric ion drag coupling was only significant above 90km at high latitudes. Propagation of magnetospheric storm effects to low latitudes in both the ionosphere and thermosphere was the focus of an ionosonde study by Forbes et al., [1988]. The recovery phase of another storm was studied by Burns et al., [1989] to investigate the thermospheric composition variations. The effect of neutral winds on magnetospheric-ionospheric electrodynamics was studied by Forbes and Harel [1989]. The neutral wind control of electrodynamic coupling in the equatorial E and F regions was studied by Biondi et al., [1988]. Samson et al., [1989] used the Goose Bay coherent scatter radar to show that dayside atmospheric gravity waves originated at an ionospheric convection shear reversal region in the 100 to 150km altitude range.

CONCLUSION

Over the past four years advancements have been made in all areas of ionospheric research. As already pointed out, the ionospheric community is a very balanced research community and, as such, contributes to our knowledge over a diverse range of sub-topics. Some of the work leads to greater confusion, again due to the complexity of the phenomena and paucity of observation. In several areas, significant new results were published during this reporting period. Some highlights are listed below.

- Global images of auroral emissions have been used to infer the temporal and spatial pattern of auroral conductances and electron precipitation. However, the single pixel representation of the fine-scale auroral structure is still in debate. This is yet another example of how phenomena on different scale sizes need to be interrelated.
- In the same vein, the need for instantaneous global "images" of the magnetospheric convection pattern has been realized and, although it is in its infancy, the AMIE technique has demonstrated its usefulness. The community has a great need for global scale time-dependent observation of the convection pattern.
- Storm dynamics in the ionosphere is a documented, but poorly understood phenomenon. However, progress has been made in quantifying the storm propagation from high to low (equatorial) latitudes. This is especially the case for the electric field penetration, F-layer dynamics, and coupled ionospheric-thermospheric effects. We still do not have an adequate representation of the storm input dynamics or its energy input profile at high latitudes.
- Much work was focused on understanding the high latitude ionospheric-electrodynamics associated with northward and southward IMF conditions. Current systems (NBZ), FTE signatures, polar cap arcs, and ionospheric density/ temperature signatures were studied. However, the major question of the northward IMF convection pattern topology, namely "distorted 2-cell" or "4-cell", remains unanswered.
- Many plasma instability mechanisms which lead to ionospheric density irregularities were quantified. A better understanding of the initial ionospheric condition associated with these instabilities was obtained. The task of how to model the competing instability mechanisms is now in hand.
- The interaction of small-scale plasma processes in a global ionospheric electrodynamic system was studied. Extensive complementary data sets were acquired and rudimentary simulations were carried out including coupling into a magnetospheric environment. A need exists for the parameterization of these small-scale processes so that their impact on global scale models can be understood.
- Active experiments were used to study growth and decay rates of plasma bubbles, density cavities, and irregularities both in the E and F regions. Such active experiments give quantifiable insight into an otherwise complex, if not apparently turbulent, phenomena.
- Ground or lightning generated VLF waves ducted through a "magnetospheric-ionospheric" system interacting with energetic magnetospheric ring current particles were studied via their ensuing precipitation into the atmosphere. Quantitative modeling of this coupled wave-particle system was successfully carried out as was the ensuing modification of the ducting channel by the precipitation.
- Ionospheric-magnetospheric coupling via the transport of plasma into the magnetosphere was quantified both at high latitudes (polar wind, ion conics, and ion beams) and at mid-latitudes (plasmaspheric ion composition). Indeed, with the exception of the cold polar wind, this coupling has now been determined empirically although the energization of ions in conics and beams requires further work.
- Coupling of the ionosphere to the thermosphere has seen the evolution of global scale coupled models. These models treat the thermospheric and ionospheric problems self consistently, and, hence, have the potential of better simulating storm dynamics, a topic of major interest to both communities.

GLOSSARY

AE: NASA atmospheric satellite program.
AKR: Auroral Kilometric Radiation.
AMIE: Assimilative Mapping of Ionospheric Electrodynamics, a computer package to best fit ionospheric currents, conductivities, and electric fields as global patterns.
AMPTE: International solar wind-magnetosphere satellite program.
Blob: Localized auroral region of enhanced plasma density in the F-region.
CEDAR: Coupling Energy and Dynamics of Atmospheric Regions.
CONDOR: Joint USA-Brazilian Rocket Program.
CUPRI: Cornell University Portable Radar Interferometer.
DE: NASA thermosphere-ionosphere-magnetosphere satellite program.
DMSP: U.S. Air Force Defense Meterological Satellite Program of satellites.
EIC: Electrostastic Ion Cyclotron plasma waves.
EISCAT: European Incoherent SCATter radar facility.
ETS: Equinox Transition Study of the thermosphere and ionosphere.
EUV: Extreme Ultra Violet region of the solar spectrum.
FLIP: Field-Line Interhemispheric Model of the University of Alabama, Huntsville.
FTE: Flux Transfer Event.
F0f2: The plasma frequency associated with the F-region peak electron density.

FPEG: Fast Pulse Electron Generator flown on the Space Shuttle.
GISMOS: Global Ionospheric Simultaneous Measurements Of Substorms.
HILAT: USAF ionosphere-magnetosphere satellite.
hmf2: The altitude of the peak electron density in the F-region.
IMF: Interplanetary Magnetic Field of solar origin.
IRI: International Reference Ionosphere model.
ISIS: Canadian ionospheric satellite program.
LEP: Lightning-induced Electron Precipitation from the ring currents.
NBZ: Northward orientated interplanetary magnetic field.
NCAR: National Center for Atmospheric Research.
Nmf2: The maximum electron density in the F-region profile.
NOAA: National Oceanic and Atmospheric Administration.
MITHRAS: Magnetosphere Ionosphere THermosphere RAdar Studies.
MSIS: Mass Spectrometer/Incoherent Scatter atmospheric model.
MU: Middle and Upper atmosphere VHF radar, Kyoto, Japan.
Patches: Localized polar cap regions of enhanced plasma density in the F-region.
PDP: Plasma Diagnostic Package flown on the Space Shuttle.
RIMS: Retarding Ion Mass Spectrometer instrument on the DE-1 satellite.
SAR: Stable Auroral Red arc.
STS: NASA Space Transport System (shuttle).
SUNDIAL: Coordinated study of the ionosphere/magnetosphere.
TDIM: Utah State University Time Dependent Ionospheric Model.
TEC: Total Electron Content along a ray path through the ionosphere.
TGCM: NCAR Thermospheric Global Circulation Model.
TID: Travelling Ionospheric Disturbance.
TIROS: NOAA weather satellite program.
UV: Ultra Violet region of the solar spectrum.
VHF: Very High Frequency radio wave.
Viking: Swedish ionospheric-magnetosphere satellite.
VLF: Very low frequency radio waves.

Acknowledgements. This research was supported by NASA grants NAG5-1484 and NAGW-1547, NSF grant ATM-89-13230, and grant AFOSR-90-0026 to Utah State University.

REFERENCES

Abe, Y., K. N. Erickson and J. R. Winckler, ELF electric turbulence near an electron beam-emitting rocket in the auroral ionosphere: ECHO 6, *Planet. Space Sci., 36*, 235-258, 1988.

Adams, G. W., J. W. Brosnahan and T. D. Halderman, Direct radar observations of TIDs in the D- and E-regions, *J. Atmos. Terr. Phys., 50*, 931-935, 1988.

Aggson, T. L., N. C. Maynard, F. A. Herrero, H. G. Mayr, L. H. Brace and M. C. Liebrecht, Geomagnetic equatorial anomaly in zonal plasma flow, *J. Geophys. Res., 92*, 311-315, 1987.

Ahn, B.-H., H. W. Kroehl, Y. Kamide, D. J. Gorney, S.-I. Akasofu and J. R. Kan, The auroral energy deposition over the polar ionosphere during substorms, *Planet. Space Sci., 37*, 239-252, 1989.

Ahn, B.-H., H. W. Kroehl, Y. Kamide and D. J. Gorney, Estimation of ionospheric electrodynamic parameters using ionospheric conductance deduced from Bremsstrahlung X-ray image data, *J. Geophys. Res., 94*, 2565-2586, 1989.

Ahn, B.-H., Y. Kamide, S.-I. Akasofu, H. W. Kroehl and D. J. Gorney, Ionospheric conductivity dependence of the cross-polar cap potential difference and global Joule heating rate, *J. Atmos. Terr. Phys., 51*, 841-850, 1989.

Anderson, D. N., J. M. Forbes and M. Codrescu, A fully analytic, low- and middle-latitude ionospheric model, *J. Geophys. Res., 94*, 1520-1524, 1989.

Ashour-Abdalla, M., H. Okuda and S. Y. Kim, Transverse ion heating in multicomponent plasmas, *Geophys. Res. Lett., 14*, 375-378, 1987.

Baker, D. N., J. B. Blake, D. J. Gorney, P. R. Higbie, R. W. Klebesadel and J. H. King, Highly relativistic magnetospheric electrons: A role in coupling to the middle atmosphere?, *Geophys. Res. Lett., 14*, 1027-1030, 1987.

Baker, K. B., R. A. Greenwald, J. M. Ruohoniemi, J. R. Dudeney, M. Pinnock, N. Mattin and J. M. Leonard, Polar Anglo-American conjugate experiment, *EOS Aug. 22*, 785, 1989.

Baginski, M. E., L. C. Hale and J. J. Olivero, Lightning-related fields in the ionosphere, *Geophys. Res. Lett., 15*, 764-767, 1988.

Banks, P. M. and W. J. Raitt, Observations of electron beam structure in space experiments, *J. Geophys. Res., 93*, 5811-5822, 1988.

Barakat, A. R., R. W. Schunk, T. E. Moore and J. H. Waite, Jr., Ion escape fluxes from the terrestrial high-latitude ionosphere, *J. Geophys. Res., 92*, 12,255-12,266, 1987.

Barakat, A. R., and R. W. Schunk, Stability of the polar wind, *J. Geophys. Res., 92*, 3409-3415, 1987.

Barakat, A. R., and R. W. Schunk, Stability of H^+ beams in the polar wind, *J. Geophys. Res., 94*, 1487-1494, 1989.

Basinska, E. M., W. J. Burke and M. A. Heinemann, A user's guide to locating flux transfer events in low-altitude satellite measurements: An S3-2 case study, *J. Geophys. Res., 94*, 6681-6691, 1989.

Basinska, E. M., W. J. Burke, S. Basu, F. J. Rich and P. F. Fougere, Low-frequency modulation of plasmas and soft electron precipitation near the dayside Cusp, *J. Geophys. Res., 92*, 3304-3314, 1987.

Basu, B., and B. Coppi, Fluctuations associated with sheared velocity regions near auroral arcs, *Geophys. Res. Lett., 15*, 417-420, 1988.

Basu, B., and B. Coppi, Velocity shear and fluctuations in the auroral regions of the ionosphere, *J. Geophys. Res., 94*, 5316-5326, 1989.

Basu, B., J. R. Jasperse, R. M. Robinson, R. R. Vondrak and D. S. Evans, Linear transport theory of auroral proton precipitation: A comparison with observations, *J. Geophys. Res., 92*, 5920-5932, 1987.

Basu, S., S. Basu, E. MacKenzie, P. F. Fougere, W. R. Coley, N. C. Maynard, J. D. Winningham, M. Sugiura, W. B. Hanson and W. R. Hoegy, Simultaneous density and electric field fluctuation spectra associated with velocity shears in the auroral oval, *J. Geophys. Res., 93*, 115,1988.

Basu, S., S. Basu, E. MacKenzie, W. R. Coley, J. R. Sharber and W. R. Hoegy, Plasma structuring by the gradient drift instability at high latitudes and comparison with velocity shear driven processes, *J. Geophys. Res., 95*, 7799-7818, 1990.

Basu, S., S. Basu, P. Stubbe, H. Kopka and J. Waaramaa, Daytime scintillations induced by high-power HF waves at Tromso, Norway, *J. Geophys. Res., 92*, 11,149-11,157, 1987.

Bell, T. F., and H. D. Ngo, Electrostatic lower hybrid waves excited by electromagnetic whistler mode waves scattering from planar magnetic-field-aligned plasma density irregularities, *J. Geophys. Res., 95*, 149-172, 1990.

Benson, R. F., and H. K. Wong, Low-altitude ISIS 1 observations of auroral radio emissions and their significance to the cyclotron maser instability, *J. Geophys. Res., 92*, 1218-1230, 1987.

Benson, R. F., M. D. Desch, R. D. Hunsucker and G. J. Romick, Ground-level detection of low- and medium-frequency auroral radio emissions, *J. Geophys. Res., 93*, 277-283, 1988a.

Benson, R. F., M. M. Mellott, R. L. Huff and D. A. Gurnett, Ordinary mode auroral kilometric radiation fine structure observed by DE 1, *J. Geophys. Res., 93*, 7515-7520, 1988b.

Bergmann, R., I. Roth and M. K. Hudson, Linear stability of the H^+ - O^+ two-stream interaction in a magnetized plasma, *J. Geophys. Res., 93*, 4005-4020, 1988.

Bering, E. A., J. E. Maggs and H. R. Anderson, The plasma wave environment of an auroral arc, *J. Geophys. Res., 92*, 7581-7605, 1987.

Bering, E. A., III, J. R. Benbrook, G. J. Byrne, B. Liao, J. R. Theall, L. J. Lanzerotti, C. G. Maclennan, A. Wolfe and G. L. Siscoe, Impulsive electric and magnetic field perturbations observed over South Pole: Flux transfer events? *Geophys. Res. Lett., 15*, 1545-1548, 1988.

Bering, E. A., III, J. R. Benbrook, H. Leverenz, J. L. Roeder, E. G. Stansbery and W. R. Sheldon, Longitudinal differences in electron precipitation near L = 4, *J. Geophys. Res., 93*, 11,385-11,403, 1988.

Berkey, F. T., and G. H. Stonehocker, A comparison of the height of the maximum electron density of the *F2*-layer from real height analysis and estimates based on M(3000)F2, *J. Atmos. Terr. Phys., 51*, 873-877, 1989.

Berkey, J. E., A. D. Richmond, R. M. Barnes, S. Gonzalez and C. A. Tepley, Solar cycle variations in *F* region electrodynamic drifts at arecibo, *J. Geophys. Res., 95*, 4303-4306, 1990.

Bernhardt, P. A., A critical comparison of ionospheric depletion chemicals, *J. Geophys. Res., 92*, 4617-4628, 1987.

Bernhardt, P. A., Cross-B convection of artificially created, negative-ion clouds and plasma depressions: Low-speed flow, *J. Geophys. Res., 93*, 8696-8704, 1988.

Bernhardt, P. A., C. A. Tepley and L. M. Duncan, Airglow enhancements associated with plasma cavities formed during ionospheric heating experiments, *J. Geophys. Res., 94*, 9071-9092, 1989b.

Bernhardt, P. A., L. M. Duncan and C. A. Tepley, Heater-induced cavities as optical tracers of plasma drifts, *J. Geophys. Res., 94*, 7003-7010, 1989a.

Bernhardt, P. A., and L. M. Duncan, The theory of ionospheric focused heating, *J. Atmos. Terr. Phys., 49*, 1107-1117, 1987.

Bernhardt, P. A., R. A. Roussel-Dupre, M. B. Pongratz, G. Haerendel, A. Valenzuela, D. A. Gurnett and R. R. Anderson, Observations and theory of the AMPTE magnetotail barium releases, *J. Geophys. Res., 92*, 5777-5794, 1987.

Bhattacharyya, A., S. J. Franke and K. C. Yeh, Characteristic velocity of equatorial *F* region irregularities determined from spaced receiver scintillation data, *J. Geophys. Res., 94*, 11,959-11,969, 1989.

Biondi, M. A., J. W. Meriwether, Jr., B. Fejer and R. Woodman, Measurements of the dynamics and coupling of the equatorial thermosphere and the *F*-region ionosphere in Peru, *J. Atmos. Terr. Phys., 50*, 937-942, 1988.

Boehm, M. H., C. W. Carlson, J. P. McFadden, J. H. Clemmons and F. S. Mozer, High-resolution sounding rocket observations of large-amplitude alfven waves, *J. Geophys. Res., 95*, 12,157-12,171, 1990.

Booker, H. G., and J. W. Tao, A scintillation theory of the fading of HF waves returned from the F-region: receiver near transmitter, *J. Atmos. Terr. Phys., 49*, 915-938, 1987.

Brace, L. H., C. R. Chappell, M. O. Chandler, R. H. Comfort, J. L. Horwitz and W. R. Hoegy, *F* region electron temperature signatures of the plasmapause based on dynamics explorer 1 and 2 measurements, *J. Geophys. Res., 93*, 1896-1908, 1988.

Bruning, K., L. P. Block, G. T. Marklund, L. Eliasson, R. Pottelette, J. S. Murphree, T. A. Potemra and S. Perraut, Viking observations above a postnoon aurora, *J. Geophys. Res., 95*, 6039-6049, 1990.

Buonsanto, M. J., A study of the daytime *E* - F1 region ionosphere at mid-latitudes, *J. Geophys. Res., 95*, 7735-7747, 1990.

Buonsanto, M. J., Comparison of incoherent scatter observations of electron density, and electron and ion

temperature at Millstone Hill with the International Reference Ionosphere, *J. Atmos. Terr. Phys., 51*, 441-468, 1989.

Buonsanto, M. J., Observed and calculated *F2* peak heights and derived meridional winds at mid-latitudes over a full solar cycle, *J. Atmos. Terr. Phys., 52*, 223-240, 1990.

Burch, J. L., Energetic particles and currents: Results from dynamics explorer, *Rev. Geophys., 26*, 215-228, 1988.

Burgess, W. C., and U. S. Inan, Simultaneous disturbance of conjugate ionospheric regions in association with individual lightning flashes, *Geophys. Res. Lett., 17*, 259-262, 1990.

Burns, A. G., T. L. Killeen, G. Crowley, B. A. Emery and R. G. Roble, On the mechanisms responsible for high-latitude thermospheric composition variations during the recovery phase of a geomagnetic storm, *J. Geophys. Res., 94*, 16,961-16,968, 1989.

Burnside, R. G., J. C. G. Walker and M. P. Sulzer, Kinematic properties of the *F* region ion velocity field inferred from incoherent scatter radar measurements at arecibo, *J. Geophys. Res., 92*, 3345-3355, 1987.

Burnside, R. G., M. P. Sulzer and J. C. G. Walker, Determination of thermospheric temperatures and neutral densities at arecibo from the ion energy balance, *J. Geophys. Res., 93*, 8642-8650, 1988.

Cai, D., T. Neubert, L. R. O. Storey, P. M. Banks, S. Sasaki, K. Abe and J. L. Burch, ELF oscillations associated with electron beam injections from the space shuttle, *J. Geophys. Res., 92*, 12,451-12,457, 1987.

Calvert, W., and K. Hashimoto, The magnetoionic modes and propagation properties of auroral radio emissions, *J. Geophys. Res., 95*, 3943-3957, 1990.

Campbell, W. H., and E. R. Schiffmacher, Quiet ionospheric currents of the southern hemisphere derived from geomagnetic records, *J. Geophys. Res., 93*, 933-944, 1988.

Candidi, M., and C.-I. Meng, Low-altitude observations of the conjugate polar cusps, *J. Geophys. Res., 93*, 923-931, 1988.

Cannata, R. W., and T. I. Gombosi, Modeling the solar cycle dependence of quiet-time ion upwelling at high geomagnetic latitudes, *Geophys. Res. Lett., 16*, 1141-1144, 1989.

Carbary, J. F., and C.-I. Meng, Correlation of cusp width with AE(12) and B_z, *Planet. Space Sci., 36*, 157-161, 1988.

Carlson, H. C., R. A. Heelis, E. J. Weber and J. R. Sharber, Coherent mesoscale convection patterns during northward interplanetary magnetic field, *J. Geophys. Res., 93*, 14,501-14,514, 1988.

Carpenter, D. L., and R. E. Orville, The excitation of active whistler mode signal paths in the magnetosphere by lightning: Two case studies, *J. Geophys. Res., 94*, 8886-8894, 1989.

Carpenter, D. L., and U. S. Inan, Seasonal, latitudinal and diurnal distributions of whistler-induced electron precipitation events, *J. Geophys. Res., 92*, 3429-3435, 1987.

Carpenter, D. L., T. F. Bell and A. J. Smith, The Siple VLF transmitter as a multi-frequency probe of the earth-ionosphere waveguide, *J. Atmos. Terr. Phys., 50*, 105-115, 1988.

Chandler, M. O., J. J. Ponthieu, T. E. Cravens, A. F. Nagy and P. G. Richards, Model calculations of minor ion populations in the plasmasphere, *J. Geophys. Res., 92*, 5885-5895, 1987.

Chappell, C. R., T. E. Moore and J. H. Waite, Jr., The ionosphere as a fully adequate source of plasma for the earth's magnetosphere, *J. Geophys. Res., 92*, 5896-5910, 1987.

Chaturvedi, P. K., J. D. Huba, S. L. Ossakow, P. Satyanarayana and J. A. Fedder, Parallel current effects on two-stream electrojet plasma instabilities, *J. Geophys. Res., 92*, 8700-8706, 1987.

Chaturvedi, P. K., M. J. Keskinen and S. L. Ossakow, Production and control of ion-cyclotron instabilities in the high latitude ionosphere by high power radio waves, *J. Atmos. Terr. Phys., 49*, 57-62, 1987.

Chaturvedi, P. K., and J. D. Huba, The interchange instability in high-latitude plasma blobs, *J. Geophys. Res., 92*, 3357-3366, 1987.

Chen, M. W., W. K. Peterson, M. Ashour-Abdalla, T. E. Moore and A. M. Persoon, Plasma characteristics of upflowing ion beams in the polar cap region, *J. Geophys. Res., 95*, 3907-3924, 1990.

Cheng, A. F., Transverse deflection and dissipation of small plasma beams and clouds in magnetized media, *J. Geophys. Res., 92*, 55-63, 1987.

Cheng, Q. C., J. R. Kan and S.-I Akasofu, Dependence of the region II field-aligned currents on ionospheric conductivity gradients, *Planet. Space Sci., 35*, 1405-1418, 1987.

Chiu, Y. T., Formation of polar cap arcs, *Geophys. Res. Lett., 16*, 743-746, 1989.

Chiu, Y. T., J. B. Cladis and W. E. Francis, Simulation of ion heating in the topside auroral ionosphere, *Geophys. Res. Lett., 15*, 1534-1537, 1988.

Cole, K. D., Electric currents in *E*-like planetary ionospheres, *Planet. Space Sci., 38*, 1061-1068, 1990.

Coley, W. R., and R. A. Heelis, Low-latitude zonal and vertical ion drifts seen by DE 2, *J. Geophys. Res., 94*, 6751-6761, 1989.

Collin, H. L., W. K. Peterson and E. G. Shelley, Solar cycle variation of some mass dependent characteristics of upflowing beams of terrestrial ions, *J. Geophys. Res., 92*, 4757-4762, 1987.

Collin, H. L., W. K. Peterson, J. F. Drake and A. W. Yau, The helium components of energetic terrestrial ion upflows: Their occurrence, morphology, and intensity, *J. Geophys. Res., 93*, 7558-7564, 1988.

Cornwall, J. M., Exact solutions and low-frequency instability of the adiabatic auroral arc model, *J. Geophys. Res., 93*, 11,429-11,435, 1988.

Crew, G. B., T. Chang, J. M. Retterer, W. K. Peterson, D. A. Gurnett and R. L. Huff, Ion cyclotron resonance heated conics: Theory and observations, *J. Geophys. Res., 95*, 3959-3985, 1990.

Crooker, N. U., Flux transfer event footprint patterns and implications for convection, *J. Geophys. Res., 95*, 10,567-10,573, 1990.

Crooker, N. U., Mapping the merging potential from the magnetopause to the ionosphere through the dayside cusp, *J. Geophys. Res., 93*, 7338-7344, 1988.

Crooker, N. U., and G. L. Siscoe, On mapping flux transfer events to the ionosphere, *J. Geophys. Res., 95*, 3795-3799, 1990.

Crowley, G., W. J. Hughes, and T. B. Jones, Observational evidence of cavity modes in the earth's magnetosphere, *J. Geophys. Res., 92*, 12,233-12,240, 1987.

Datlowe, D. W., and W. L. Imhof, Cyclotron resonance precipitation of energetic electrons from the inner magnetosphere, *J. Geophys. Res., 95*, 6477-6491, 1990.

De Groot, J. S., and K. Mizuno, The effect of the ion acoustic decay instability on microwave-plasma interactions, *J. Geophys. Res., 94*, 1537-1540, 1989.

Delcourt, D. C., C. R. Chappell, T. E. Moore, and J. H. Waite, Jr., A three-dimensional numerical model of ionospheric plasma in the magnetosphere, *J. Geophys. Res., 94*, 11,893-11,920, 1989b.

Delcourt, D. C., T. E. Moore, J. H. Waite, Jr., and C. R. Chappell, Polar wind ion bands after neutral sheet acceleration, *J. Geophys. Res., 94*, 3773-3778, 1989a.

Demars, H. G., and R. W. Schunk, Comparison of solutions to bi-maxwellian and maxwellian transport equations for subsonic flows, *J. Geophys. Res., 92*, 5969-5990, 1987.

Demars, H. G., and R. W. Schunk, Temperature anisotropies in the terrestrial ionosphere and plasmasphere, *Rev. Geophys., 25*, 1659-1679, 1987.

Demars, H. G., and R. W. Schunk, Solutions to bi- maxwellian transport equations for the polar wind, *Planet. Space Sci., 37*, 85-96, 1989.

Djuth, F. T., B. Thide, H. M. Ierkic, and M. P. Sulzer, Large F-region electron-temperature enhancements generated by high-power HF radio waves, *Geophys. Res. Lett., 14*, 953-956, 1987b.

Djuth, F. T., and C. A. Gonzales, Temporal evolution of the HF-enhanced plasma line in sporadic *E*, *J. Geophys. Res., 93*, 196-208, 1988.

Djuth, F. T., R. J. Jost, H. M. Ierkic, M. P. Sulzer, and S. T. Noble, Observations of HF-enhanced ion waves in the ionosphere, *Geophys. Res. Lett., 14*, 194-197, 1987a.

Earle, G. D., M. C. Kelley, and G. Ganguli, Large velocity shears and associated electrostatic waves and turbulence in the auroral F region, *J. Geophys. Res., 94*, 15,321-15,333, 1989.

Earle, G. D., and M. C. Kelley, Spectral studies of the sources of ionospheric electric fields, *J. Geophys. Res., 92*, 213-224, 1987.

Eccles, J. V., W. J. Raitt, and P. M. Banks, A numerical model of the electrodynamics of plasma within the contaminant gas cloud of the space shuttle orbiter at low earth orbit, *J. Geophys. Res., 94*, 9049-9063, 1989.

Elgin, J. B., D. C. Cooke, M. F. Tautz, and E. Murad, Modeling of atmospherically induced gas phase optical contamination from orbiting spacecraft, *J. Geophys. Res., 95*, 12,197-12,208, 1990.

Engebretson, M. J., B. J. Anderson, L. J. Cahill, Jr., R. L. Arnoldy, T. J. Rosenberg, D. L. Carpenter, W. B. Gail, and R. H. Eather, Ionospheric signatures of cusp latitude Pc 3 pulsations, *J. Geophys. Res., 95*, 2447-2456, 1990.

Erlandson, R. E., L. J. Cahill, Jr., R. L. Kauffman, C. J. Pollock, and R. L. Arnoldy, ARCS 3 ionospheric artificial argon ion beam injections: waves near the heavy ion gyrofrequencies, *J. Geophys. Res., 94*, 2645-2653, 1989.

Evans, D. S., G. T. Davidson, H. D. Voss, W. L. Imhof, J. Mobilia, and Y. T. Chiu, Interpretation of electron spectra in morningside pulsating aurorae, *J. Geophys. Res., 92*, 12,295-12,306, 1987.

Farley, D., and J. Providakes, The variation with T_e and T_i of the velocity of unstable ionospheric two-stream waves, *J. Geophys. Res., 94*, 15,415-15,420, 1989.

Farrell, W. M., D. A. Gurnett, P. M. Banks, R. I. Bush, and W. J. Raitt, An analysis of whistler mode radiation from the spacelab 2 electron beam, *J. Geophys. Res., 93*, 153-161, 1988.

Farrell, W. M., D. A. Gurnett, and C. K. Goertz, Coherent Cerenkov radiation from the spacelab 2 electron beam, *J. Geophys. Res., 94*, 443-452, 1989.

Fejer, B. G., E. R. de Paula, I. S. Batista, E. Bonelli, and R. F. Woodman, Equatorial *F* region vertical plasma drifts during solar maxima, *J. Geophys. Res., 94*, 12,049-12,054, 1989.

Fejer, B. G., M. C. Kelley, C. Senior, O. de la Beaujardiere, J. A. Holt, C. A. Tepley, R. Burnside, M. A. Abdu, J. H. A. Sobral, R. F. Woodman, Y. Kamide, and R. Lepping, Low- and mid-latitude ionospheric electric fields during the January 1984 GISMOS campaign, *J. Geophys. Res., 95*, 2367-2377, 1990.

Fejer, J. A., F. T. Djuth, H. M. Ierkic, and M. P. Sulzer, Simultaneous observations of the enhanced plasma line and the reflected HF wave at Arecibo, *J. Atmos. Terr. Phys., 51*, 721-725, 1989.

Fejer, J. A., and M. P. Sulzer, Observation of suprathermal electron fluxes during ionospheric modification experiments, *J. Geophys. Res., 92*, 3441-3444, 1987.

Fesen, C. G., G. Crowley, and R. G. Roble, Ionospheric effects at low latitudes during the March 22, 1979 geomagnetic storm, *J. Geophys. Res., 94*, 5405-5417, 1989.

Fesen, C. G., and V. J. Abreu, Modeling the 6300-Å low-latitude nightglow, *J. Geophys. Res., 92*, 1231-1239, 1987.

Fontheim, E. G., L. H. Brace, and J. D. Winningham, Properties of low-energy electron precipitation in the cleft during periods of unusually high ambient electron temperatures, *J. Geophys. Res., 92*, 12,267-12,273, 1987.

Forbes, J. M., M. Codrescu, and T. J. Hall, On the utilization of ionosonde data to analyze the latitudinal penetration of ionospheric storm effects, *Geophys. Res. Lett., 15*, 249-252, 1988.

Forbes, J. M., and M. Harel, Magnetosphere-thermosphere coupling: An experiment in interactive modeling, *J. Geophys. Res., 94*, 2631-2644, 1989.

Forbes, J. M., and R. G. Roble, Thermosphere-ionosphere coupling: An experiment in interactive modeling, *J. Geophys. Res., 95*, 201-208, 1990.

Foster, J. C., Reply to Kamide and Richmond, *Geophys. Res. Lett., 14*, 160-161, 1987.

Foster, J. C., C. del Pozo, K. Groves, and J.-P. St. Maurice, Radar observations of the onset of current driven instabilities in the topside ionosphere, *Geophys. Res. Lett., 15*, 160-163, 1988.

Foster, J. C., and J. Aarons, Enhanced anti-sunward convection and *F* region scintillations at mid-latitude during storm onset, *J. Geopys. Res., 93*, 11,537-11,542, 1988.

Foster, J. C., T. Fuller-Rowell, and D. S. Evans, Quantitative patterns of large-scale field-aligned currents in the auroral ionosphere, *J. Geophys. Res., 94*, 2555-2564, 1989.

Frank, L. A., W. R. Paterson, M. Ashour-Abdalla, D. Schriver, W. S. Kurth, D. A. Gurnett, N. Omidi, P. M. Banks, R. I. Bush, and W. J. Raitt, Electron velocity distributions and plasma waves associated with the injection of an electron beam into the ionosphere, *J. Geophys. Res., 94*, 6995-7001, 1989.

Franke, S. J., and C. H. Liu, Analysis of a long period fading component in saturated VHF amplitude scintillation observed at Ascension Island, *J. Atmos. Terr. Phys., 49*, 421-431, 1987.

Fraser-Smith, A. C., Centered and eccentric geomagnetic dipoles and their poles, 1600-1985, *Rev. Geophys., 25*, 1-16, 1987.

Friis-Christensen, E., M. A. McHenry, C. R. Clauer, and S. Vennerstrom, Ionospheric traveling convection vortices observed near the polar cleft: A triggered response to sudden changes in the solar wind, *Geophys. Res. Lett., 15*, 253-256, 1988.

Fujita, S., Duct propagation of hydromagnetic waves in the upper ionosphere. 2. Dispersion characteristics and loss mechanism, *J. Geophys. Res., 93*, 14,674-14,682, 1988.

Fujita, S., and T. Tamao, Duct propagation of hydromagnetic waves in the upper ionosphere. 1. Electromagnetic field disturbances in high latitudes associated with localized incidence of a shear Alfven wave, *J. Geophys. Res., 93*, 14,665-14,673, 1988.

Fukao, S., J. P. McClure, A. Ito, T. Sato, I. Kimura, T. Tsuda, and S. Kato, First VHF radar observation of midlatitude *F*-region field-aligned irregularities, *Geophys. Res. Lett., 15*, 768-771, 1988.

Fuller-Rowell, T. J., and D. S. Evans, Height-integrated Pedersen and Hall conductivity patterns inferred from the TIROS-NOAA satellite data, *J. Geophys. Res., 92*, 7606-7618, 1987.

Fuselier, S. A., D. M. Klumpar, W. K. Peterson, and E. G. Shelley, Direct injection of ionospheric O^+ into the dayside low latitude boundary layer, *Geophys. Res. Lett., 16*, 1121-1124, 1989.

Gail, W. B., and U. S. Inan, Characteristics of wave-particle

interactions during sudden commencements. 2. Spacecraft observations, *J. Geophys. Res., 95*, 139-147, 1990.

Gail, W. B., U. S. Inan, R. A. Helliwell, D. L. Carpenter, S. Krishnaswamy, T. J. Rosenberg, and L. J. Lanzerotti, Characteristics of wave-particle interactions during sudden commencements. 1. Ground-based observations, *J. Geophys. Res., 95*, 119-137, 1990.

Ganguli, G., and P. J. Palmadesso, Electrostatic ion instabilities in the presence of parallel currents and transverse electric fields, *Geophys. Res. Lett., 15*, 103-106, 1988.

Ganguli, S. B., H. G. Mitchell, Jr., and P. J. Palmadesso, Behavior of ionized plasma in the high latitude topside ionosphere: The polar wind, *Planet. Space Sci., 35*, 703-713, 1987.

Ganguli, G., Y. C. Lee, P. J. Palmadesso, and S. L. Ossakow, D.C. electric field stabilization of plasma fluctuations due to a velocity shear in the parallel ion flow, *Geophys. Res. Lett., 16*, 735-738, 1989.

Ganguly, S., and D. Coco, Incoherent scattering from the collision dominated *D*-region. Comparison of theories with experimental data, *J. Atmos. Terr. Phys., 49*, 549-563, 1987.

Ganguly, S., R. A. Behnke, and B. A. Emery, Average electric field behavior in the ionosphere above arecibo, *J. Geophys. Res., 92*, 1199-1210, 1987.

Gilchrist, B. E., P. M. Banks, T. Neubert, P. R. Williamson, N. B. Myers, W. J. Raitt, and S. Sasaki, Electron collection enhancement arising from neutral gas jets on a charged vehicle in the ionosphere, *J. Geophys. Res., 95*, 2469-2475, 1990.

Gledhill, J. A., I. S. Dore, C. K. Goertz, R. Haggard, W. J. Hughes, M. W. J. Scourfield, D. P. Smits, P. H. Stoker, P. R. Sutcliffe, P. A. Wakerley, and A. D. M. Walker, A magnetospheric substorm observed at Sanae, Antarctica, *J. Geophys. Res., 92*, 2461-2475, 1987.

Goerke, R. T., P. J. Kellogg, and S. J. Monson, An analysis of whistler mode radiation from a 100 mA electron beam, *J. Geophys. Res., 95*, 4277-4283, 1990.

Gombosi, T. I., and A. F. Nagy, Time-dependent modeling of field-aligned current-generated ion transients in the polar wind, *J. Geophys. Res., 94*, 359-369, 1989.

Gombosi, T. I., and T. L. Killeen, Effects of thermospheric motions on the polar wind: A time-dependent numerical study, *J. Geophys. Res., 92*, 4725-4729, 1987.

Gombosi, T. I., and R. W. Schunk, A comparative study of plasma expansion events in the polar wind, *Planet. Space Sci., 36*, 753-764, 1988.

Gorney, D. J., Solar cycle effects on the near-earth space environment, *Rev. Geophys., 28*, 315-336, 1990.

Grebowsky, J. M., H. A. Taylor, Jr., M. W. Pharo, III, and N. Reese, Thermal ion perturbations observed in the vicinity of the space shuttle, *Planet. Space Sci., 35*, 501-513, 1987a.

Grebowksy, J. M., H. A. Taylor, Jr., M. W. Pharo, III, and N. Reese, Thermal ion complexities observed within the spacelab 2 bay, *Planet. Space Sci., 35*, 1463-1469, 1987b.

Grebowsky, J. M., and N. Reese, Another look at equatorial metallic ions in the *F* region, *J. Geophys. Res., 94*, 5427-5440, 1989.

Grebowksy, J. M., W. R. Hoegy, and T. C. Chen, Solar maximum-minimum extremes in the summer noontime polar cap *F* region ion composition: The measurements, *J. Geophys. Res., 95*, 12,269-12,276, 1990.

Greenspan, M. E., Origins of enhanced field-aligned current at the edge of an auroral arc, *J. Geophys. Res., 94*, 12,037-12,042, 1989.

Greenwald, R. A., K. B. Baker, J. M. Ruohoniemi, J. R. Dudeney, M. Pinnock, N. Mattin, and J. M. Leonard, Simultaneous conjugate observations of dynamic variations in high-latitude dayside convection due to changes in IMF *By*, *J. Geophys. Res., 95*, 8057-8072, 1990.

Groves, K. M., M. C. Lee, and S. P. Kuo, Spectral broadening of VLF radio signals traversing the ionosphere, *J. Geophys. Res., 93*, 14,683-14,687, 1988.

Hagan, M. E., Effects of geomagnetic activity in the winter thermosphere. 2. Magnetically disturbed conditions, *J. Geophys. Res., 93*, 9937-9944, 1988.

Hairston, M. R., and R. A. Heelis, Model of the high-latitude ionospheric convection pattern during southward interplanetary magnetic field using DE 2 data, *J. Geophys. Res., 95*, 2333-2343, 1990.

Hajkowicz, L. A., and R. D. Hunsucker, A simultaneous observation of large-scale periodic tids in both hemispheres following an onset of auroral disturbances, *Planet. Space Sci., 35*, 785-791, 1987.

Hallinan, T. J., J. Winckler, P. Malcolm, H. C. Stenbaek-Nielsen, and J. Baldridge, Conjugate echoes of artificially injected electron beams detected optically by means of new image processing, *J. Geophys. Res., 95*, 6519-6532, 1990.

Hansen, J. D., G. J. Morales, and J. E. Maggs, Daytime saturation of thermal cavitons, *J. Geophys. Res., 94*, 6833-6840, 1989.

Hansen, P. J., and J. R. Henley, Evolution of *F* region barium releases: Phenomenological effects of background turbulence, *J. Geophys. Res., 93*, 957-962, 1988.

Hardy, D. A., M. S. Gussenhoven, and D. Brautigam, A statistical model of auroral ion precipitation, *J. Geophys. Res., 94*, 370-392, 1989.

Hardy, D. A., M. S. Gussenhoven, R. Raistrick and W. J. McNeil, Statistical and functional representations of the pattern of auroral energy flux, number flux, and conductivity, *J. Geophys. Res., 92*, 12,275-12,294, 1987.

Harker, K. J., and P. M. Banks, Near fields in the vicinity of pulsed electron beams in space, *Planet. Space Sci., 35*, 11-19, 1987.

Hastings, D. E., and J. Blandino, Bounds on current collection from the far field by plasma clouds in the ionosphere, *J. Geophys. Res., 94*, 2737-2744, 1989.

Heelis, R. A., Electrodynamics and plasma processes in the ionosphere, *Rev. Geophys., 25*, 419-431, 1987.

Heelis, R. A., Studies of ionospheric plasma and electrodynamics and their application to ionosphere-magnetosphere coupling, *Rev. Geophys., 26*, 317-328, 1988.

Heelis, R. A., W. B. Hanson, and G. J. Bailey, Distributions of He^+ at middle and equatorial latitudes during solar maximum, *J. Geophys. Res., 95*, 10,313-10,320, 1990.

Heelis, R. A., and J. F. Vickrey, Magnetic field-aligned coupling effects on ionospheric plasma structure, *J. Geophys. Res., 95*, 7995-8008, 1990.

Heelis, R. A., and W. R. Coley, Global and local joule heating effects seen by DE 2, *J. Geophys. Res., 93*, 7551-7557, 1988.

Heppner, J. P., B. G. Ledley, M. L. Miller, P. A.Marionni, M. B. Pongratz, D. W. Slater, T. J. Hallinan, and D. Rees, Search for auroral belt *E*// fields with high-velocity barium ion injections, *J. Geophys. Res., 94*, 393-425, 1989.

Heppner, J. P., and N. C. Maynard, Empirical high-latitude electric field models, *J. Geophys. Res., 92*, 4467-4489, 1987.

Hoegy, W. R., and R. F. Benson, DE/ISIS conjunction comparisons of high-latitude electron density features, *J. Geophys. Res., 93*, 5947-5954, 1988.

Hoffman, R. A., The magnetosphere, ionosphere, and atmosphere as a system: Dynamics explorer 5 years later, *Rev. Geophys., 26*, 209-214, 1988.

Hoffman, R. A., M. Sugiura, N. C. Maynard, R. M. Candey, J. D. Craven, and L. A. Frank, Electrodynamic patterns in the polar region during periods of extreme magnetic quiescence, *J. Geophys. Res., 93*, 14,515 14,541, 1988.

Hollweg, J. V., Resonance absorption of propagating fast waves in a cold plasma, *Planet. Space Sci., 38*, 1017-1030, 1990.

Holt, J. M., R. H. Wand, J. V. Evans, and W. L. Oliver, Empirical models for the plasma convection at high latitudes from Millstone Hill observations, *J. Geophys. Res., 92*, 203-212, 1987.

Hones, E. W. Jr., J. D. Craven, L. A. Frank, D. S. Evans, and P. T. Newell, The horse-collar aurora: A frequent pattern of the aurora in quiet times, *Geophys. Res. Lett., 16*, 37-40, 1989.

Horwitz, J. L., Parabolic heavy ion flow in the polar magnetosphere, *J. Geophys. Res., 92*, 175-185, 1987.

Horwitz, J. L., R. H. Comfort, and C. R. Chappell, A statistical characterization of plasmasphere density structure and boundary locations, *J. Geophys. Res., 95*, 7937-7947, 1990.

Horwitz, J. L., R. H. Comfort, P. G. Richards, M. O. Chandler, C. R. Chappell, P. Anderson, W. B. Hanson, and L. H. Brace, Plasmasphere-ionosphere coupling. 2. Ion composition measurements at plasmaspheric and ionospheric altitudes and comparison with modeling results, *J. Geophys. Res., 95*, 7949-7959, 1990.

Hudson, M. K., and I. Roth, Simulations of active ion injection experiments on ARCS 3, *J. Geophys. Res., 93*, 8768-8772, 1988.

Hultqvist, B., R. Lundin, K. Stasiewicz, L. Block, P.-A. Lindqvist, G. Gustafsson, H. Koskinen, A. Bahnsen, T. A. Potemra, and L. J. Zanetti, Simultaneous observation of upward moving field-aligned energetic electrons and ions on auroral zone field lines, *J. Geophys. Res., 93*, 9765-9776, 1988.

Hunsucker, R. D., and J. K. Hargreaves, A study of gravity waves in ionospheric electron content at L = 4, *J. Atmos. Terr. Phys., 50*, 167-172, 1988.

Hunton, D. E., A. A. Viggiano, W. Swider, J. F. Paulson, and C. Sherman, Mass spectrometric measurements of SF6 chemical releases from sounding rockets, *J. Geophys. Res., 92*, 8827-8830, 1987.

Inan, U. S., VLF heating of the lower ionosphere, *Geophys. Res. Lett., 17*, 729-732, 1990.

Inan, U. S., Waves and instabilities, *Rev. Geophys., 25*, 588-598, 1987.

Inan, U. S., M. Walt, H. D. Voss, and W. L. Imhof, Energy spectra and pitch angle distributions of lightning-induced electron precipitation: Analysis of an event observed on the S81-1(SEEP) Satellite, *J. Geophys. Res., 94*, 1379-1401, 1989.

Inan, U. S., D. C. Shafer, W. Y. Yip, and R. E. Orville, Subionospheric VLF signatures of nighttime D region perturbations in the vicinity of lightning discharges, *J. Geophys. Res., 93*, 11,455-11,472, 1988.

Inan, U. S., and D. L. Carpenter, Lightning-induced electron precipitation events observed at $L \sim 2.4$ as phase and amplitude perturbations on subionospheric VLF signals, *J. Geophys. Res., 92*, 3293-3303, 1987.

Imhof, W. L., H. D. Voss, D. W. Datlowe, and J. Mobilia, Isolated electron precipitation regions at high latitudes, *J. Geophys. Res., 93*, 2649-2660, 1988.

Isham, B., W. Birkmayer, T. Hagfors, and W. Kofman, Observations of small-scale plasma density depletions in arecibo HF heating experiments, *J. Geophys. Res., 92*, 4629-4637, 1987.

Jacobson, A. R., D. J. Simons, and G. Nalesso, A model of ionospheric image structure underneath a braking, cross-field plasma jet, *J. Atmos. Terr. Phys., 49*, 599-605, 1987.

Jacobson, A. R., and R. C. Carlos, Coherent-array HF Doppler sounding of traveling ionospheric disturbances: I. Basic technique, *J. Atmos. Terr. Phys., 51*, 297-309, 1989a.

Jacobson, A. R., and R. C. Carlos, Coherent-array HF Doppler sounding of traveling ionospheric disturbances: II. Assessment of errors, *J. Atmos. Terr. Phys., 51*, 879-895, 1989b.

James, H. G., U. S. Inan, and M. T. Rietveld, Observations on the DE 1 spacecraft of ELF/VLF waves generated by an ionospheric heater, *J. Geophys. Res., 95*, 12,187-12,195, 1990.

Jarvis, M. J., A. J. Smith, F. T. Berkey, and D. L.Carpenter, Wave-induced burst precipitation events detected with a digital ionosonde, *Geophys. Res. Lett., 17*, 61-64, 1990.

Johnson, J. R., T. Chang, G. B. Crew, and M. Andre, Equatorially generated ULF waves as a source for the turbulence associated with ion conics, *Geophys. Res. Lett., 16*, 1469-1472, 1989.

Johnson, R. M., and J. G. Luhmann, Cross correlation of high-latitude upper mesospheric neutral winds with AE and Kp, *J. Geophys. Res., 93*, 8625-8632, 1988.

Jones, A. V., R. L. Gattinger, P. Shih, J. W. Meriwether, V. B. Wickwar, and J. Kelly, Optical and radar characterization of a short-lived auroral event at high latitude, *J. Geophys. Res., 92*, 4575-4589, 1987.

Kamide, Y., and A. D. Richmond, Comment on 'ionospheric convection associated with discrete levels of particle precipitation', *Geophys. Res. Lett., 14*, 158-159, 1987.

Kamide, Y., Y. Ishihara, T. L. Killeen, J. D. Craven, L. A. Frank, and R. A. Heelis, Combining electric field and aurora observations from DE 1 and 2 with ground magnetometer records to estimate ionospheric electromagnetic quantities, *J. Geophys. Res., 94*, 6723-6738, 1989.

Kan, J. R., Generation of field-aligned currents in magnetosphere-ionosphere coupling in a MHD plasma, *Planet. Space Sci., 35*, 903-912, 1987.

Kan, J. R., A theory of patchy and intermittent reconnections for magnetospheric flux transfer events, *J. Geophys. Res., 93*, 5613-5623, 1988.

Kan, J. R., and F. Cao, Effect of field-aligned potential drop in a global magnetosphere-ionosphere coupling model, *J. Geophys. Res., 93*, 7571-7577, 1988.

Kan, J. R., L. Zhu, and S.-I Akasofu, A theory of substorms: Onset and subsidence, *J. Geophys. Res., 93*, 5624-5640, 1988.

Katz, I., G. A. Jongeward, V. A. Davis, M. J. Mandell, R. A. Kuharski, J. R. Lilley, Jr., W. J. Raitt, D. L. Cooke, R. B. Torbert, G. Larson, and D. Rau, Structure of the bipolar plasma sheath generated by SPEAR 1, *J. Geophys. Res., 94*, 1450-1458, 1989.

Kaufmann, R. L., and D. J. Larson, Electric field mapping and auroral Birkeland currents, *J. Geophys. Res., 94*, 15,307-15,319, 1989.

Kaufmann, R. L., D. N. Walker, J. C. Holmes, C. J. Pollock, R. L. Arnoldy, L. J. Cahill, Jr., and P. M. Kintner, Heavy ion beam-ionosphere interactions: Charging and neutralizing the payload, *J. Geophys. Res., 94*, 453-471, 1989.

Kelley, M. C., C. E. Seyler, and S. Zargham, Collisional interchange instability 2. A comparison of the numerical simulations with the in situ experimental data, *J. Geophys. Res., 92*, 10,089-10,094, 1987.

Kelley, M. C., D. T. Farley, and J. Rottger, The effect of cluster ions on anomalous VHF backscatter from the summer polar mesosphere, *Geophys. Res. Lett., 14*, 1031-1034, 1987.

Kellogg, P. J., S. J. Monson, and B. A. Whalen,Observation of an antenna-plasma instability, *J. Geophys. Res., 95*, 7773-7788, 1990.

Keskinen, M. J., H. G. Mitchell, J. A. Fedder, P. Satyanarayana, S. T. Zalesak, and J. D. Huba, Nonlinear evolution of the Kelvin-Helmholtz instability in the high-latitude ionosphere, *J. Geophys. Res., 93*, 137-152, 1988.

Killeen, T. L., Energetics and dynamics of the earth's

thermosphere, *Rev. Geophys., 25*, 433-454, 1987.

Killeen, T. L., J. D. Craven, L. A. Frank, J.-J. Ponthieu, N. W. Spencer, R. A. Heelis, L. H. Brace, R. G. Roble, P. B. Hays, and G. R. Carignan, On the relationship between dynamics of the polar thermosphere and morphology of the aurora: Global-scale observations from dynamics explorers 1 and 2, *J. Geophys. Res., 93*, 2675-2692, 1988.

Kivelson, M. G., and D. J. Southwood, Hydromagnetic waves and the ionosphere, *Geophys. Res. Lett., 15*, 1271-1274, 1988.

Klobuchar, J. A., and M. A. Abdu, Equatorial ionospheric irregularities produced by the Brazilian ionospheric modification experiment (BIME), *J. Geophys. Res., 94*, 2721-2726, 1989.

Klobuchar, J. A., and M. C. Lee, Periodic amplitude variations as precursors of plumes of equatorial ionospheric irregularities, *J. Atmos. Terr. Phys., 51*, 733-738, 1989.

Knipp, D. J., A. D. Richmond, G. Crowley, O. de la Beaujardiere, E. Friis-Christensen, D. S. Evans, J. C. Foster, I. W. McCrea, F. J. Rich, and J. A. Waldock, Electrodynamic patterns for September 19, 1984, *J. Geophys. Res., 94*, 16,913-16,923, 1989.

Kondo, T., B. A. Whalen, A. W. Yau, and W. K. Peterson, Statistical analysis of upflowing ion beam and conic distributions at DE 1 altitudes, *J. Geophys. Res., 95*, 12,091-12,102, 1990.

Kozyra, J. U., C. E. Valladares, H. C. Carlson, M. J. Buonsanto, and D. W. Slater, A Theoretical study of the seasonal and solar cycle variations of stable aurora red arcs, *J. Geophys. Res., 95*, 12,219-12,234, 1990.

Kozyra, J. U., E. G. Shelley, R. H. Comfort, L. H. Brace, T. E. Cravens, and A. F. Nagy, The role of ring current O^+ in the formation of stable auroral red arcs, *J. Geophys. Res., 92*, 7487-7502, 1987.

Kudeki, E., and D. T. Farley, Aspect sensitivity of equatorial electrojet irregularities and theoretical implications, *J. Geophys. Res., 94*, 426-434, 1989.

Kudeki, E., B. G. Fejer, D. T. Farley, and C. Hanuise, The condor equatorial electrojet campaign: radar results, *J. Geophys. Res., 92*, 13,561-13,577 1987.

Kuo, S. P., and F. T. Djuth, A thermal instability for the spread-F echoes from HF-heated ionosphere, *Geophys. Res. Lett., 15*, 1345-1348, 1988.

Kuo, S. P., M. C. Lee, and F. T. Djuth, A new interpretation of plasma-line overshoot phenomena, *Geophys. Res. Lett., 14*, 961-964, 1987.

Kuo, S. P., and M. C. Lee, Intensity modulation of HF heater-induced plasma lines, *J. Geophys. Res., 95*, 2463-2464, 1990.

Kuo, S. P., and M. C. Lee, Parametric excitation of whistler waves by HF heater, *J. Atmos. Terr. Phys., 51*, 727-731, 1989.

Kuo, S. P., and M. C. Lee, Thermal filamentation instability driven by the auroral electrojet current, *J. Geophys. Res., 93*, 265-269, 1988.

LaBelle, J., Radio noise of auroral origin: 1968-1988, *J. Atmos. Terr. Phys., 51*, 197-211, 1989.

LaBelle, J., and P. M. Kintner, The measurement of wavelength in space plasmas, *Rev. Geophys., 27*, 495-518, 1989.

LaBelle, J., R. J. Sica, C. Kletzing, G. D. Earle, M. C. Kelley, D. Lummerzheim, R. B. Torbert, K. D. Baker, and G. Berg, Ionization from soft electron precipitation in the auroral *F* region, *J. Geophys. Res., 94*, 3791-3798, 1989.

Lai, S. T., W. J. McNeil, and E. Murad, Amplification of critical velocity ionization by a pulsed neutral beam, *Geophys. Res. Lett., 17*, 737-740, 1990a.

Lai, S. T., E. Murad, and W. J. McNeil, Critical ionization velocity in a mixture of species, *Planet. Space Sci., 38*, 1011-1016, 1990b.

Lai, S. T., and E. Murad, Critical ionization velocity experiments in space, *Planet. Space Sci., 37*, 865-872, 1989.

Lai, S. T., H. A. Cohen, T. L. Aggson, and W. J. McNeil, The effect of photoelectrons on boom-satellite potential differences during electron beam ejection, *J. Geophys. Res., 92*, 12,319-12,325, 1987.

Lai, S., W. F. Denig, E. Murad, and W. J. McNeil, The role of plasma processes in the space shuttle environment, *Planet. Space Sci., 36*, 841-849, 1988.

Lakhina, G. S., M. Mond, and E. Hameiri, Ballooning mode instability at the plasmapause, *J. Geophys. Res., 95*, 4007-4016,1990.

Lee, M. C., S. V. Nghiem, and C. Yoo, Effects of irregularity anisotropy on Faraday polarization fluctuations, *J. Geophys. Res., 94*, 15,421-15,424, 1989.

Liao, C. P., J. P. Friedberg, and M. C. Lee, Explosive spread F caused by lightning-induced electromagnetic effects, *J. Atmos. Terr. Phys., 51*, 751-758, 1989.

Lilensten, J., D. Fontaine, W. Kofman, L. Eliasson, C. Lathuillere, and E. S. Oran, Electron energy budget in the high-latitude ionosphere during Viking/EISCAT coordinated measurements, *J. Geophys. Res., 95*, 6081-6092, 1990.

Lockwood, M., K. Suvanto, J.-P. St. Maurice, K. Kikuchi, B. J. I. Bromage, D. M. Willis, S. R. Crothers, H. Todd, and S. W. H. Cowley, Scattered power from non-thermal, F-region plasma observed by EISCAT---evidence for coherent echoes?, *J. Atmos. Terr. Phys., 50*, 467-485, 1988.

Lockwood, M., and M. F. Smith, Low-altitude signatures of the cusp and flux transfer events, *Geophys. Res. Lett., 16*, 879-882, 1989.

Lockwood, M., M. F. Smith, C. J. Farrugia, and G. L. Siscoe, Ionospheric ion upwelling in the wake of flux transfer events at the dayside magnetopause, *J. Geophys. Res., 93*, 5641-5654, 1988.

Lockwood, M., B. J. I. Bromage, R. B. Horne, J.-P. St. Maurice, D. M. Willis, and S. W. H. Cowley, Non-maxwellian ion velocity distributions observed using EISCAT, *Geophys. Res. Lett., 14*, 111-114, 1987.

Lotko, W., B. U. O. Sonnerup, and R. L. Lysak, Nonsteady boundary layer flow including ionospheric drag and parallel electric fields, *J. Geophys. Res., 92*, 8635-8648, 1987.

Lu, G., P. H. Reiff, M. R. Hairston, R. A. Heelis, and J. L. Karty, Distribution of convection potential around the polar cap boundary as a function of the interplanetary magnetic field, *J. Geophys. Res., 94*, 13,447-13,461, 1989.

Lyons, L. R., O. de la Beaujardiere, G. Rostoker, J. S. Murphree, and E. Friis-Christensen, Analysis of substorm expansion and surge development, *J. Geophys. Res., 95*, 10,575-10,589, 1990.

Lysak, R. L., Theory of auroral zone PiB pulsation spectra, *J. Geophys. Res., 93*, 5942-5946, 1988.

Ma, T.-Z., and R. W. Schunk, A fluid model of high voltage spheres in the ionosphere, *Planet. Space Sci., 37*, 21-47, 1989.

Ma, T.-Z., and R. W. Schunk, A two-dimensional model of plasma expansion in the ionosphere, *Planet. Space Sci.,38*, 723-741, 1990.

Machida, S., and C. K. Goertz, Computer simulation of the Farley-Buneman instability and anomalous electron heating in the auroral ionosphere, *J. Geophys. Res., 93*, 9993-10,000, 1988.

Maggs, J. E., Nonlinear evolution of the auroral electron beam, *J. Geophys. Res., 94*, 3631-3651, 1989.

Mandell, M. J., J. R. Lilley, Jr., I. Katz, T. Neubert, and N. B. Myers, Computer modeling of current collection by the charge-2 mother payload, *Geophys. Res. Lett., 17*, 135-138, 1990.

Marklund, G. T., L. G. Blomberg, T. A. Potemra, J. S. Murphree, F. J. Rich, and K. Stasiewicz, A new method to derive "instantaneous" high-latitude potential distributions from satellite measurements including auroral imager data, *Geophys. Res. Lett., 14*, 439-442, 1987.

Marklund, G. T., L. G. Blomberg, K. Stasiewicz, J. S. Murphree, R. Pottelette, L. J. Zanetti, T. A. Potemra, D. A. Hardy, and F. J. Rich, Snapshots of high-latitude electrodynamics using Viking and DMSP F7 observations, *J. Geophys. Res., 93*, 14,479-14,492, 1988.

Maruyama, T., A diagnostic model for equatorial spread *F*. 1. Model description and application to electric field and neutral wind effects, *J. Geophys. Res., 93*, 14,611-14,622, 1988.

Maynard, N. C., J. J. Sojka, R. W. Schunk, J. P. Heppner, and L. H. Brace, A test of convection models for IMF B_Z north, *Planet. Space Sci., 38*, 1077-1089, 1990.

Maynard, N. C., T. L. Aggson, F. A. Herrero, and M. C. Liebrecht, Average low-latitude meridional electric fields from DE 2 during solar maximum, *J. Geophys. Res., 93*, 4021-4037, 1988.

McFadden, J. P., C. W. Carlson, and M. H. Boehm, Structure of an energetic narrow discrete arc, *J. Geophys. Res., 95*, 6533-6547, 1990.

McHenry, M. A., and C. R. Clauer, Modeled ground magnetic signatures of flux transfer events, *J. Geophys. Res., 92*, 11,231-11,240, 1987.

McNeil, W. J., S. T. Lai, and E. Murad, Interplay between collective and collisional processes in critical velocity ionization, *J. Geophys. Res., 95*, 10,345-10,356, 1990.

Mende, S. B., J. H. Doolittle, R. M. Robinson, R. R. Vondrak, and F. J. Rich, Plasma drifts associated with a system of sun-aligned arcs in the polar cap, *J. Geophys. Res., 93*, 256-264, 1988.

Mendillo, M., J. Baumgardner, and J. Providakes, Ground-based imaging of detached arcs, ripples in the diffuse aurora, and patches of 6300-Å emission, *J. Geophys. Res., 94*, 5367-5381, 1989.

Menietti, J. D., J. L. Burch, and D. L. Gallagher, Statistical study of ion flows in the dayside and nightside plasmasphere, *Planet. Space Sci., 36*, 693-702, 1988.

Miah, M. A., Observation of low energy particle precipitation at low altitude in the equatorial zone, *J.Atmos. Terr. Phys., 51*, 541-549, 1989.

Milikh, G. M., Role of chemical effects in the formation of electron concentration depletions during HF heating of the ionosphere, *J. Atmos. Terr. Phys., 52*, 119-123, 1990.

Min-Yun, Z., E. Nielsen, W. B. Hanson, and T. A. Potemra, Polar convection and Birkeland currents during strongly positive IMF *By*, *J. Geophys. Res., 92*, 3417-3422, 1987.

Mizera, P. F., D. J. Gorney, and D. S. Evans, On the conjugacy of the aurora: High and low latitudes, *Geophys. Res. Lett., 14*, 190-193, 1987.

Morrill, J., and W. Benesch, Plasma preconditioning and the role of elevated vibrational temperature in production of excited *N2* vibrational distributions, *J. Geophys. Res., 95*, 7711-7724, 1990.

Moses, J. J., G. L. Siscoe, R. A. Heelis, and J. D. Winningham, A model for multiple throat structures in the polar cap flow entry region, *J. Geophys. Res., 93*, 9785-9790, 1988.

Moses, J. J., G. L. Siscoe, R. A. Heelis, and J. D. Winningham, Polar cap deflation during magnetospheric substorms, *J. Geophys. Res., 94*, 3785-3789, 1989.

Moses, J. J., G. L. Siscoe, N. U. Crooker, and D. J. Gorney, IMF *By* and day-night conductivity effects in the expanding polar cap convection model, *J. Geophys. Res., 92*, 1193-1198, 1987.

Murphy, G., and I. Katz, The POLAR code wake model: Comparison with in situ observations, *J. Geophys. Res., 94*, 9065-9070, 1989.

Murphy, G. B., D. L. Reasoner, A. Tribble, N. D'Angelo, J. S. Pickett, and W. S. Kurth, The plasma wake of the shuttle orbiter, *J. Geophys. Res., 94*, 6866-6872, 1989.

Myers, N. B., W. J. Raitt, B. E. Gilchrist, P. M. Banks, T. Neubert, P. R. Williamson, and S. Sasaki, A comparison of current-voltage relationships of collectors in the earth's ionosphere with and without electron beam emission *Geophys. Res. Lett., 16*, 365-368, 1989.

Nakada, M. P., Auroral pulsations from ionospheric winds, *J. Geophys. Res., 94*, 15,425-15,429, 1989.

Nakada, M. P., Parallel electric fields from ionospheric winds, *J. Geophys. Res., 92*, 11,248-11,252, 1987.

Nakamura, T., J. R. Kan, and T. Tamao, Closure of field-aligned currents carried by super-alfvenic auroral electrons, *J. Geophys. Res., 94*, 5485-5489, 1989.

Neubert, T., and K. J. Harker, Magnetic fields in the vicinity of pulsed electron beams in space, *Planet. Space Sci., 36*, 469-470, 1988.

Neubert, T., M. J. Mandell, S. Sasaki, B. E. Gilchrist, P. M. Banks, P. R. Williamson, W. J. Raitt, N. B. Meyers, K. I. Oyama, and I. Katz, The sheath structure around a negatively charged rocket payload, *J. Geophys. Res., 95*, 6155-6165, 1990b.

Neubert, T., P. M. Banks, B. E. Gilchrist, A. C. Fraser-Smith, P. R. Williamson, W. J. Raitt, N. B. Myers, and S. Sasaki, The interaction of an artificial electron beam with the earth's upper atmosphere: Effects on spacecraft charging and the near-plasma environment, *J. Geophys. Res., 95*, 12,209-12,217, 1990a.

Neubert, T., T. F. Bell, and L. R. O. Storey, Resonance between coherent whistler mode waves and electrons in the topside ionosphere, *J. Geophys. Res., 92*, 255-265, 1987.

Neubert, T., T. F. Bell, L. R. O. Storey, and D. A. Gurnett, The space shuttle as a platform for observations of ground-based transmitter signals and whistlers, *J. Geophys. Res., 92*, 11,262-11,268, 1987.

Newberry, I. T., R. H. Comfort, P. G. Richards, and C. R. Chappell, Thermal He^+ in the plasmasphere: Comparison of observations with numerical calculations, *J. Geophys. Res., 94*, 15,265-15,276, 1989.

Newell, P. T., and C.-I. Meng, An event of distinct ion polar rain, *Geophys. Res. Lett., 15*, 1165-1168, 1988.

Newman, A. L., H. C. Carlson, Jr., G. P. Mantas, and F. T. Djuth, Thermal response of the F-region ionosphere for conditions of large HF-induced electron-temperature enhancements, *Geophys. Res. Lett., 15*, 311-314, 1988.

Niciejewski, R. J., J. W. Meriwether, Jr., A. V. Jones, R. I. Gattinger, C. E. Valladares, V. B. Wickwar, and J. Kelly, Ground-based observations of $O2^+$ 1N band enhancements relative to $N2^+$ 1N band emission, *Planet. Space Sci., 37*, 131-143, 1989.

Niciejewski, R. J., J. W. Meriwether, Jr., F. G. McCormac, J. H. Hecht, A. B. Christensen, G. G. Sivjee, D. J. Strickland, G. Swenson, S. B. Mende, A. Vallance Jones, R. L. Gattinger, H. C. Carlson, and C. E. Valladares, Coordinated satellite and ground-based measurements of the energy characteristics of a sun-aligned arc over Sondre Stromfjord, *J. Geophys. Res., 94*, 17,201-17,213, 1989.

Nishikawa, K.-I., G. Ganguli, Y. C. Lee, and P. J. Palmadesso, Simulation of electrostatic turbulence due to sheared flows parallel and transverse to the magnetic field, *J. Geophys. Res., 95*, 1029-1038, 1990.

Nishikawa, K.-I, L. A. Frank, and C. Y. Huang, Three-dimensional simulation of whistler mode excited by the spacelab 2 electron beam, *J. Geophys. Res., 94*, 6855-6865, 1989.

Noble, S. T., F. T. Djuth, R. J. Jost, W. E. Gordon, A. Hedberg, B. Thide, H. Derblom, R. Bostrom, E. Nielsen, P. Stubbe, and H. Kopka, Multiple frequency radar observations of high-latitude *E* region irregularities in the HF modified ionosphere, *J. Geophys. Res., 92*, 13,613-

13,627, 1987.
Okano, S., and J. S. Kim, Observations of a SAR-ARC associated with an isolated magnetic substorm, *Planet. Space Sci., 35*, 475-482, 1987.
Okuda, H., and J. Berchem, Injection and propagation of a nonrelativistic electron beam and spacecraft charging, *J. Geophys. Res., 93*, 175-195, 1988.
Okuda, H., and M. Ashour-Abdalla, Ion acoustic instabilities excited by injection of an electron beam in space, *J. Geophys. Res., 93*, 2011-2015, 1988.
Oliver, W. L., Neutral and ion composition changes in the *F* region over Millstone Hill during the equinox transition study, *J. Geophys. Res., 95*, 4129-4134, 1990.
Olsen, R. C., L. E. Weddle, and J. L. Roeder, Plasma wave observations during ion gun experiments, *J. Geophys. Res., 95*, 7759-7771, 1990.
Ono, T., T. Hirasawa, and C.-I Meng, Weak auroral emissions and particle precipitations in the dusk auroral oval, *J. Geophys. Res., 94*, 11,933-11,947, 1989.
Osherovich, V. A., Physical nature of the diffuse plasma resonances in the ionosphere, *J. Geophys. Res., 92*, 316-320, 1987.
Osherovich, V. A., The physical nature of the upper subsidiary diffuse resonances, *J. Geophys. Res., 94*, 5530-5532, 1989.
Pangia, M. J., C. S. Lin, and J. N. Barfield, A correlative study of Pc 5 magnetic pulsations with substorm onsets, *J. Geophys. Res., 95*, 10,699-10,702, 1990.
Parish, J. L., W. F. Denig, and W. J. Raitt, Delay time for the onset of beam plasma discharge, *Planet. Space Sci., 35*, 1123-1126, 1987.
Paterson, W. R., and L. A. Frank, Hot ion plasmas from the cloud of neutral gases surrounding the space shuttle, *J. Geophys. Res., 94*, 3721-3727, 1989.
Person, J. C., D. Resendes, H. Petschek, and D. E. Hastings, Effects of collisional processes on the critical velocity hypothesis, *J. Geophys. Res., 95*, 4039-4055, 1990.
Persoon, A. M., D. A. Gurnett, W. K. Peterson, J. H. Waite, Jr., J. L. Burch, and J. L. Green, Electron density depletions in the nightside auroral zone, *J. Geophys. Res., 93*, 1871-1895, 1988.
Pfaff, R. F., M. C. Kelley, E. Kudeki, B. G. Fejer, and K. D. Baker, Electric field and plasma density measurements in the strongly driven daytime equatorial electrojet. 1. The unstable layer and gradient drift waves, *J. Geophys. Res., 92*, 13,578-13,596, 1987a.
Pfaff, R. F., M. C. Kelley, E. Kudeki, B. G. Fejer, and K. D. Baker, Electric field and plasma density measurements in the strongly driven daytime equatorial electrojet. 2. Two-stream waves, *J. Geophys. Res., 92*, 13,597-13,612, 1987b.
Pickett, J. S., N. D'Angelo, and W. S. Kurth, Plasma density fluctuations observed during space shuttle orbiter water releases, *J. Geophys. Res., 94*, 12,081-12,086, 1989.
Pike, C. P., D. J. Knecht, R. A. Viereck, E. Murad, I. L. Kofsky, M. A. Maris, N. H. Tran, G. Ashley, L. Twist, M. E. Gersh, J. B. Elgin, A. Berk, A. T. Stair, Jr., J. P. Bagian, and J. F. Buchli, Release of liquid water from the space shuttle, *Geophys. Res. Lett., 17*, 139-142, 1990.
Pingree, J. E., and B. G. Fejer, On the height variation of the equatorial *F*-region vertical plasma drifts, *J. Geophys. Res., 92*, 4763-4766, 1987.
Pollock, C. J., R. L. Arnoldy, R. E. Erlandson, and L. J. Cahill, Observations of the plasma environment during an active ionospheric ion beam, *J. Geophys. Res., 93*, 11,473-11,493, 1988.
Porter, H. S., F. Varosi, and H. G. Mayr, Iterative solution of the multistream electron transport equation. I. Comparison with laboratory beam injection experiments, *J. Geophys. Res., 92*, 5933-5959, 1987.
Potemra, T. A., H. Vo, D. Venkatesan, L. L. Cogger, R. E. Erlandson, L. J. Zanetti, P. F. Bythrow, and B. J. Anderson, Periodic auroral forms and geomagnetic field oscillations in the 1400 MLT region, *J. Geophys. Res., 95*, 5835-5844, 1990.
Poulsen, W. L., T. F. Bell, and U. S. Inan, Three-dimensional modeling of subionospheric VLF propagation in the presence of localized *D* region perturbations associated with lightning, *J. Geophys. Res., 95*, 2355-2366, 1990.
Pritchett, P. L., Spatial coherence during pulsed injection of electron beams, *J. Geophys. Res., 95*, 10,671-10,677, 1990.
Pritchett, P. L., H. Karimabadi, and N. Omidi, Generation mechanism of whistler waves produced by electron beam injection in space, *Geophys. Res. Lett., 16*, 883-886, 1989.
Pritchett, P. L., and R. M. Winglee, The plasma environment during particle beam injection into space plasmas. 1. Electron beams, *J. Geophys. Res., 92*, 7673-7688, 1987.
Providakes, J., D. T. Farley, B. G. Fejer, J. Sahr, W. E. Swartz, I. Haggstrom, A. Hedberg, and J. A. Nordling, Observations of auroral *E*-region plasma waves and electron heating with EISCAT and a VHF radar interferometer, *J. Atmos. Terr. Phys., 50*, 339-356, 1988.
Rasmussen, C. E., J. J. Sojka, R. W. Schunk, V. B. Wickwar, O. de la Beaujardiere, J. Foster, and J. Holt, Comparison of simultaneous Chatanika and Millstone Hill temperature measurements with ionospheric model predictions, *J. Geophys. Res., 93*, 1922-1932, 1988.
Rasmussen, C. E., and R. W. Schunk, A three-dimensional time-dependent model of the plasmasphere, *J. Geophys. Res., 95*, 6133-6144, 1990.
Rasmussen, C. E., and R. W. Schunk, Ionospheric convection driven by NBZ currents, *J. Geophys. Res., 92*, 4491-4504, 1987.
Rasmussen, C. E., and R. W. Schunk, Ionospheric convection inferred from interplanetary magnetic field-dependent Birkeland currents, *J. Geophys. Res., 93*, 1909-1921, 1988.
Rasmussen, C. E., and R. W. Schunk, Multistream hydrodynamic modeling of interhemispheric plasma flow, *J. Geophys. Res., 93*, 14,557-14,565, 1988.
Rasmussen, C. E., R. W. Schunk, and V. B. Wickwar, A photochemical equilibrium model for ionospheric conductivity, *J. Geophys. Res., 93*, 9831-9840, 1988.
Rees, M. H., D. Lummerzheim, R. G. Roble, J. D. Winningham, J. D. Craven, and L. A. Frank, Auroral energy deposition rate characteristic electron energy and ionospheric parameters derived from dynamics explorer 1 images, *J. Geophys. Res., 93*, 12,841-12,860, 1988.
Rees, M. H., and D. Lummerzheim, Characteristics of auroral electron precipitation derived from optical spectroscopy, *J. Geophys. Res., 94*, 6799-6815, 1989.
Reeves, G. D., P. M. Banks, T. Neubert, K. J. Harker, and D. A. Gurnett, VLF wave emissions by pulsed and DC electron beams in space. 2. Analysis of Spacelab 2 results, *J. Geophys. Res., 95*, 6505-6517, 1990.
Reeves, G. D., P. M. Banks, T. Neubert, R. I. Bush, P. R. Williamson, and A. C. Fraser-Smith, VLF wave emissions by pulsed and DC electron beams in space 1. Spacelab 2 observations, *J. Geophys. Res., 93*, 14,699-14,718, 1988.
Reeves, G. D., P. M. Banks, A. C. Fraser-Smith, T. Neubert, R. I. Bush, D. A. Gurnett, and W. J. Raitt, VLF wave stimulation by pulsed electron beams injected from the space shuttle, *J. Geophys. Res., 93*, 162-174, 1988.
Reiff, P. H., H. L. Collin, J. D. Craven, J. L. Burch, J. D. Winningham, E. G. Shelley, L. A. Frank, and M. A. Friedman, Determination of auroral electrostatic potentials using high- and low-altitude particle distributions, *J. Geophys. Res., 93*, 7441-7465, 1988.
Rich, F. J., D. A. Hardy, R. H. Redus, and M. S. Gussenhoven, Northward IMF and patterns of high-latitude precipitation and field-aligned currents: The February 1986 storm, *J. Geophys. Res., 95*, 7893-7913, 1990.
Rich, F. J., and M. S. Gussenhoven, The absence of region 1/region 2 field-aligned currents during prolonged quiet times, *Geophys. Res. Lett., 14*, 689-692, 1987.
Rich, F. J., and N. C. Maynard, Consequences of using simple analytical functions for the high-latitude convection electric field, *J. Geophys. Res., 94*, 3687-3701, 1989.
Richards, P. G., and D. G. Torr, Auroral modeling of the 3371 Å emission rate: Dependence on characteristic electron energy, *J. Geophys. Res., 95*, 10,337-10,344, 1990.
Richards, P. G., and D. G. Torr, Ratios of photoelectron to EUV ionization rates for aeronomic studies, *J. Geophys. Res., 93*, 4060-4066, 1988.
Richards, P. G., D. G. Torr, M. J. Buonsanto, and K. L. Miller, The behavior of the electron density and temperature at Millstone Hill during the equinox transition study September, 1984, *J. Geophys. Res., 94*, 16,969-16,975, 1989.
Richmond, A. D., and R. G. Roble, Electrodynamic effects of thermospheric winds from the NCAR thermospheric general circulation model, *J. Geophys. Res., 92*, 12,365-12,376, 1987.
Richmond, A. D., and Y. Kamide, Mapping electrodynamic features of the high-latitude ionosphere from localized observations: Technique, *J. Geophys. Res., 93*, 5741-5759, 1988.
Richmond, A. D., Y. Kamide, S.-I. Akasofu, D. Alcayde, M. Blanc, O. de la Beaujardiere, D. S. Evans, J. C. Foster, E. Friis-Christensen, J. M. Holt, R. J. Pellinen, C. Senior, and A. N. Zaitzev, Global measures of ionospheric electrodynamic activity inferred from combined incoherent scatter radar and ground magnetometer observations, *J. Geophys. Res., 95*, 1061-1071, 1990.
Richmond, A. D., Y. Kamide, B.-H. Ahn, S.-I. Akasofu, D. Alcayde, M. Blanc, O. de la Beaujardiere, D. S. Evans, J. C. Foster, E. Friis-Christensen, T. J. Fuller-Rowell, J. M. Holt, D. Knipp, H. W. Kroehl, R. P. Lepping, R. J. Pellinen, C. Senior, and A. N. Zaitzev, Mapping electrodynamic features of the high-latitude ionosphere from localized observations: Combined incoherent-scatter radar and magnetometer measurements for January 18-19, 1984, *J. Geophys. Res., 93*, 5760-5776, 1988.
Riggin, D., and A. Kadish, Nonlocal theory of long-wavelength plasma waves associated with sporadic *E* layers, *J. Geophys. Res., 94*, 1495-1500, 1989.
Roberts, W. T., Jr., J. L. Horwitz, R. H. Comfort, C. R. Chappell, J. H. Waite, Jr., and J. L. Green, Heavy ion density enhancements in the outer plasmasphere, *J. Geophys. Res., 92*, 13,499-13,512, 1987.
Robinson, R. M., C. R. Clauer, O. de la Beaujardiere, J. D. Kelly, E. Friis-Christensen, and M. Lockwood, Sondrestrom and EISCAT radar observations of poleward-moving auroral forms, *J. Atmos. Terr. Phys., 52*, 411-420, 1990.
Robinson, R. M., G. T. Davidson, R. R. Vondrak, W. E. Francis, and M. Walt, A technique for interpretation of auroral Bremsstrahlung X-ray spectra, *Planet. Space Sci.,37*, 1053-1062, 1989.
Robinson, R. M., R. R. Vondrak, J. D. Craven, L. A. Frank, and K. Miller, A comparison of ionospheric conductances and auroral luminosities observed simultaneously with the Chatanika radar and the DE 1 auroral imagers, *J. Geophys. Res., 94*, 5382-5396, 1989.
Robinson, R. M., and R. R. Vondrak, Electrodynamic properties of auroral surges, *J. Geophys. Res., 95*, 7819-7832, 1990.
Robinson, R. M., R. R. Vondrak, and E. Friis-Christensen, Ionospheric currents associated with a sun-aligned arc connected to the auroral oval, *Geophys. Res. Lett. 14*, 656-659, 1987.
Robinson, R. M., R. R. Vondrak, K. Miller, T. Dabbs, and D. Hardy, On calculating ionospheric conductances from the flux and energy of precipitating electrons, *J. Geophys. Res., 92*, 2565-2569, 1987.
Robinson, R. M., R. R. Vondrak, D. Hardy, M. S. Gussenhoven, T. A. Potemra, and P. F. Bythrow, Electrodynamics of very high latitude arcs in the morning sector auroral zone, *J. Geophys. Res., 93*, 913-922, 1988.
Robinson, R. M., J. D. Winningham, J. R. Sharber, J. L. Burch, and R. Heelis, Plasma and field properties of suprathermal electron bursts, *J. Geophys. Res., 94*, 12,031-12,036, 1989.
Roble, R. G., E. C. Ridley, A. D. Richmond, and R. E. Dickinson, A coupled thermosphere/ionosphere general circulation model, *Geophys. Res. Lett., 15*, 1325-1328, 1988.
Roble, R. G., E. C. Ridley, and R. E. Dickinson, On the global mean structure of the thermosphere, *J. Geophys. Res., 92*, 8745-8758, 1987.
Rodger, A. S., and J. Aarons, Studies of ionospheric *F*-region irregularities from geomagnetic mid-latitude conjugate regions, *J. Atmos. Terr. Phys., 50*, 63-72, 1988.
Rohrbaugh, R. P., W. B. Hanson, B. A. Tinsley, B. L. Cragin, J. P. McClure, and A. L. Broadfoot, Images of transequatorial bubbles based on field-aligned airglow observations from Haleakala in 1984-1986, *J. Geophys.Res., 94*, 6763-6770, 1989.
Ronchi, C., P. L. Similon, and R. N. Sudan, A nonlocal linear theory of the gradient drift instability in the equatorial electrojet, *J. Geophys. Res., 94*, 1317-1326, 1989.
Ronchi, C., R. N. Sudan, and P. L. Similon, Effect of short-scale turbulence on kilometer wavelength irregularities in the equatorial electrojet, *J. Geophys. Res., 95*, 189-200, 1990.
Rosenberg, T. J., D. L. Detrick, P. F. Mizera, D. J.Gorney, F. T. Berkey, R. H. Eather, and L. J. Lanzerotti, Coordinated ground and space measurements of an auroral surge over South Pole, *J. Geophys. Res., 92*, 11,123-11,132, 1987.
Rosenberg, T. J., R. Wei, D. L. Detrick, and U. S. Inan, Observations and modeling of wave-induced microburst electron precipitation, *J. Geophys. Res., 95*, 6467-6475, 1990.
Ruohoniemi, J. M., R. A. Greenwald, K. B. Baker, J. P. Villain, and M. A. McCready, Drift motions of small-scale irregularities in the high-latitude *F* region: An experimental comparison with plasma drift motions, *J. Geophys. Res., 92*, 4553-4564, 1987.
Ruohoniemi, J. M., R. A. Greenwald, J. P. Villain, K. B. Baker, P. T. Newell, and C.-I. Meng, Coherent HF radar backscatter from small-scale irregularities in the dusk sector of the subauroral ionosphere, *J. Geophys. Res., 93*, 12,871-12,882, 1988.
Ruohoniemi, J. M., R. A. Greenwald, K. B. Baker, J .-P. Villain, C. Hanuise, and J. Kelly, Mapping high-latitude plasma convection with coherent HF radars, *J. Geophys. Res., 94*, 13,463-13,477, 1989.
Sa, L. A. D., A wave-particle-wave interaction mechanism as a cause of VLF triggered emissions, *J. Geophys. Res., 95*, 12,277-12,286, 1990.
Saflekos, N. A., J. L. Burch, M. Sugiura, D. A. Gurnett, and J. L. Horwitz, Observations of reconnected flux tubes within the mid-altitude cusp, *J. Geophys. Res., 95*, 8037-8055, 1990.
Sagawa, E., A. W. Yau, B. A. Whalen, and W. K. Peterson, Pitch angle distributions of low-energy ions in the near-earth magnetosphere, *J. Geophys. Res., 92*, 12,241-12,254, 1987.
Sahai, Y., J. A. Bittencourt, H. Takahashi, N. R. Teixeira, J. H. A. Sobral, B. A. Tinsley, and R. P. Rohrbaugh, Multispectral optical observations of ionospheric *F*-region storm effects at low latitude, *Planet. Space Sci., 36*, 371-381, 1988.
Samir, U., R. H. Comfort, K. H. Wright, Jr., and N. H. Stone,

Intercomparison among plasma wake models for plasmaspheric and ionospheric conditions, *Planet. Space Sci., 35*, 1477-1487, 1987.

Samir, U., R. H. Comfort, N. Singh, K. S. Hwang, and N. H. Stone, Insight into theory-experiment comparisons of wake measurements in the plasmasphere, *Planet. Space Sci., 37*, 873-880, 1989.

Samson, J. C., R. A. Greenwald, J. M. Ruohoniemi, A. Frey, and K. B. Baker, Goose Bay radar observations of earth-reflected, atmospheric gravity waves in the high-latitude ionosphere, *J. Geophys. Res., 95*, 7693-7709, 1990.

Samson, J. C., R. A. Greenwald, J. M. Ruohoniemi, and K. B. Baker, High-frequency radar observations of atmospheric gravity waves in the high-latitude ionosphere, *Geophys. Res. Lett., 16*, 875-878, 1989.

Sandahl, I., L. Eliasson, A. Pellinen-Wannberg, G. Rostoker, L. P. Block, R. E. Erlandson, E. Friis-Christensen, B. Jacobsen, H. Luhr, and J. S. Murphree, Distribution of auroral precipitation at midnight during a magnetic storm, *J. Geophys. Res., 95*, 6051-6072, 1990.

Sandholt, P. E., B. Jacobsen, B. Lybekk, A. Egeland, P. F. Bythrow, and D. A. Hardy, Electrodynamics of the polar cusp ionosphere; A case study, *J. Geophys. Res., 94*, 6713-6722, 1989.

Satyanarayana, P., M. J. Keskinen, P. K. Chaturvedi, and S. L. Ossakow, Effects of ion collisions on quasi-linear heating by the current-driven ion cyclotron instability in the high-latitude ionosphere, *J. Geophys. Res., 94*, 5510-5514, 1989.

Satyanarayana, P., Y. C. Lee, and J. D. Huba, Transverse Kelvin-Helmholtz instability with parallel electron dynamics and coulomb collisions, *J. Geophys. Res., 92*, 8813-8820, 1987.

Scales, W. A., and P. M. Kintner, Artificial ion beam instabilities. 1. Linear theory, *J. Geophys. Res., 95*, 10,623-10,641, 1990a.

Scales, W. A., and P. M. Kintner, Artificial ion beam instabilities. 2. Simulations, *J. Geophys. Res., 95*, 10,643-10,653, 1990b.

Schriver, D., M. Ashour-Abdalla, H. Collin, and N. Lallande, Ion beam heating in the auroral zone, *J. Geophys. Res., 95*, 1015-1028, 1990.

Schriver, D., and M. Ashour-Abdalla, Linear instabilities in multicomponent plasmas and their consequences for the auroral zone, *J. Geophys. Res., 93*, 2633-2641, 1988.

Schunk, R. W., A mathematical model of the middle and high latitude ionosphere, *PAGEOPH, 127*, 255-303, 1988.

Schunk, R. W., and J. J. Sojka, Ionospheric climate and weather modeling, *EOS, 69, 11*, 153-168, 1988.

Schunk, R. W., and J. J. Sojka, A theoretical study of the lifetime and transport of large ionospheric density structures, *J. Geophys. Res., 92*, 12,343-12,351, 1987.

Schunk, R. W., J. J. Sojka, and M. D. Bowline, Theoretical study of the effect of ionospheric return currents on the electron temperature, *J. Geophys. Res., 92*, 6013-6022, 1987.

Schunk, R. W., and J. J. Sojka, A three-dimensional time-dependent model of the polar wind, *J. Geophys. Res., 94*, 8973-8991, 1989.

Senbetu, L., and J. R. Henley, Distribution of plasma density and potential around a mesothermal ionospheric object, *J. Geophys. Res., 94*, 5441-5448, 1989.

Senior, C., J. R. Sharber, O. de la Beaujardiere, R. A. Heelis, D. S. Evans, J. D. Winingham, M. Sugiura, and W. R. Hoegy, *E* and *F* region study of the evening sector auroral oval: A Chatanika/dynamics explorer 2/NOAA 6 comparison, *J. Geophys. Res., 92*, 2477-2494, 1987.

Sentman, D. D., Approximate Schumann resonance parameters for a two-scale-height ionosphere, *J. Atmos. Terr. Phys., 52*, 35-46, 1990.

Sentman, D. D., Detection of elliptical polarization and mode splitting in discrete Schumann resonance excitations, *J. Atmos. Terr. Phys., 51*, 507-519, 1989.

Sergeev, V. A., O. A. Aulamo, R. J. Pellinen, M. K. Vallinkoski, T. Bosinger, C. A. Cattell, R. C. Elphic, and D. J. Williams, Non-substorm transient injection events in the ionosphere and magnetosphere, *Planet. Space Sci., 38*, 231-239, 1990.

Seyler, C. E., Jr., Nonlinear 3-D evolution of bounded kinetic alfven waves due to shear flow and collisionless tearing instability, *Geophys. Res. Lett., 15*, 756-759, 1988.

Sheldon, W. R., J. R. Benbrook, and G. J. Byrne, The effect of mid-latitude electron precipitation on the geoelectric field, *J. Atmos. Terr. Phys., 50*, 1019-1023, 1988.

Shoucri, M., G. J. Morales, and J. E. Maggs, Modification of the ionospheric electron velocity distribution function due to resonant absorption of HF waves, *J. Geophys. Res., 92*, 246-254, 1987.

Sica, R. J., R. W. Schunk, and P. J. Wilkinson, A study of the undisturbed mid-latitude ionosphere using simultaneous multiple site ionosonde measurements during the Sundial-86 campaign, *J. Geophys. Res., 95*, 8271-8279, 1990.

Sica, R. J., R. W. Schunk, and C. E. Rasmussen, Can the high latitude ionosphere support large field-aligned ion drifts?, *J. Atmos. Terr. Phys., 50*, 141-152, 1988.

Singh, L., T. R. Tyagi, Y. V. Somayajulu, P. N. Vijayakumar, R. S. Dabas, B. Loganadham, S.Ramakrishna, P. V. S. Rama Rao, A. Dasgupta, G.Navneeth, J. A. Klobuchar, and G. K. Hartmann, A multi-station satellite radio beacon study of ionospheric variations during total solar eclipses, *J. Atmos. Terr. Phys., 51*, 271-278, 1989.

Singh, N., and D. G. Torr, Effects of ion temperature anisotropy on the interhemispheric plasma transport during plasmaspheric refilling, *Geophys. Res. Lett., 17*, 925-928, 1990.

Singh, N., and K. S. Hwang, Electric potential structures and propagation of electron beams injected from a spacecraft into a plasma, *J. Geophys. Res., 93*, 10,035-10,040, 1988.

Singh, N., K. S. Hwang, D. G. Torr, and P. Richards, Temporal features of the outflow of heavy ionospheric ions in response to a high altitude plasma cavity, *Geophys. Res. Lett., 16*, 29-32, 1989.

Slater, D. W., C. Gurgiolo, J. U. Kozyra, E. W. Kleckner, and J. D. Winningham, A possible energy source to power stable auroral red arcs: precipitating electrons, *J. Geophys. Res., 92*, 4543-4552, 1987.

Smith, M. F., and M. Lockwood, The pulsating CUSP, *Geophys. Res. Lett., 17*, 1069-1072, 1990.

Sojka, J. J., Global scale, physical models of the *F* region ionosphere, *Rev. Geophys., 27*, 371-403, 1989.

Sojka, J. J., R. W. Schunk, and G. L. Wrenn, A comparison of f_0F2 obtained from a time-dependent ionospheric model with Argentine Islands' data for quiet conditions, *J. Atmos. Terr. Phys., 50*, 1027-1039, 1988.

Sojka, J. J., and R. W. Schunk, A model study of how electric field structures affect the polar cap *F* region, *J. Geophys. Res., 93*, 884-896, 1988.

Sojka, J. J., R. W. Schunk, J. D. Craven, L. A. Frank, J. Sharber, and J. D. Winningham, Modeled *F* region response to auroral dynamics based upon dynamics explorer auroral observations, *J. Geophys. Res., 94*, 8993-9008, 1989.

Sojka, J. J., and R. W. Schunk, Theoretical study of the seasonal behavior of the global ionosphere at solar maximum, *J. Geophys. Res., 94*, 6739-6749, 1989.

Sojka, J. J., and R. W. Schunk, Theoretical study of the high-latitude ionosphere's response to multicell convection patterns, *J. Geophys. Res., 92*, 8733-8744, 1987.

Sojka, J. J., R. W. Schunk, and J. A. Whalen, The longitude dependence of the dayside F region trough: A detailed model-observation comparison, *J. Geophys. Res., 95*, 15,275-15,280, 1990.

Spiro, R. W., R. A. Wolf, and B. G. Fejer, Penetration of high-latitude-electric-field effects to low latitudes during SUNDIAL 1984, *Ann. Geophys. 6*, 39-50, 1988.

Stenbaek-Nielsen, H. C., E. M. Wescott, D. Rees, A. Valenzuela, and N. Brenning, Non-solar UV produced ions observed optically from the 'CRIT I' critical velocity ionization experiment, *J. Geophys. Res., 95*, 7749-7757, 1990.

Stenzel, R. L., and J. M. Urrutia, Whistler wings from moving electrodes in a magnetized laboratory plasma, *Geophys. Res. Lett., 16*, 361-364, 1989.

Stern, D. P., Substorm Electrodynamics, *J. Geophys. Res., 95*, 12,057-12,067, 1990.

St.-Maurice, J.-P., A unified theory of anomalous resistivity and joule heating effects in the presence of ionospheric *E* region irregularities, *J. Geophys. Res., 92*, 4533-4542, 1987.

St.-Maurice, J. P., J. C. Foster, J. M. Holt, and C. Del Pozo, First results on the observation of 440-MHz high-latitude coherent echoes from the E region with the Millstone Hill radar, *J. Geophys. Res., 94*, 6771-6798, 1989.

Sulzer, M. P., H. M. Ierkic, and J. A. Fejer, Observational limitations on the role of Langmuir cavitons in ionospheric modification experiments at arecibo, *J. Geophys. Res., 94*, 6841-6854, 1989.

Suszcynsky, D. M., N. D'Angelo, and R. L. Merlino, An experimental study of electrostatic ion cyclotron waves in a two-ion component plasma, *J. Geophys. Res., 94*, 8966-8972, 1989.

Svenes, K. R., J. Troim, B. N. Maehlum, M. Friedrich, K. M. Torkar, G. Holmgren, and W. F. Denig, RAM-Wake measurements obtained from the ionospheric sounding rocket *MAIMIK*, *Planet. Space Sci., 38*, 653-663, 1990.

Swartz, W. E., J. F. Providakes, M. C. Kelley, and J. F. Vickrey, The effect of strong velocity shears on incoherent scatter spectra: A new interpretation of unusual high latitude spectra, *Geophys. Res. Lett., 15*, 1341-1344, 1988.

Swift, D. W., Simulation of the ejection of plasma from the polar ionosphere, *J. Geophys. Res., 95*, 12,103-12,118, 1990.

Tepley, C. A., and R. B. Kerr, Variations in the proton concentration and flux of the topside ionosphere at arecibo during the September 1984 equinox transition study, *J. Geophys. Res., 94*, 16,977-16,986, 1989.

Thide, B., A. Hedberg, J. A. Fejer, and M. P. Sulzer, First observations of stimulated electromagnetic emission at arecibo, *Geophys. Res. Lett., 16*, 369-372, 1989.

Torr, M. R., D. G. Torr, P. Bhatt, W. Swift, and H. Dougani, Ca^+ emission in the sunlit ionosphere, *J. Geophys. Res., 95*, 2379-2387, 1990.

Tribble, A. C., J. S. Pickett, N. D'Angelo, and G. B. Murphy, Plasma density, temperature and turbulence in the wake of the Shuttle Orbiter, *Planet. Space Sci., 37*, 1001-1010, 1989.

Tsunoda, R. T., High-latitude *F* region irregularities: a review and synthesis, *Rev. Geophys., 26*, 719-760, 1988.

Tsunoda, R. T., R. C. Livingston, J. F. Vickrey, R. A. Heelis, W. B. Hanson, F. J. Rich, and P. F. Bythrow, Dayside observations of thermal-ion upwellings at 800-km altitude: An ionospheric signature of the cleft ion fountain, *J. Geophys. Res., 94*, 15,277-15,290, 1989.

Tulunay, Y. K., and J. M. Grebowsky, Hemispheric differences in the morphology of the high latitude ionosphere measured at ~500 km, *Planet. Space Sci., 35*, 821-826, 1987.

Valladares, C. E., M. C. Kelley, and J. F. Vickrey, Plasma line observations in the auroral oval, *J. Geophys. Res., 93*, 1997-2003, 1988.

Vampola, A. L., Electron precipitation in the vicinity of a VLF transmitter, *J. Geophys. Res., 92*, 4525-4532, 1987.

Villain, J.-P., C. Hanuise, R. A. Greenwald, K. B. Baker, and J. M. Ruohoniemi, Obliquely propagating ion acoustic waves in the auroral *E* region: Further evidence of irregularity production by field-aligned electron streaming, *J. Geophys. Res., 95*, 7833-7846, 1990.

Villain, J. P., R. A. Greenwald, K. B. Baker, and J. M. Ruohoniemi, HF radar observations of *E* region plasma irregularities produced by oblique electron streaming, *J. Geophys. Res., 92*, 12,327-12,342, 1987.

Villalon, E., Ionospheric electron acceleration by electromagnetic waves near regions of plasma resonances, *J. Geophys. Res., 94*, 2717-2720, 1989.

Weber, E. J., M. C. Kelley, J. O. Ballenthin, S. Basu, H. C. Carlson, J. R. Fleischman, D. A. Hardy, N. C. Maynard, R. F. Pfaff, P. Rodriguez, R. E. Sheehan, and M. Smiddy, Rocket measurements within a polar cap arc: Plasma, particle, and electric circuit parameters, *J. Geophys. Res., 94*, 6692-6712, 1989.

Wei, C. Q., and L. C. Lee, Ground magnetic signatures of moving elongated plasma clouds, *J. Geophys. Res., 95*, 2405-2418, 1990.

Whalen, J. A., The daytime *F* layer trough and its relation to ionospheric-magnetospheric convection, *J. Geophys. Res., 94*, 17,169-17,184, 1989.

Whalen, J. A., Daytime *F* layer trough observed on a macroscopic scale, *J. Geophys. Res., 92*, 2571-2576, 1987.

Williams, E. R., G. W. Watkins, T. A. Blix, E. V. Thrane, G. Entzian, G. von Cossart, K. M. Greisiger, W. Singer, J. Taubenheim, M. Friedrich, C. M. Hall, J. R. Katan, J. Lastovicka, B. A. de la Moreno, S. V. Pakhomov, H. Ranta, Z. T. Rapoport, V. M. Sinelnikov, D. Samardjiev, G. Nestorov, H. H. Sauer, and P. Stauning, The ionosphere: morphology, development and coupling, *J. Atmos. Terr. Phys., 49*, 777, 1987.

Wilson, G. R., C. W. Ho, J. L. Horwitz, N. Singh, and T. E. Moore, A new kinetic model for time-dependent polar plasma outflow: Initial results, *Geophys. Res. Lett., 17*, 263-266, 1990.

Winglee, R. M., Electron beam injection during active experiments. 2. Collisional effects, *J. Geophys. Res., 95*, 6191-6207, 1990.

Winglee, R. M., M. Ashour-Abdalla, and R. D. Sydora, Heating of ionospheric O^+ ions by shear Alfven waves, *J. Geophys. Res., 92*, 5911-5919, 1987.

Winglee, R. M., P. B. Dusenbery, H. L. Collin, C. S. Lin and A. M. Persoon, Simulations and observations of heating of auroral ion beams, *J. Geophys. Res., 94*, 8943-8965, 1989.

Winglee, R. M., and P. J. Kellogg, Electron beam injection during active experiments. 1. Electro-magnetic wave emissions, *J. Geophys. Res., 95*, 6167-6190, 1990.

Winningham, J. D., D. T. Decker, J. U. Kozyra, J. R. Jasperse, and A. F. Nagy, Energetic (>60 eV) atmospheric photoelectrons, *J. Geophys. Res., 94*, 15,335-15,348, 1989.

Wolfe, A., D. Venkatesan, R. Slawinski, and C. G. Maclennan, A conjugate area study of Pc 3 pulsations near cusp latitudes, *J. Geophys. Res., 95*, 10,695-10,698, 1990.

Yeh, H.-C, and J. C. Foster, Storm time heavy ion outflow at mid-latitude, *J. Geophys. Res., 95*, 7881-7891, 1990.

Yeh, H.-C., J. C. Foster, J. M. Holt, R. H. Redus, and F. J. Rich, Radar and satellite observations of the storm time cleft, *J. Geophys. Res., 95*, 12,075-12,090, 1990.

Yu, M. Y., P. K. Shukla, and R. S. B. Ong, Scattering of electromagnetic waves by electron acoustic waves, *Planet. Space Sci., 35*, 295-298, 1987.

Zanetti, L. J., T. A. Potemra, R. E. Erlandson, P. F. Bythrow, B. J. Anderson, J. S. Murphree, and G. T. Marklund, Polar region Birkeland current, convection, and aurora for northward interplanetary magnetic field, *J. Geophys. Res., 95*, 5825-5833, 1990.

Zargham, S., and C. E. Seyler, Collisional and inertial

dynamics of the ionospheric interchange instability, *J. Geophys. Res.*, *94*, 9009-9027, 1989.

Zargham, S., and C. E. Seyler, Collisional interchange instability. 1. Numerical simulations of intermediate-scale irregularities, *J. Geophys. Res.*, *92*, 10,073-10,088, 1987.

Zhu, L., and J. R. Kan, Effects of ionospheric recombination time scale on the auroral signature of substorms, *J. Geophys. Res.*, *95*, 10,389-10,398, 1990.

Zhu, L., and J. R. Kan, Ground magnetic signatures of multiple field-aligned current sheets in flux transfer events, *J. Geophys. Res.*, *94*, 6655-6664, 1989.

Zhu, L., and J. R. Kan, Time evolution of the westward-traveling surge on an ionospheric time scale, *Planet. Space Sci.*, *35*, 145-151, 1987.

J. J. Sojka, Center for Atmospheric and Space Sciences, Utah State University, Logan, UT 84322.

(Received Februrary 2, 1991;
accepted February 15, 1991.)

A Small Satellite Constellation for "Imaging" Magnetospheric Electrodynamics

J. J. Sojka
Center for Atmospheric and Space Sciences
Utah State University

and

F. J. Redd
Center for Space Engineering
Utah State University

To Be Presented At:

XXVII COSPAR
The Hague
June 1990

A SMALL SATELLITE CONSTELLATION FOR "IMAGING" MAGNETOSPHERIC ELECTRODYNAMICS

J. J. Sojka,* F. J. Redd**

*Center for Atmospheric and Space Sciences, Utah State University, Logan, UT
**Center for Space Engineering, Utah State University, Logan, UT

ABSTRACT

Our understanding of the global scale magnetospheric electrodynamics system will, even after ISTP missions, still be only qualitative. Indeed, it is only the auroral imagers which enable us to have a 2-D time-dependent glimpse of the complexity of the magnetosphere. The imagers will, however, not be able to map the key electric fields and currents responsible for the complex dynamics of the magnetosphere. A 2-D time-dependent look at the electric fields and currents is desperately needed.

Alternative space measurement technologies must be pursued to achieve mapping of these key electrical fields. A system consisting of a constellation of 50 small satellites is described to achieve the "imaging" of these parameters. Each small satellite will support a single, simple electric field (and/or current) measurement instrument, and will use off-the-shelf technology to support the experiment. Data sampling rates, onboard storage, and telemetry will be minimized to achieve the single overall scientific goal; namely, the global 2-D mapping of the electric field (and/or current) from altitudes of 500 to 800 km, every fifteen minutes.

INTRODUCTION

A major aspect of scientific research in the Thermospheric-Ionospheric-Magnetospheric (TIM) system has been via community wide collaborative campaigns and programs (GISMOS, CEDAR, WITS, CDAW, etc.); the object being to better understand the larger scale phenomena. In most cases the global scale is not observed, although the advent of global auroral imaging is beginning to change this. For most of these campaigns and programs an understanding of the global transport of energy, or mass, or electrodynamics is the major goal. At present, the observations are limited to local observations or 1D satellite coverage.

The future ISTP program will be similarly restricted. Indeed, the magnetospheric community identifies these 3-D problems as major questions not satisfactorily addressed by the ISTP program [Banks et al., 1988]. These same problems are also critical to the future GEM program [Roederer et al., 1988]. Both of these reports are based on community wide input.

A global distribution of simultaneous electric field observations is needed. Both hemispheres need to be covered to identify IMF and other hemispheric asymmetries. No global imagery of the electric field is currently possible, and ground based global coverage on this scale is impractical. Hence, in situ measurements need to be made. A single satellite produces a 1D cut and therefore to get global coverage a constellation i.e. a fleet of satellites is needed. In this paper we consider a constellation of 50 small satellites. By varying the individual orbit parameters, i.e., ascending node, inclination, UT of ascending node, etc., an optimized coverage is obtained. Circular orbits whose altitudes range from 500 to 1000 km would be sufficient. Each satellite could produce as little as one electric field measurement every 0.1 second (i.e. 1 km. along the satellite track). Higher frequency data collection would not produce significantly better 2-D coverage or resolution.

PRESENT DAY MAGNETOSPHERIC ELECTRIC FIELD STATUS

A wide variety of empirical and semi-empirical models of the magnetospheric electric field as mapped into the high latitude ionosphere currently exists [Volland, 1978; Heppner, 1977; Heelis et al., 1982; Foster, 1983; Heppner and Maynard, 1987]. However, these models are based upon either extensive satellite data bases or ground based incoherent scatter radar data sets. In either case the instantaneous or simultaneous data coverage is extremely limited, to either a satellite track or locally high resolution ground radar data. By binning (or sorting) the data according to magnetic or solar indices, data sets of improved spatial coverage are achieved. This is the basis for the empirical models.

The resulting models no longer have temporal (substorm or even storm) dependencies. Even their gross morphologies are contested. Our community is faced with the quandary of deciding between "distorted two-cell" versus "four or multiple cell" descriptions of the convection electric field under IMF Bz northward conditions. Since both interpretations are based upon the same satellite data sources, namely, the Dynamics Explorers, there is great difficulty in finding "ground truth" data against which the models can be compared.

In specific study periods where a global picture of the convection is needed, several methods are used to construct this convection pattern. One method is to scale an empirical electric field for the required magnetic and IMF conditions. A parameter such as the cross polar cap potential [Reiff and Luhmann, 1986] is computed and used to define the scaling factor. A more eleborate scheme is to define the polar cap potential along its boundary and then use this to define the global potential [Lu et al., 1989]. In either case, dynamics is introduced via the change in magnetic or solar indices and hence different choices of convection patterns. Figure 1 shows an example of how difficult it is to define this boundary potential from limited satellite coverage [from Lu et al., 1989]. Two orbits of DE-2 are compared with the corresponding global convection patterns. The electric fields in the cusp and Harang regions are very poorly defined.

A second method is to use all the electrodynamic data available, currents, conductivities, and electric field data to self-consistently deduce the best global picture of the currents and electric fields. This technique has been pioneered by Richmond [Richmond et al., 1988] and is referred to as the Assimilative Mapping of Ionosphere Electrodynamics (AMIE). At present, even this technique is unable to produce significant results because of the lack of data. The process relies heavily upon a statistical electric field model when data is sparse, and consequently, it loses its self consistent attributes. Figure 2 shows an example of how sparse the data distribution typically is [from Richmond et al., 1988]. Using ground based radars and magnetometers as well as satellite data, the coverage is still too sparse to be meaningfully inverted into a global scale convection pattern.

Although ground based coverage could be somewhat enhanced the cost of new facilities alone would be prohibitive, and these facilities would be unable to operate continously. At present, the incoherent scatter type radars give the most extensive and reliable data, but these radars can only operate for a few days per month. Installing one or two more such facilities would clearly not result in a major difference in coverage. They would produce additional, but still only local measurements.

THE ELECTRIC FIELD (ELF) SATELLITE

The design and development of these small ELF satellites has to take on novel measures to ensure that 50 can be procured (afforded), deployed (globally), and yet give good scientific quality data. This was the goal of Dr Frank Redd's* NASA sponsored Space Design Course for 1989-1990. A group of 18 students participated in the design of the various satellite subsytem/ mission

components of such a 50 satellite mission. A final project report has been prepared by Redd and Olsen [1990]. The salient features of this study are summarized in the following subsections and Section 4.

3.1 Design Considerations. The primary performance driver for this mission is the need to measure the attitude of each satellite very accurately while making the 3 axis electric field measurements. In addition, it is necessary to know the induced electric field generated by the satellite as it crosses the magnetic field lines. This must then be factored out of the measurements. The electric field booms must rotate in order to balance photoelectric effects and aid in the measure of the V X B bias.

3.2 Electric Field Sensing System. The 3 axis system will consist of 3 orthogonal sets of insulated booms with conductive spheres attached to the ends as shown in Figure 3. The electrical potential across each boom will be measured. Photoelectric charge build up on the booms is minimized by having the satellite rotate. To achieve the desired accuracy, the spheres must be separated by at least 1 meter and be rotating at no more than 10 radians per second. Since the rotation causes a sinusoidal variation in the output, potential readings must be taken at least every 0.1 seconds to get the desired resolution. Four booms (a 2.75m Weitzmann Quadrupole Stacer boom system) lie in a plane perpendicular to the spin axis. The fifth (a 1.65m Weitzmann Monopole Stacer boom) lies along the spin axis. A 5cm radius gold plated aluminum sphere is mounted at the end of each boom.

3.3 Attitude Control and Determination System. The satellite is modelled as a spinning oblate platform which spins at 10 rpm. The orientation or attitude of each satellite will not be controlled, but the spin rate will be controlled to 10 ± 2rpm. An on-board cold gas propellant system will be used to spin-up the satellite initially as well as make any necessary spin rate adjustments. Two 2-axis magnetometers, 2 sun sensors, and 1 horizon crossing sensor are used to determine the attitude of each ELF satellite. By using different combinations of these 5 sensors, the attitude of the satellite can be determined at all times during the orbit. Some of the data will be redundant, but this redundancy can be used to enhance the accuracy of the readings. These readings will lie within the $\pm$ 1 degree error in attitude knowledge margin.

3.4 Data Processing System. The data processing system is sized to store up to 24 hours worth of data. These data include the electrical field potential as well as the attitude readings. This system will also handle housekeeping functions on-board the satellite. Sampling 6, 12 bit words every 0.1 seconds leads to a daily on board storage capability of only 7.8 M bytes.

3.5 Communication System. Because the attitude of each ELF satellite will not be controlled and each satellite can maintain a different orientation, a virtually omni-directional antenna is needed on-board for communication. A stripline wraparound antenna meets this requirement. Frequencies in the S-band will be used for receiving instructions and transmitting the collected data to a ground station. Data will be transmitted twice per day to one ground station. The ground station will use a 4.3 m parabolic dish with tracking capabilities. The actual location of this ground station is yet to be determined. Each satellite will take a maximum of 82 seconds to transmit the stored data. It is expected that each satellite will pass within range of the ground station at least twice per day.

3.6 Power System. The satellite's power will come from solar cells wrapped around the exterior of the spacecraft. Since the satellites will not generally be placed in sun synchronous orbits, they will have to function in the dark as well. Therefore, the solar cells will be backed up with batteries. The minimum power generation will be 12.77 W which will be sufficient to cover the power requirements of all systems.

3.7 ELF Satellite Structure and Configuration. The cylindrical primary structure is 45 cm in diameter and 35 cm high. It will be composed of 0.16 to 0.32 cm thick aluminum honeycomb. Most subsystem components will be mounted on this plate as shown by Figure 4. Individual

component covers will provide radiation shielding as required.

A 50 ELF SATELLITE MISSION

Having designed the ELF satellite, the next step is to consider the ELF constellation deployment. Two different scenarios were considered by Redd and Olsen [1990]. The first considers using Orbital Sciences Corporation's Pegasus as a dedicated launch vehicle. The second option looks at piggyback opportunities on McDonnell Douglas's Delta II launch vehicle. The following discussion centers on the Pegasus vehicle to provide 8 launches with 6 satellites per launch. Pegasus will insert the payloads into 550km altitude orbits for a minimum lifetime orbit of 7 years. When the proper orbit is reached, one of the 6 satellites will be ejected. The rest of the cluster will remain attached to the upper stage. This stage will then be manouvered to a slightly different altitude (about 75km higher) or a slightly different inclination (about 2.5 degrees) where another ELF will be ejected. This sequence will be repeated until all ELFs are deployed. By slightly changing the altitude and/or inclination of each satellite, the satellites will be dispersed further by orbital perturbations caused by the earth's oblateness.

Figure 5a shows the initial 8 orbit planes viewed from above the north pole. After six months each set of 6 satellites are dispersed from these orbits to produce the coverage shown in Figure 5b. In order to make the improved scientific measurements data from all satellites will be compared during a small time interval. Figure 5c shows the resulting satellite orbit segments for a 20 minute time interval. The ensuing observational coverage is the key parameter in deciding how to select the initial 8 Pegasus launches.

CONCLUSION

The concept of globally "imaging" the magnetospheric electric field at ionospheric altitudes (500 to 1000km) has been considered. A constellation of 50 small ELF satellites simultaneously measuring the in-situ electric field has been outlined. This small ELF satellite has been designed to minimize mass and cost (Redd and Olsen,1990). Each ELF satellite has a mass of 19 kg and costs less than $250,000 for the hardware. These ELF satellites would be lauched six at a time by Pegasus or four at a time as a secondary payload by the Delta II. Based upon the Pegasus launch senario, where one vehicle costs $7 million, a total of 9 launches would be needed. This would result in a mission cost of $90 million (assuming each ELF costs $0.5 million) or $171 million (assuming each ELF costs $2.0 million). Such a mission would fall in the NASA small to moderate mission category while the scientific data from such a mission would have a major impact on the ionospheric, thermospheric, and magnetospheric disiplines.

Acknowledgments : This research was supported by NASA contracts NAGW-77 and NAGW-1547 and AFOSR grant AFOSR-90-0026 to Utah State University.

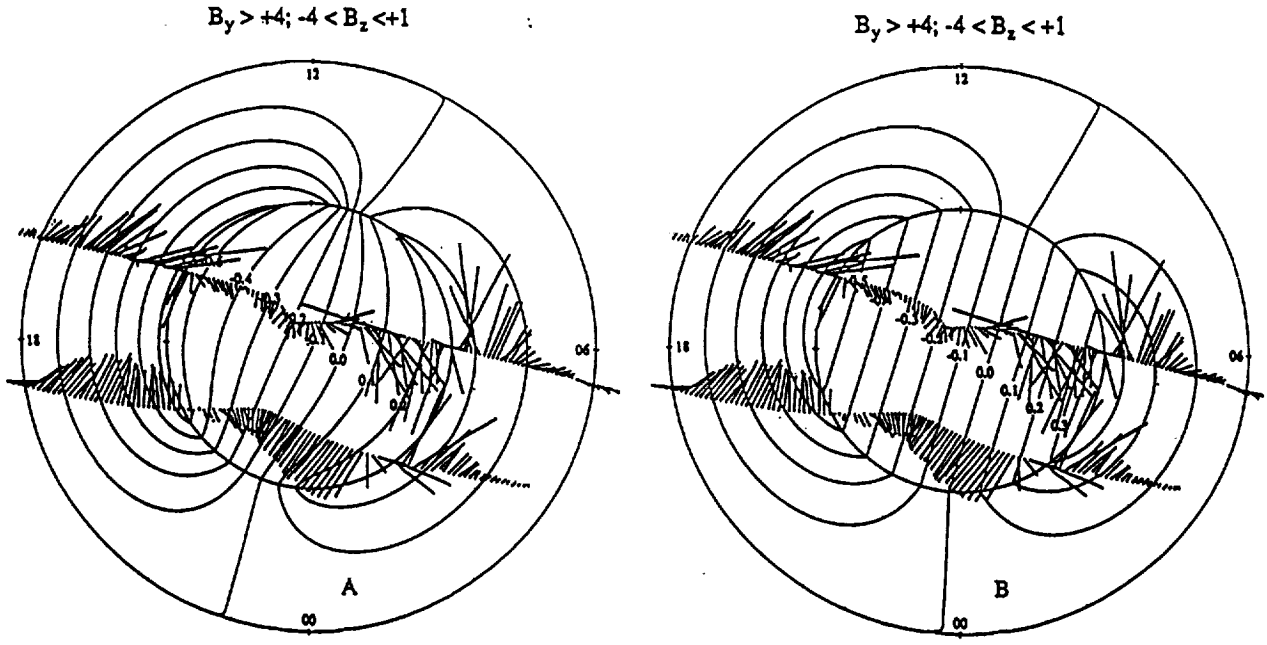

From: Lu et al., JGR, 1989.

Figure 1

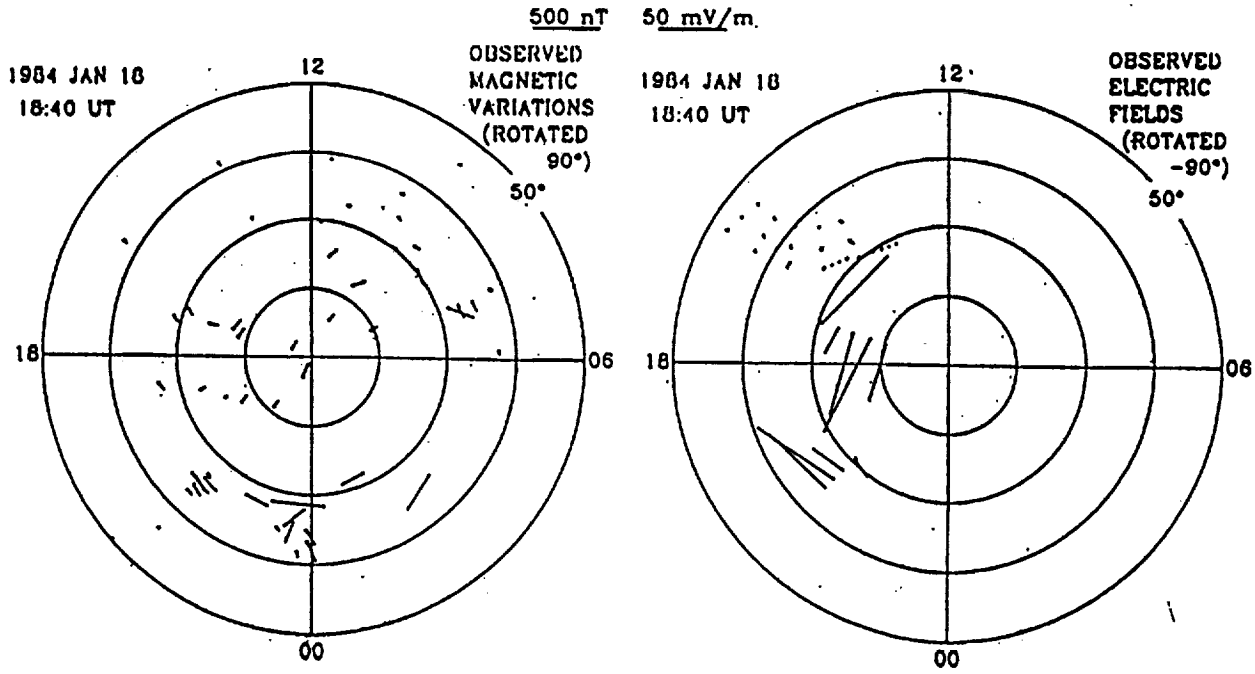

From: Richmond et al., JGR, 1988.

Figure 2

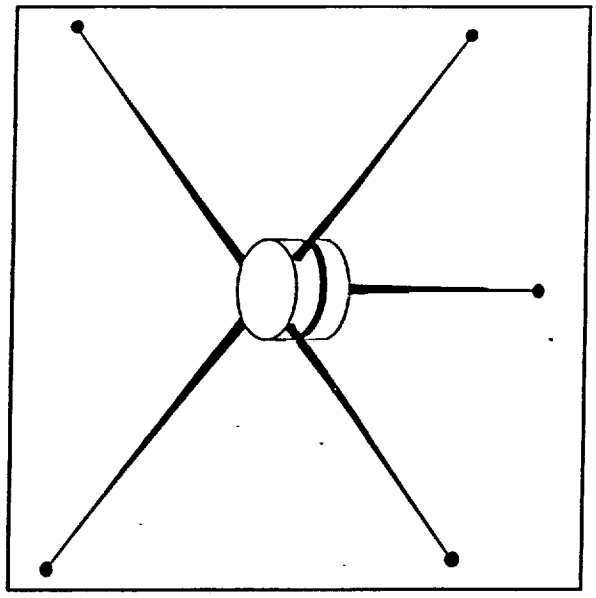

Figure 3 Close-up exterior view of an ELF satellite

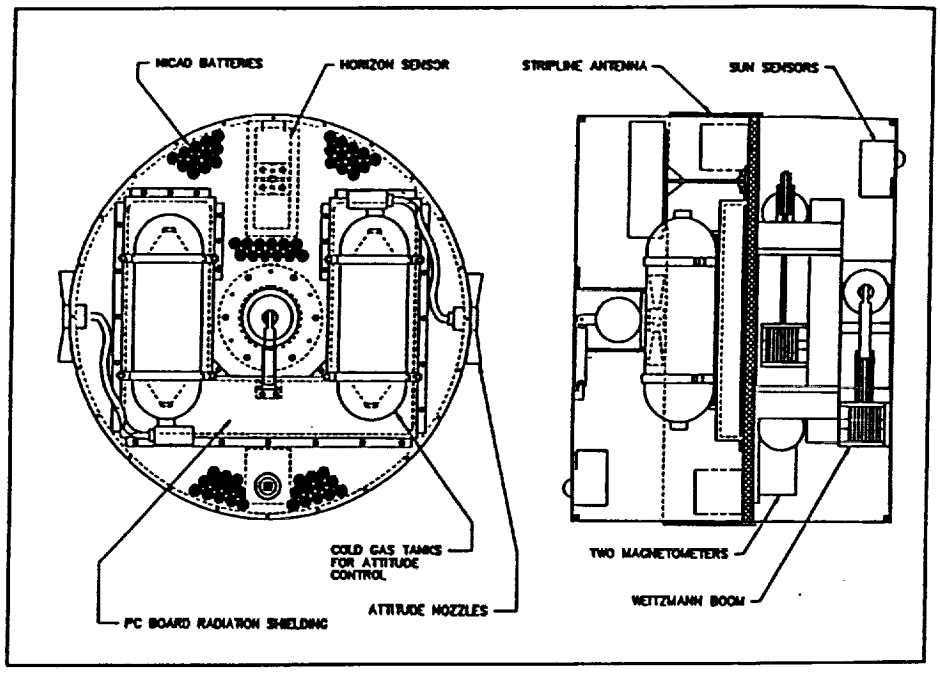

Figure 4 Internal layout of the subsystem components

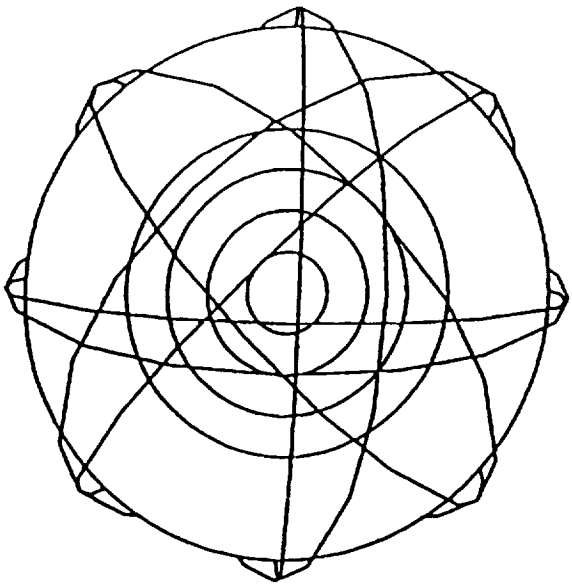

Figure 5a View from the North Pole of the orbits after all 8 Pegasus launches. Satellites are still in clusters of 6.

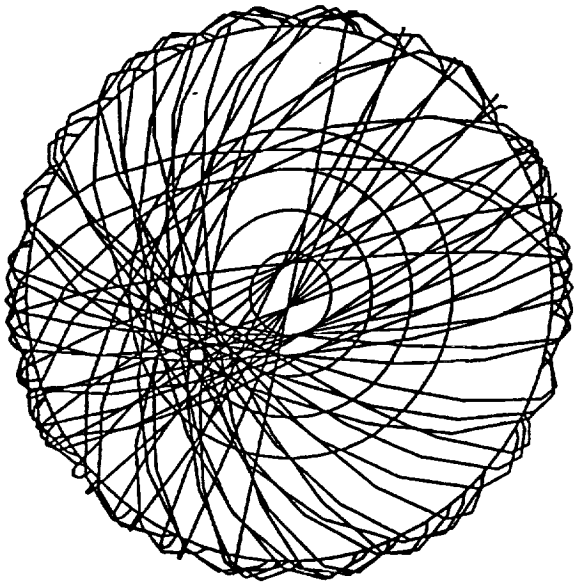

Figure 5b Constellation configuration after 6 months

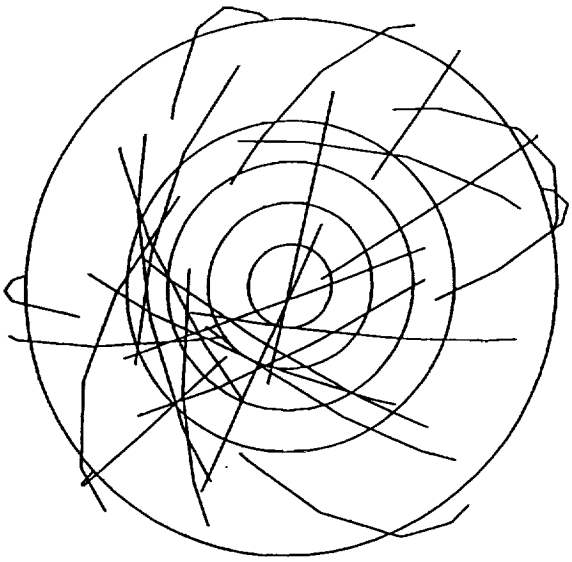

Figure 5c Global coverage during a 20 minute time span 6 months after deployment

Ionospheric Simulation Compared with Dynamics Explorer Observations for 22 November 1981

J. J. SOJKA, M. BOWLINE AND R. W. SCHUNK

Center for Atmospheric and Space Sciences, Utah State University, Logan

J. D. CRAVEN AND L. A. FRANK

Department of Physics and Astronomy, University of Iowa, Iowa City

J. R. SHARBER AND J. D. WINNINGHAM

Southwest Research Institute, San Antonio, Texas

L. H. BRACE

Goddard Space Flight Center, Greenbelt, Maryland

Submitted to:

Journal of Geophysical Research

August 1990

Revised May 1991

ABSTRACT

Dynamics Explorer (DE)-2 electric field and particle data have been used to constrain the inputs of a Time-Dependent Ionospheric Model (TDIM) for a simulation of the ionosphere on 22 November 1981. The simulated densities have then been critically compared with the DE-2 electron density observations. This comparison uncovers a model-data disagreement in the morning sector trough; generally good agreement of the background density in the polar cap and evening sector trough; and a difficulty in modelling the observed polar F-layer patches. From this comparison, the consequences of structure in the electric field and precipitation inputs can be seen. This is further highlighted during a substorm period for which DE-1 auroral images were available. Using these images, a revised dynamic particle precipitation pattern was used in the ionospheric model; the resulting densities were different from the original simulation. With this revised dynamic precipitation model, improved density agreement is obtained in the auroral/polar regions where the plasma convection is not stagnant. However, the dynamic study also reveals a difficulty of matching dynamic auroral patterns with static empirical convection patterns. In this case, the matching of the models produced intense auroral precipitation in a stagnation region, which, in turn, led to exceedingly large TDIM densities.

I. INTRODUCTION

Theoretical models of the terrestrial ionosphere and thermosphere have now attained global-scale [*Sojka and Schunk*, 1985; *Roble et al.*, 1987; *Fuller-Rowell et al.*, 1987]. Such models require global-scale inputs, especially for the magnetospheric parameters. At the present time, no global-scale theoretical model of the magnetosphere exists. Hence, statistical (empirical) models of the magnetospheric electric field [*Volland*, 1978; *Heelis et al.*, 1982; *Sojka et al.*, 1986; *Heppner and Maynard*, 1987] and auroral precipitation [*Spiro et al.*, 1982; *Hardy et al.*, 1985; *Evans*, 1987] are used as inputs to ionospheric and thermospheric models. Such studies are handicapped because statistical inputs cannot readily be adapted to simulate the spatial variations and temporal dynamics of geomagnetic storms and substorms. To minimize some of these difficulties, models have used in-situ satellite observations of auroral precipitation and electric fields, combined with Defense Meteorological Satellite Program (DMSP) images and ground-based incoherent scatter radar observations of electric fields, to define the auroral and convection boundaries [*Sojka et al.*, 1983; *Rasmussen et al.*, 1986b]. With the availability of global auroral images from the Dynamics Explorer 1 (DE-1) satellite, it is possible to directly define a magnetospheric auroral input on the scale needed by the ionospheric and thermospheric models.

In a previous study, we investigated methods to provide a description of the energy flux and characteristic energy of the auroral precipitation based on DE-1 images [*Sojka et al.*, 1989]. The resulting precipitation models were compared with in-situ DE-2 particle measurements. *Rees et al.* [1988] have carried out image-to-precipitation calculations and used similar in-situ cross checks on the auroral precipitation. In our previous study, a particularly dynamic auroral period was chosen because it provided excellent image sensitivity. Unfortunately, the magnetospheric convection was also dynamic, and because of the northward turning of the IMF during the selected period, a realistic convection model could not be defined. The study did, however, show the ionospheric dependence on the auroral dynamics.

For this study we used a period where both the precipitation and convection patterns could

be compared with DE data. In addition, the IMF data was available and was found to be reasonably behaved.

Section 2 describes the selected data period, while Section 3 describes the quiet day inputs and model-observation comparison. In Section 4, the major substorm disturbance in this period is analyzed. Results of this study are summarized in Section 5.

II. 22 NOVEMBER 1981

This day was selected for a variety of reasons based upon both data availability and geomagnetic conditions. During this 24-hour period, the three-hourly Kp dropped from 3+ to 2 (see top panel in Figure 1); the average three-hourly Kp was 2+. Several substorms occurred during this day as shown by the short duration peaks in the AE index in the bottom panel of Figure 1. Between 0730 and 0935 UT at least two substorms occurred and the AE reached values of 750 during this time. This was the strongest disturbance; for the rest of the period the AE index averaged around 200 with brief departures to nearly 500. These departures being associated with other smaller substorms. Because these substorms were only moderate intensity they would not lead to a significant perturbation of the auroral F-region. At 0150, 1540, and 2300 UT the DE-1 auroral images show the substorms and confirm they are moderate compared to the 0730 and 0900 UT substorms. Hence, the 0730 to the 0935 UT period will be considered in detail as a substorm period while the other substorms will be averaged over and considered as a quiet period.

The Interplanetary Magnetic Field (IMF) data were also available and two components are shown in Figure 1 (middle panel). For almost the entire period the IMF had the same sector morphology, namely southward IMF with *By* positive. In Figure 1 (middle panel), the *By* component is about 4 nT (gamma) positive until about 2100 UT when it approaches zero and then it oscillates about this value for the remaining three hours. The *Bz* component is negative (southward) all day with the exception of a one-hour period from 1030 to 1130 UT. During this brief period, the *Bz* component is weakly positive, less than one nT. There appears to be no correlation between the northward turning at ~1130 and subsequent southward turning of the IMF at 1330 UT and the substorms, as indicated by the AE index. However, the decreasing Kp is probably correlated with the *Bz* component approaching zero from its initial -5 nT value.

The IMF southward condition implies that a two-cell convection pattern is appropriate, while the long period of *By* positive implies that the convection pattern would have a well defined skewing. This corresponds to the *Heppner and Maynard* [1987] BC pattern. In our previous DE-

TDIM study [*Sojka et al.*, 1989], it was not possible to define the convection pattern. However, this study begins with the convection pattern established; this will be demonstrated in the next section.

A further reason for selecting this period was the availability of DE-1 auroral images from the SAI instrument. The shaded bars on the UT time axis of Figure 1 indicate the four periods for which auroral images were taken. Our attention will be focused upon the 0635 to 0935 UT period when substorms were present. A third reason for focusing on this day was that it can be well represented by a "quiet" day with a three-hour substorm period superimposed. Finally, during this 24-hour period data were available from a number of DE-2 orbits for almost all the instruments.

III. QUIET DAY STUDY

The 22nd of November 1981 can be characterized as a quiet day with a superimposed pair of substorms occurring at 0730 and 0900 UT. In this section, the quiet day aspect of this 24-hour period will be analyzed. Data from several instruments on DE-2 will be used to help define the magnetospheric drivers for the ionosphere and, subsequently, to compare the model ionospheric densities with the in-situ observed densities. During this 24-hour period, data is available from 11 partial DE-2 orbits out of a possible 15 orbits. Five of these northern hemisphere passes have been selected for detailed presentation because complete data sets for the Vector Electric Field Instrument (VEFI), Low Altitude Plasma Instrument (LAPI), and Langmuir Probe (LANG) are available. These five orbits represent the variability found during this 24-hour period, including one pass during the substorm . Figure 2 shows the selected passes, approximated as straight lines, in the polar magnetic coordinates with a *Hardy et al.* [1985] auroral oval shown as the shaded region. Each DE-2 passage is labeled with the approximate time at which the orbit crossed the dawn-side northern high latitude region. This time will be used as the reference for discussions about specific orbits.

3.1. *Electric Field*

Data from the VEFI instrument was used to verify the use of the *Heppner and Maynard* [1987] BC electric field model to simulate plasma convection on this day. The DE-2 ac and dc electric field instrumentation [*Maynard et al.*, 1981] was designed for three-axis measurements using the symmetric double-probe floating potential technique with cylindrical antennas providing 21.4 m baselines. As described by *Maynard et al.* [1982], the Z-axis (east-west geographic) antenna failed to deploy; hence, measurements were restricted to the two components in the orbit plane. The dc data for most purposes are presented in spacecraft coordinates in which the two components are resolved into a horizontal component E_x (positive in the direction of the spacecraft velocity vector) and a vertically upward component. A correction for contact potentials is

determined for each pass using an assumption that the 45° latitude points are at zero potential. For presentation and analysis, the *Ex* component is examined after **v** x **B** fields from the satellite's motion and co-rotation have been removed.

From Figure 2 it can be argued that the missing electric field component on this day is of secondary importance because the orbits lie primarily along the dawn-dusk meridian. The dominant electric field component in this region is along the VEFI E_x direction. This electric field component is available and, hence, its path integral gives a reasonable approximation to the cross polar-cap potential. For this day there are no DE-2 retarding potential analyzer (RPA) data to infer the missing electric field component.

Five passes of VEFI data were compared with the *Heppner and Maynard* [1987] BC electric field model (HM-BC). Figure 3 shows the comparison between the VEFI and HM-BC electric potential for the five orbits shown in Figure 2. In this figure, each panel corresponds to a single pass and is labeled with the orbit time. The HM-BC pattern has the strong electric field in the dawn sector of the polar cap; this asymmetry is associated with the positive IMF *By*. In the potential plots shown in Figure 3, the strong electric fields are associated with regions of large gradients in the potential. The VEFI data, especially the top two panels, show even larger asymmetries in the electric field. This is consistent with the IMF data (Figure 1), which shows that the *By* component is strongest for the first 8 hours of this day. Toward the end of this period, later than 2100 UT, the IMF *Bz* and *By* components become very weak and the convection pattern is expected to depart from the BC pattern. This change is also manifested in the decrease in Kp (Figure 1). The Heppner and Maynard potential patterns have been parameterized and made Kp dependent by *Rich and Maynard* [1989], but we have not included this variation in our simulation. In this instance we believe that the departure from the BC convection pattern as *Bz* approaches zero is more significant than the 30% reduction in Kp, and because we don't know how the convection pattern changed, we adopt a constant BC pattern for the quiet period. The comparison of the electric potential magnitude is best at the latter times when the Kp is lower. At the earlier times, the electric potential variations observed by VEFI are larger than the BC model. By simply changing

the Kp better agreement is not obtained, because the model smooths out these regions of strong electric fields.

3.2. *Auroral Precipitation*

The *Hardy et al.* [1985] auroral precipitation model for Kp=3 was compared to the DE-2 plasma observations. The LAPI instrument on DE-2 consisted of 15 divergent parabolic-plate electrostatic analyzers, each of which provided differential spectral measurements of electrons and positive ions over the energy range from ~ 5 eV to ~ 30 keV with a 1 sec temporal resolution. The analyzer fields-of-view were selected to provide optimal sampling within and outside of the particle source and loss cones at DE-2 altitudes (500--1000 km). For the observations on 22 November 1981, 31-point energy spectral measurements were made for electrons at pitch angles 0°, 7.5°, 15°, 30°, 45°, 60°, 105°, 135°, 165°, and 172.5°. Further details and calibration information on LAPI may be found in *Winningham et al.* [1981].

For each LAPI spectrum, the precipitating electron energy flux from 50 to 20,000 eV was integrated to give an auroral energy flux. Figure 4 shows these energy fluxes for the five selected orbits. Also shown in this figure is the *Hardy et al.* [1985], Kp=3 energy flux at the satellite locations. The auroral precipitation is both more structured and more confined than the statistical oval. For the first half of the day, the LAPI observations are comparable to the model predictions in the oval regions. However, toward the end of the day as the activity decreases (see Figure 1), the LAPI data show lower fluxes of precipitating electrons than the model. In the first three passes shown in Figure 4, the model fluxes are in conflict with the observations in the polar region, i.e., no precipitation is observed while the model suggests about 0.2 erg/cm^2 s should be present. This descrepancy is not severe when it is realized that these three passes are not truly in the polar cap, but just touch the dayside cusp region (see Figure 2). In this region, the difficulty of using a statistical model is highlighted by the model's dayside oval width being significantly wider in latitude than was actually present. The remaining two orbits do cross the polar cap and the fluxes do decrease as expected (see Figure 4, bottom two panels). Hence, the polar cap problem in the first three passes in Figure 4 indicates that the actual oval was somewhat more expanded on the

dayside than the Kp=3 oval we have adopted. This is consistent with the magnetic indices, which were initially at a Kp=3+ level. For the purposes of this study, the Kp=3 oval appears to be reasonable and, hence, we adopted the Hardy Kp=3 model to describe the auroral precipitation for the quiet day and for consistency with the adoption of a fixed convection pattern.

3.3. *Ionospheric Model*

Our ionospheric model was initially developed as a mid-latitude, multi-ion (NO^+, O_2^+, N_2^+, and O^+) model by *Schunk and Walker* [1973]. The time-dependent ion continuity and momentum equations were solved as a function of altitude for a co-rotating plasma flux tube including diurnal variations and all relevant *E* and *F* region processes. This model was extended to include high latitude effects due to convection electric fields and particle precipitation by *Schunk et al.* [1975, 1976]. A simplified ion energy equation was also added which was based on the assumption that local heating and cooling processes dominate (valid below 500 km). The trajectories for plasma motion were determined as the plasma moved in response to convection electric fields. A further extension of the model to include the minor ions N^+ and He^+, an updated photochemical scheme, and the mass spectrometer/incoherent scatter (MSIS) atmospheric model is described in *Schunk and Raitt* [1980].

The addition of "constant" plasma convection and empirical models for particle precipitation is described in *Sojka et al.* [1981a, b]. More recently, the ionospheric model has been extended by *Schunk and Sojka* [1982] to include ion thermal conduction and diffusion-thermal heat flow so that the ion temperature is now rigorously calculated at all altitudes between 120 and 1000 km. The adopted ion energy equation and conductivities are those given by *Conrad and Schunk* [1979]. Also, time-dependent plasma convection and particle precipitation inputs have been used with the basic high-latitude model so that magnetospheric storm and substorm conditions could be studied [*Sojka and Schunk*, 1983, 1984].

For the quiet day aspect of this study, the above ionospheric model was run for a 24-hour

period during which the magnetospheric and solar inputs were fixed. This produced a "diurnally reproducible" electron density data set. The solar conditions were represented by a solar flux F10.7 value of 180. Based upon the indices in Figure 1 and the DE data shown in the previous two sections, the magnetospheric inputs (convection and precipitation) were, respectively, the *Heppner and Maynard* [1987] BC model and the *Hardy et al.* [1985] Kp=3 model. Since both of these models are extensively discussed in the respective references, no further discussion is given here. A neutral atmosphere is also needed; the MSIS model was used for this input [*Hedin*, 1987]. For the MSIS model, the above F10.7 value and Ap=11 were used as input parameters. A simple meridional 200 m/s neutral wind model blowing from 1300 MLT to 0100 MLT was adopted for the dark polar regions. The validity of this wind is difficult to quantify since no IMF dependent wind model is presently available. *Rees and Fuller-Rowell* [1988] used their coupled thermosphere and ionosphere to study the IMF *By* dependence of the high latitude. At latitudes poleward of ~75°, a strong asymmetry is found in the F-region neutral wind as a function of IMF *By*, but at latitudes equatorward of this a meridional wind peaking at ~0100 MLT is found. Since the wind only affects the F-layer at the latitudes equatorward of 75°, this simple wind is consistent with that from the more physical coupled ionosphere-thermosphere model. The TDIM produced a data base of electron densities for magnetic latitudes poleward of 50° over the 100 to 800 km altitude range.

The quiet-day ionospheric simulation for 22 November 1981 is shown in Plate 1 as a UT series of snapshots of N_mF_2 (top panels), h_mF_2 (2nd from top panels), molecular ion density at 300 km (third row), and O+ at 800 km (bottom panels). Six UT snapshots uniformly distributed throughout the day are shown. N_mF_2 indicates how significant the UT control of the polar ionosphere is: at 0100 UT the polar densities are below 4×10^5 cm^{-3}, while at 1700 UT the polar densities everywhere approach 1×10^6 cm^{-3}. Apart from the absolute density differences, the polar cap density is structured. A "tongue of ionization" is evident at most times and is seen as the channel of high densities moving through the cusp region into the polar cap. This tongue extends

first in a westward direction and then over the pole in a predominantly anti-sunward direction. The dawn polar cap has significantly higher densities than does the dusk polar cap. All these density structures are associated with the convection pattern, the IMF *By* positive Heppner and Maynard pattern. The density variation with UT is controlled by the location of the transition from daylight produced ionization to darkness (solar terminator) in relation to the cusp region where plasma enters the polar cap. As this terminator region approaches the cusp, the density in the polar cap increases (compare densities at 0500 and 1700 UT). This effect has been observed by ground -based incoherent scatter radars [*de la Beaujardiere et al.*, 1985].

The second panel from the top shows the height of the *F*-region peak density (h_mF_2). In sunlight, the peak lies just below 300 km, whereas inside the dark polar cap it ranges from as low as 220 km up to 400 km. The highest values are located in the polar cap dawn sector just poleward of the cusp. In this region, the electric fields are the largest (largest flow speeds) and the flow is predominantly towards the magnetic pole. This results in a strong upward drift, i.e., the electric field is perpendicular to the tilted magnetic field which gives rise to an upward **E** x **B** drift. However, on the other side of the pole, this flow leads to a downward drift which appears as the region of lowest h_mF_2 values.

In the vicinity of the peak (300 km), the molecular ions do not show significant polar cap densities or structure (third row). The molecular ions instead, are enhanced in the auroral oval and the sunlit region. This is consistent with the fast recombination time for the molecular ions which inhibits transport effects. Only a very small transport enhancement in the molecular ions can be seen in the region of the high h_mF_2 where the plasma moves into the polar cap.

At 800 km, the ion density variation (bottom panel, Plate 1) is similar to the N_mF_2 variation. For a diurnally reproducible study such as this quiet day, this is not surprising since the topside time constant, on the order of an hour, is 'fast' compared to the times at which the model inputs are changing. This would not be the case during a substorm [*Sojka and Schunk*, 1983, 1984].

3.4. *Electron Density Comparison*

The computed electron densities were compared with those measured by the Langmuir Probe (LANG) on DE-2. The Langmuir Probe instrument was designed to perform in-situ measurements of the electron temperature and the electron and ion densities in the ionosphere. Two independent sensors were connected to individual adaptive sweep voltage circuits and, hence, the LP can continuously track the changing electron temperature and spacecraft potential while autoranging electrometers adjust their gain in response to the changing plasma density. The control signals used to achieve this automatic tracking provide a continuous monitor of the ionospheric parameters. Additionally, internal data storage circuits permit high resolution, high data rate sampling of selected volt-ampere curves for transmission to the ground to verify or correct the inflight processed data. The availability of analog telemetry channels in the DE spacecraft permits the transmission of raw electrometer data from either of the two sensors. Further details can be found in *Krehbiel et al.* [1981].

Figure 5 shows the electron density along the five orbits for the LANG and the TDIM. In each panel the logarithm to the base 10 of the density (cm^{-3}) is plotted against UT. Overall, the model densities track the observed densities fairly well, but there are a few exceptions to this. In the dawn sector at the beginning of each pass, the model is consistently lower than the observations (see arrows labeled A). The LANG density structure in the center of the polar cap is also missing from the model (see arrows labeled B) and the location of the structure in the dusk sector trough (arrows labeled C) does not always coincide with the observed location. Ignoring for the time being the dawn trough discrepancy (A), the density comparison for these five orbits ranges from good to almost excellent (orbit 1400 UT). This is also the case for the other orbits (not shown) for which LANG data were available where the differences fall into the same categories found in Figure 5. These differences are discussed and related to the geophysical conditions in the following section.

3.5 *Quiet-Day Discussion*

Both the LANG observations and the model show that the density does not peak in the auroral region, but rather the peak density is found in the polar cap (see Figure 5). This is because the densities are all in the topside ionosphere at the satellite altitude where the role of plasma transport is more important than that of the auroral precipitation [*Sojka and Schunk*, 1984]. The DE-2 altitude ranges from 800 km on the dawnside to 400 km on the dusk end of each passage (see Figure 2), and hence, the measurements were made above the *F*-region peak. Agreement is also present in the dynamic range of the observed densities with, of course, the exception of the dawn trough region.

The disagreement in observed and modelled densities found in the morning sector trough region was unexpected, since this region is believed to be relatively independent of the magnetospheric inputs. Figure 6 shows the relevant ionospheric morphology in this region. A circle represents the region where the model densities are low relative to the LANG densities. This circle is located equatorward of the nocturnal auroral region and is in darkness; the straight line represents the solar terminator. Passing through this region is the 0735 UT DE-2 satellite track. In the TDIM, the plasma present in the large circle has co-rotated to this region from around midnight. During this co-rotation the plasma flux tubes have remained equatorward of the auroral oval (see dashed line in Figure 6). These co-rotational and auroral conditions are consistent with the VEFI observations (Figure 3) in that the electric potential is not changing with latitude ($E \approx 0$) and the LAPI (Figure 4) data which indicates the region to be equatorward of the auroral precipitation. The TDIM densities in these flux tubes are maintained by the upward induced drift caused by the generally equatorward neural winds. Although this mechanism is adequate to maintain the ionosphere around midnight, it is unable to do so just prior to sunrise [*Sojka et al.*, 1981b]. This is the first attempt to check the topside densities in the trough at these pre-sunrise times. The model densities are clearly too low in this region for the first four orbits shown in Figure 5, although the final orbit does agree better with the model. An extensive check has been made to confirm that the observed densities are accurate, and LANG data from other days confirms this

trend. This result has led us to begin a follow-up study to determine what is missing in the TDIM nighttime trough processes. The obvious candidate is a downward plasma flux from the plasmasphere, which was set to zero in the simulation owing to a lack of measurements of this parameter.

Polar cap density structures, as highlighted by the B arrows in Figure 5, are not expected to be present in the TDIM. The model uses only statistically smooth inputs for the magnetospheric convection and precipitation and, hence, no source for multiple structures in the polar cap is present. However, this picture is somewhat over simplified; certain aspects of the structure can be related to the presently used inputs. For the first two orbits in Figure 5, the first B arrow points to a region in the polar cap where the density increases from about 3×10^4 to 3×10^5 cm^{-3} over a very small distance. Figure 3 VEFI data show that this is the region of largest electric fields in the polar cap. These measured electric fields are stronger than those obtained from the HM-BC input to the TDIM simulation. These electric fields are responsible for convecting plasma through the cusp region into the polar cap. The polar cap density features then depend upon the plasma and convection in the vicinity of the cusp. Such a cusp control can be seen in N_mF_2 as a function of UT in Plate 1. These convecting density structures have been reported [*Weber et al.*, 1984, 1986] and are referred to as F-layer patches. Morphologically, they are present during IMF southward conditions, while their sizes and locations depend on the variability in the cusp convection in ways not fully understood. Earlier TDIM ionospheric studies have shown that significant polar cap density structuring is possible even with smooth inputs [*Sojka and Schunk*, 1987; *Rasmussen et al.*, 1986a]. In this study, the HM-BC model does not have a strong enough electric field to reproduce the structures observed along the first two orbits shown in Figure 5. Density structure B' in the 2210 UT pass (Figure 5, bottom panel) is a larger feature. Towards the end of the quiet period, the IMF *Bz* component approached zero and, hence, the actual convection pattern must have changed. This density feature may well be the equivalent of the TDIM density enhancement from 2220 to 2223 UT in the same orbit panel of Figure 5. The B' density structure is certainly

not a precipitation feature (Figure 4) since no appreciable precipitation is present.

The C arrows in Figure 5 highlight the third region where differences are present between the modelled and observed densities. In this case, the differences are not systematic and are not present in all cases. This region is the afternoon sector trough. Here, the depleted trough densities are associated with a combination of the convection-co-rotation balance and the presence of the auroral equatorward boundary [*Sojka et al.*, 1981a]. For the orbit at 1400 UT, an almost perfect agreement is found in the densities (Figure 5) and the convection (Figure 3), while for the orbit at 2210 UT, the observed trough is significantly more poleward and a similar difference is seen in the convection at that time. Hence, the differences highlighted by the C arrows are probably associated with the electric field variability not present in the HM-BC convection model. At present, there are no methods available to reconstruct the variability in the electric field data.

What about the "substorms"? In Figure 5 the 0735 UT pass occurred during the substorm period. However, it does not look especially different from the other orbits. Neither the convection (Figure 3) nor the precipitation (Figure 4) appear significantly more disturbed. Nevertheless, the DE-1 spin-scan auroral imager (SAI) data do show significant differences in the precipitation during this time. The next section looks at this substorm period in depth.

IV. THE 0635-0935 UT SUBSTORM PERIOD

4.1. *Auroral Imagery*

The high-altitude satellite DE-1 obtained continuous sequences of auroral images in time intervals in excess of four hours for some orbits during the fall of 1981. The satellite is equipped with a spin-scan auroral imager (SAI) that comprises three scanning photometers with off-axis parabolic reflectors as the primary optical elements. Two of these imaging photometers provide global auroral images at visible wavelengths, each utilizing any of 12 filters selected by ground command. The third photometer is capable of auroral imaging at vacuum ultraviolet (VUV) wavelengths with a similar selection of one of its 12 filters. In typical operation, a 30° x 120° image is obtained every 12 minutes for each photometer. The images are centered in the Earth nadir direction, with the 30° angular width of each image aligned transverse to the plane of satellite rotation and the coplanar satellite orbital plane. A detailed description of the imaging instrumentation is given by *Frank et al.* [1981].

During the substorm period, images were obtained every 12 minutes from 0635 to 0912 UT. A total of 14 images show the auroral dynamics during this period. Images were taken simultaneously at 557 and 630 nm in the visible spectrum and in the vacuum ultraviolet (VUV) over the 123--160 nm bandwidth. On this day the 630 nm intensities were very low and because of statistical considerations were not suitable for use in the energy flux-characteristic energy analysis described by *Sojka et al.* [1989]. Plate 2 shows the VUV images for this substorm period and the color key gives the observed SAI photometer compressed pixel counts. From these observations, the auroral dynamics is evident. In the evening and night sectors, discrete auroral forms are present over a large region and they display a significant temporal variation, i.e., changes in these structures are seen from one image to the next. Substorm onsets are observed in the 0723 and then the 0836 UT images. None of these spatial or temporal features are present in the statistical auroral model used in the quiet-day study.

To use the images in Plate 2 as an input to the TDIM, they must be converted to

precipitating energy fluxes. The lower panels in each pair of images in Plate 2 show these energy fluxes. *Sojka et al.* [1989] discussed at length the procedures used to convert the SAI images to energy flux. In this study, two levels of conversion were considered; the first is the relative energy flux which conserves the auroral spatial and temporal variability, and the second is the absolute energy flux calibration. As has been noted by *Sojka et al.* [1989] and others [*Rees et al.* 1988], the second part is extremely difficult to do from first principles. The procedure used here is to obtain the relative auroral dynamics (spatial and temporal) from the images and then to scale the energy fluxes to achieve consistency with the LAPI data. This follows the general procedures described by *Sojka et al.* [1989]. The energy fluxes were computed from the VUV images by the algorithm described by *Rees et al.* [1988]. These energy fluxes were within a factor of two of the LAPI energy fluxes, which statistically was the same as found by *Sojka et al.* [1989]. Hence, the same scaling factor was used to scale all the computed image energy fluxes to the LAPI level. The resulting energy fluxes are shown in the lower panel of each pair in Plate 2 with a color key in ergs/cm^{2}s. The 14 images span the entire image period and during this time the auroral region undergoes significant changes. The AE index peaks at 0800 and again at 0930 UT, which roughly correspond to the times of maximum expansion in the substorms.

4.2. *Substorm Density Comparison*

The TDIM was rerun using energy fluxes obtained from DE-1 images to simulate the ionospheric response to the auroral dynamics during the substorm period. From Figure 1 it can be argued that prior to about 0635 UT the auroral conditions were quiet, i.e., the AE index was relatively small and varied smoothly. On this basis, the previous quiet-day TDIM densities were used as the initial conditions at 0635 UT for the substorm simulation. During the substorm period, insufficient data were available to define a dynamic convection model and, hence, the HM-BC model was used again. Therefore, only the auroral inputs were changed for the substorm simulation. The Hardy empirical auroral model was replaced with a time varying sequence of image energy fluxes. These images occur at 12 minute intervals. In using the image energy

fluxes, each was assigned an image UT (the middle of its 12 minute period) and then energy fluxes at a given location were obtained by linearly interpolating between two images that occurred before and after the required TDIM UT.

In creating the dynamic auroral model from the SAI images, it was difficult to infer the characteristic energy of the precipitation on this day. This is because the characteristic energy is deduced from the ratio of emissions at different wavelengths. The 630 nm emission is crucial for this ratio calculation. As already pointed out, the 630 nm had low count rates, hence, these data could not constrain this parameter. The computed ionospheric densities do, however, depend upon the characteristic energy. In the Appendix, a parametric study of this dependence is given. Based on the limited data available, we adopted a characteristic energy model; the SAI images, the LAPI data, and the *Hardy et al.* [1985] characteristic energies were used to define this model. The model defines the characteristic energy in the polar cap to be 1 KeV and equatorward of the oval to be 5 KeV. Inside the oval in the morning sector it is also 5 KeV, while in the afternoon-evening oval it is 3 KeV. In this model the oval is defined as regions where the energy flux exceeded 0.5 erg/cm^{2}s.

Figure 7 compares the substorm TDIM (Adopted E_0 line), the quiet day TDIM (Original Simulation line), and the LANG observations for the 0735 UT DE-2 pass. The model/measurement discrepancy in the dawn sector trough is, as expected, unchanged. In the polar cap, especially the dusk sector, the new model densities are in significantly better agreement with the LANG observations. However, the earlier similarity between model and data in the dusk sector trough is changed and now there is a marked difference in densities. The substorm TDIM (Adopted E_0) densities are almost an order of magnitude larger than the LANG trough densities, whereas the quiet day TDIM densities were only a factor of two larger than the LANG densities. This feature is significant and will be discussed in the following section. A second northern hemisphere DE-2 LANG pass occurred later in the substorm period. Figure 8 shows the LANG density (crosses), as well as the quiet day (solid line, Original Simulation) and substorm (solid line, Adopted E_0) simulation densities. This pass occurred between 0915 and 0935 UT, which

was toward the end of the image sequence and at the time of the second peak in the AE index (see Figure 1). Because several hours have elapsed since the beginning of the substorm, the simulation is independent of the initial quiet conditions. This is in contrast to the pass at 0735 UT which occurred near the beginning of the image sequence. In Figure 8, the substorm simulation shows significantly better agreement with the observed densities. It lacks the sharp polar cap density structures, but this is to be expected due to the lack of convection structure in the model. As with Figure 7, the biggest disagreement occurs in the dusk sector auroral oval/trough region. In this case, the trough minimum is matched reasonably well; however, the model predicts a huge density maximum in the oval at 0928 UT. The following section describes in depth how the discrepancy in Figure 7 arose. The argument to be presented also applies to the density difference shown in Figure 8.

4.3. *Substorm Discussion*

The density comparison in the polar regions indicates that the dynamic auroral TDIM simulation yields a better agreement with the data (see Figure 7). However, of concern is the larger discrepancy produced in the dusk sector trough. In order to understand this, Figure 9 is used to graphically display the plasma mechanisms leading to this greater difference. The circle indicates the region where the substorm TDIM produced the larger densities. This region lies in a region of auroral emissions, as indicated by the shaded region in Figure 9. In comparison, the original oval does not coincide with this circle (compare Figure 9 with Figures 6 or 2). Hence, the images show that during the substorm period, auroral precipitation extends considerably more equatorward in this local time sector than predicted by the statistical oval. In fact, this interpretation is consistent with the LAPI data which show strong precipitation equatorward of the statistical oval (see Figure 4, the 0735 UT pass at about 0753 UT).

Also shown in Figure 9 are the trajectories of two plasma flux tubes that form this enhanced density region. On each trajectory the small circles mark hourly intervals. One of the trajectories (labeled *a*) is for plasma convecting around from the dayside and stagnating in the

circle. This trajectory is responsible for the high TDIM densities because the plasma stagnates in a region of high auroral energy fluxes. However, such a scenario is extremely unlikely; stagnation occurs only in regions equatorward of the auroral oval where the magnetospheric electric field tends to cancel the co-rotational electric field. Hence, the inability to dynamically modify the convection pattern during the substorm has resulted in the "spurious" high TDIM densities. Furthermore, as seen in Figure 7, there is almost no dusk sector trough in this substorm simulation. From this it can be deduced that the magnetospheric electric field must have penetrated to lower latitudes. The single DE-2 substorm pass at 0735 UT in Figure 3 indicates that this is the case. The second plasma flux tube trajectory (labeled *b*) shown in Figure 9 represents the typical poleward edge of the dusk sector trough. Here, the plasma is convecting sunward inside the oval to the region of interest. High TDIM densities are associated with this flux tube because it is in a region of high precipitation for several hours. The DE-2 orbit track at 0735 UT is superimposed on Figure 9 as the line with small crosses.

V. SUMMARY

In this study we have used an extensive DE data base to both constrain inputs to the TDIM and then check the simulated densities. This has been done for both a quiet period and a substorm period. The quiet period had a duration of about 24 hours, while the substorm duration was 3 hours and occurred 6.5 hours into the quiet period. This is the most extensive high latitude TDIM-data comparison carried out to date. Aspects of the study can almost be regarded as looking at ionospheric "weather" rather than the usual "climatology." Such a capability can only arise when the inputs constraining the model are available with adequate resolution and coverage. Under ideal conditions the combined DE-1 and DE-2 data bases can almost achieve this resolution, as the study has shown.

The study can be summarized by the following key findings:

(1) The quiet-day study produced very good agreement between modelled and observed electron densities in the topside ionosphere with two important

exceptions.

(a) Across the polar region the DE-2 LANG densities showed fine structure (F-layer patches) in addition to the overall regional density morphology. Such fine structure is associated with the "weather" variability in the magnetospheric inputs. These cannot be completely described by the present day observations. The full extent of this structure is, therefore, missing from the simulated densities.

(b) A surprising discrepancy arose in the pre-sunrise mid-latitude trough. The TDIM densities were an order of magnitude lower than those observed by DE-2. This discrepancy was not restricted to this day; the measured densities were similar in this region over many days. This region is also independent of the magnetospheric inputs and so does not rely on good resolution in the DE inputs. A follow-up study has been initiated to elucidate the source of this marked discrepancy.

(2) The substorm study showed remarkably good agreement with the observed densities with again two exceptions.

(a) The observed fine structuring of the polar cap densities was even more marked during the substorm period. During a substorm, the highest degree of "weather" is present. No method of achieving both the temporal and spatial coverage is available to describe the source of this structure.

(b) Although the auroral image sequence produces a very good description of the global substorm, the associated convection electric field is not available. This can lead to drastic errors in the model prediction. In this case, the dusk sector stagnation occurred inside the auroral oval. The ensuing TDIM density enhancement was over an order of magnitude greater than observed. Such a discrepancy is purely an artifact of not having the necessary electric field measurements to couple the auroral and convection patterns self-

consistently.

This study shows again the importance of using extensive data bases to constrain the global and temporal behavior of the magnetospheric inputs to the ionospheric (and thermospheric) system. Even under quiet conditions, as shown by this study, simplifying model assumptions need to be verified. Under dynamic substorm conditions, even simple mismatching between inputs leads to major errors in calculated ionospheric densities. More work is needed in deducing an empirical means of making convection and precipitation patterns self-consistent during temporal variations. This would be even more useful as global auroral imagery becomes a standard replacement for statistical auroral inputs. The major "weather" aspects will require not only high resolution imagery of the precipitation, but also information concerning the structure in the convection pattern. It is the structure in the convection pattern that produces the density fine structure, as shown simplistically in the TDIM polar cap structure of Plate 1.

Acknowledgements. This research was supported by NASA grants NAGW-1547, NAGW-77 and NAG5-1484 to Utah State University, by NASA contract NAS5-33031 to Southwest Research Institute. At the University of Iowa this research was supported in part by NASA under grants NAG5-483 and NAGW-1536. The VEFI data was made available to us by J. Heppner and N. Maynard. The expertise of R. Dvorsky greatly simplified the auroral image analysis.

APPENDIX

The depth into the thermosphere that an auroral electron can penetrate and the altitude distribution of ionization depend upon several factors. The most important factor is the energy of the electron. When a flux of electrons travels through the ionosphere, the energy is characterized not by a single value, but by the initial energy spectrum. A lengthly calculation is needed to deduce the associated altitude distribution of ionization. To simulate this process, the TDIM selects between ionization profiles for different characteristic energies, different seasons, and different solar cycle conditions. These basic ionization profiles were computed using the Strickland auroral deposition code (*R. Daniel*, private communication, 1988).

Figure 10 shows the sensitivity of the TDIM density calculation to the characteristic energy. The substorm simulation described in Section 4 was repeated three times for three fixed charac-

teristic energies. In each case, the energy fluxes varied as shown in Plate 2, i.e., according to the image variability. Three results for typical auroral energies are shown in Figure 10, namely 1, 3, and 5 KeV. Since the densities shown in Figure 10 are along the DE-2 track used in Figure 7, they are all in the topside ionosphere. In this region, the lowest energies contribute the most ionization, although the integrated ionization is largest for the most energetic electrons. The curves shown in Figure 10 indicate that a factor of 2 to 4 density difference can be anticipated for the expected uncertainty in the auroral electron energy.

For the Adopted E_0 data shown in Figures 7 and 8, the following simple auroral characteristic energy distribution was adopted:

1) Inside the polar cap, poleward of the auroral oval magnetic latitude, $E_0 = 1$ KeV.

2) Inside the afternoon-evening sector oval, $E_0 = 3$ KeV.

3) Inside the morning sector oval, $E_0 = 5$ KeV.

4) Equatorward of oval, $E_0 = 5$ KeV.

In this case the oval is defined as a region where the auroral energy flux exceeds 0.5 erg/cm^{2}s.

REFERENCES

Conrad, J. R., and R. W. Schunk, Diffusion and heat flow equations with allowance for large temperature differences between interacting species, *J. Geophys. Res., 84*, 811-822, 1979.

de la Beaujardiere, O., V. B. Wickwar, G. Coudal, J. M. Holt, J. D. Craven, L. A. Frank, L. H. Brace, D. S. Evans, J. D. Winningham, and R. A. Heelis, Universal Time dependence of nighttime *F* region densities at high latitudes, *J. Geophys. Res., 90*, 4319-4332, 1985.

Evans, D. S., Global statistical patterns of auroral phenomena, in *Quantitative Modelling of Magnetosphere-Ionosphere Coupling Processes*, pp. 325-330, Kyoto Sangyo University, Kyoto, Japan 1987.

Frank, L. A., J. D. Craven, K. L. Ackerson, M. R. English, R. H. Eather, and R. L. Carovillano, Global auroral imaging instrumentation for the Dynamics Explorer mission, *Space Sci. Instrum., 5*, 369-393, 1981.

Fuller-Rowell, T. J., D. Rees, S. Quegan, R. J. Moffett, and G. J. Bailey, Interactions between neutral thermospheric composition and the polar ionosphere using a coupled ionosphere-thermosphere model, *J. Geophys. Res., 92*, 7744-7748, 1987.

Hardy, D. A., M. S. Gussenhoven, and E. Holeman, A statistical model of auroral electronprecipitation, *J. Geophys. Res., 90*, 4229-4248, 1985.

Hedin, A. E., MSIS-86 Thermospheric Model, *J. Geophys. Res., 92*, 4649-4662, 1987.

Heelis, R. A., J. K. Lowell, and R. W. Spiro, A model of the high-latitude ionospheric convection pattern, *J. Geophys. Res., 87*, 6339-6345, 1982.

Heppner, J. P., and N. C. Maynard, Empirical high-latitude electric field models, *J. Geophys. Res., 92*, 4467-4489, 1987.

Krehbiel, J. P., L. H. Brace, R. F. Theis, W. H. Pinkus, and R. B. Kaplan, The Dynamics Explorer langmuir probe instrument, *Space Sci. Instrum., 5*, 493-502, 1981.

Maynard, N. C., E. A. Bielecki, and H. F. Burdick, Instrumentation for vector electric field

measurements from DE-B, *Space Sci. Instrum., 5*, 523, 1981.

Maynard, N. C., J. P. Heppner, and A. Egeland, Intense variable electric fields at ionospheric altitudes in the high-latitude regions as observed by DE-2, *Geophys. Res., Lett., 9*, 981, 1982.

Rasmussen, C. E., R. W. Schunk, and J. J. Sojka, Effects of different convection models upon the high-latitude ionosphere, *J. Geophys. Res., 91*, 6999-7005, 1986*a*.

Rasmussen, C. E., R. W. Schunk, J. J. Sojka, V. B. Wickwar, O. de la Beaujardiere, J. Foster, J. Holt, D. S. Evans, and E. Nielsen, Comparison of simultaneous Chatanika and Millstone Hill observations with ionospheric model predicitons, *J. Geophys. Res., 91*, 6986-6998, 1986*b*.

Rees, D. and T. J. Fuller-Rowell, Seasonal and geomagnetic response of the thermosphere and ionosphere, *AGARD-CP-441*, 21.1-7, 1989.

Rees, M. H., D. Lammerzheim, R. G. Roble, J. D. Winningham, J. D. Craven, and L. A. Frank, Auroral energy deposition rate, characteristic electron energy, and ionospheric parameters derived from Dynamics Explorer 1 images, *J. Geophys. Res., 93*, 12841-12860, 1988.

Rich, F. J. and N. C. Maynard, Consequences of using simple analytical functions for the high-latitude convection electric field, *J. Geophys. Res., 94*, 3687-3701, 1989.

Roble, R. G., E. C. Ridley, and R. E. Dickinson, On the global mean structure of the thermosphere, *J. Geophys. Res., 92*, 8745-8758,1987.

Schunk, R. W. and W. J. Raitt, Atomic nitrogen and oxygen ions in the daytime high-latitude F region, *J. Geophys. Res., 85*, 1255-1272, 1980.

Schunk, R. W. and J. J. Sojka, Ion temperature variations in the daytime high-latitude F region, *J. Geophys. Res., 87*, 5169-5183, 1982.

Schunk, R. W. and J. C. G. Walker, Theoretical ion densities in the lower ionosphere, *Planet. Space Sci., 21*, 1875-1896, 1973.

Schunk, R. W., W. J. Raitt, and P. M. Banks, Effect of electric fields on the daytime high-latitude E and F regions, *J. Geophys. Res., 80*, 3121-3130, 1975.

Schunk, R. W., P. M. Banks, and W. J. Raitt, Effects of electric fields and other processes upon the nighttime high latitude F layer, *J. Geophys. Res., 81*, 3271-3282, 1976.

Sojka, J. J., and R. W. Schunk, A theoretical study of the high latitude F region's response to magnetospheric storm inputs, *J. Geophys. Res., 88,* 2112-2122, 1983.

Sojka, J. J., and R. W. Schunk, A theoretical F region study of ion compositional and temperature variations in response to magnetospheric storm inputs, *J. Geophys. Res., 89,* 2348-2358, 1984.

Sojka, J. J., and R. W. Schunk, A theoretical study of the global F region for June solstice, solar maximum, and low magnetic activity, *J. Geophys. Res., 90*, 5285-5298, 1985.

Sojka, J. J., and R. W. Schunk, A theoretical study of the high-latitude ionosphere's response to multicell convection patterns, *J. Geophys. Res., 92,* 8733-8744, 1987.

Sojka, J. J., W. J. Raitt, and R. W. Schunk, A theoretical study of the high-latitude winter F region at solar minimum for low magnetic activity, *J. Geophys. Res., 86*, 609-621,1981a.

Sojka, J. J., W. J. Raitt, and R. W. Schunk, Theoretical predictions for ion composition in the high-latitude winter *F* region for solar minimum and low magnetic activity, *J. Geophys. Res., 86,* 2206-2216, 1981b.

Sojka, J. J., R. W. Schunk, J. D. Craven, L. A. Frank, J. Sharber, and J. D. Winningham, Modeled F region response to auroral dynamics based upon Dynamics Explorer auroral observations, *J. Geophys. Res., 94*, 8993-9008, 1989.

Sojka, J. J., R. W. Schunk, J. V. Evans, J. M. Holt, and R. H. Wand, Comparison of model high-latitude electron densities with Millstone Hill observations, *J. Geophys. Res., 88*, 7783-7793, 1983.

Sojka, J. J., C. E. Rasmussen, and R. W. Schunk, An interplanetary magnetic field dependent model of the ionospheric convection electric field, *J. Geophys. Res, 91*, 11,281-11,290, 1986.

Spiro, R. W., P. H. Reiff, and L. J. Maher, Precipitating electron energy flux and auroral zone conductances: An empirical model, *J. Geophys. Res., 87*, 8215-8227, 1982.

Volland, H., A model of the magnetospheric electric convection field, *J. Geophys. Res., 83,* 2695-2699, 1978.

Weber, E. J., J. Buchau, J. G. Moore, J. R. Sharber, R. C. Livingston, J. D. Winningham, and B. W. Reinisch, *F* Layer ionization patches in the polar cap, *J. Geophys. Res., 89,* 1683-1694, 1984.

Weber, E. J., J. A. Klobuchar, J. Buchau, H. C. Carlson, Jr., R. C. Livingston, O. de la Beaujardiere, M. McCready, J. G. Moore, and G. J. Bishop, Polar cap F-layer patches: Structure and dynamics, *J. Geophys. Res., 91,* 12,121-12,129, 1986.

Winningham, J. D., J. L. Burch, N. Eaker, V. A. Blevins, and R. A. Hoffman, The low altitude plasma instrument (LAPI), *Space Sci. Instrum., 5,* 465-475, 1981.

ILLUSTRATIONS

Figure 1. Geomagnetic and IMF indices for 22 November 1981, and a chart indicating when DE-1 auroral images were available (gray shading on the UT axis). The 3-hourly Kp index is plotted in the top panel while the auroral electroject index, AE, is plotted in the bottom panel. Two components of the IMF, *By* and *Bz*, are plotted in the middle panel.

Figure 2. DE-2 orbit tracks in the northern hemisphere in dipole latitude-MLT coordinates in a polar format. These five orbits are used to highlight the electric field and particle precipitation data. In the dawn sector, the DE-2 altitude is about 800 km which decreases to below 400 km in the dusk sector. A *Hardy et al.* [1985] Kp=3 oval is shown for reference, as the shaded region. The shading corresponds to energy fluxes larger than 0.25 ergs/cm^2 s.

Figure 3. Electric potential along the DE-2 satellite track for five northern hemisphere passes on 22 November 1981. The electric potential computed from the VEFI electric field data (dashed line) is compared with that from the *Heppner and Maynard* [1987] BC Kp=3 model (solid line) is shown as the solid line. The five satellite tracks are shown in Figure 2.

Figure 4. Electron precipitation flux along the DE-2 satellite track for five northern hemisphere passes on 22 November 1981. The precipitation flux computed from the LAPI electron instrument (dashed line) is compared with that from the *Hardy et al.* [1985] Kp=3 model (solid line). The energy flux is in ergs/cm^{2}s. The five satellite tracks are identical to those used in Figure 3 and shown in Figure 2.

Figure 5. Electron density along the DE-2 satellite track for five northern hemisphere passes on 22 November 1981. The electron density from the LANG instrument ("+" symbols) is compared

with that from the TDIM (solid line). The electron density is in cm^{-3}. The five satellite tracks are identical to those in Figures 2-4.

Figure 6. Schematic view of the plasma/DE-2 geometry in the low density pre-dawn trough region plotted in a dipole latitude-MLT polar format. This region is shown as a circle on the line representing a DE-2 satellite track, and the dashed line represents a co-rotational plasma trajectory. The shaded region shows the *Hardy et al.* [1985] auroral oval, while the terminator is shown as the solid line across the dayside. The format is the same as for a single panel of Figure 5.

Figure 7. Electron density comparison during the 0735 UT substorm on 22 November 1981. The DE-2 LANG data are compared with the TDIM simulations. Two TDIM simulations are shown, the original (from Figure 5) and the storm case labeled Adopted E_0.

Figure 8. Second substorm electron density comparison on 22 November 1981. The DE-2 LANG data are compared with the TDIM simulations. The figure layout is identical to that of Figure 7.

Figure 9. Schematic view of the plasma/DE-2 geometry in the "stagnation" dusk trough region plotted in a dipole latitude-MLT polar format. This region is shown as the intersection of the solid, crossed, line representing a DE-2 satellite track and the solid, circled line (labeled *a*) representing a plasma trajectory. The shaded region shows the auroral precipitation inferred from an appropriate DE-1 SAI auroral image (> 0.25 $ergs/cm^2s$).

Figure 10. Model electron density variation along the DE-2 orbit track during the 0735 UT storm period. Each curve represents the TDIM simulation for different characteristic energies. In each case the SAI images were used to determine the energy flux for the auroral precipitation. The

densities are in electrons/cm^3. This is the same orbit shown in Figure 7.

Plate 1. Color coded snapshots of the quiet-day ionospheric simulation at six equally spaced times. Top row corresponds to N_mF_2, 2nd row to h_mF_2, 3rd row to the molecular ion density at 300 km, and the bottom row to the electron density at 800 km. Data are color coded in magnetic latitude-MLT polar format from 50 degrees to the pole. The polar dial format is identical to that used in Figures 2, 6, and 9. Color keys are given on the right side of each row.

Plate 2. Fourteen DE-1 VUV auroral images and the inferred auroral energy fluxes during the substorm period on 22 November 1981. The top panel in each pair is the VUV compressed count rate image, while the lower panel is the energy flux in the same polar plot used in Plate 1. Color keys are given on the right side of each row.

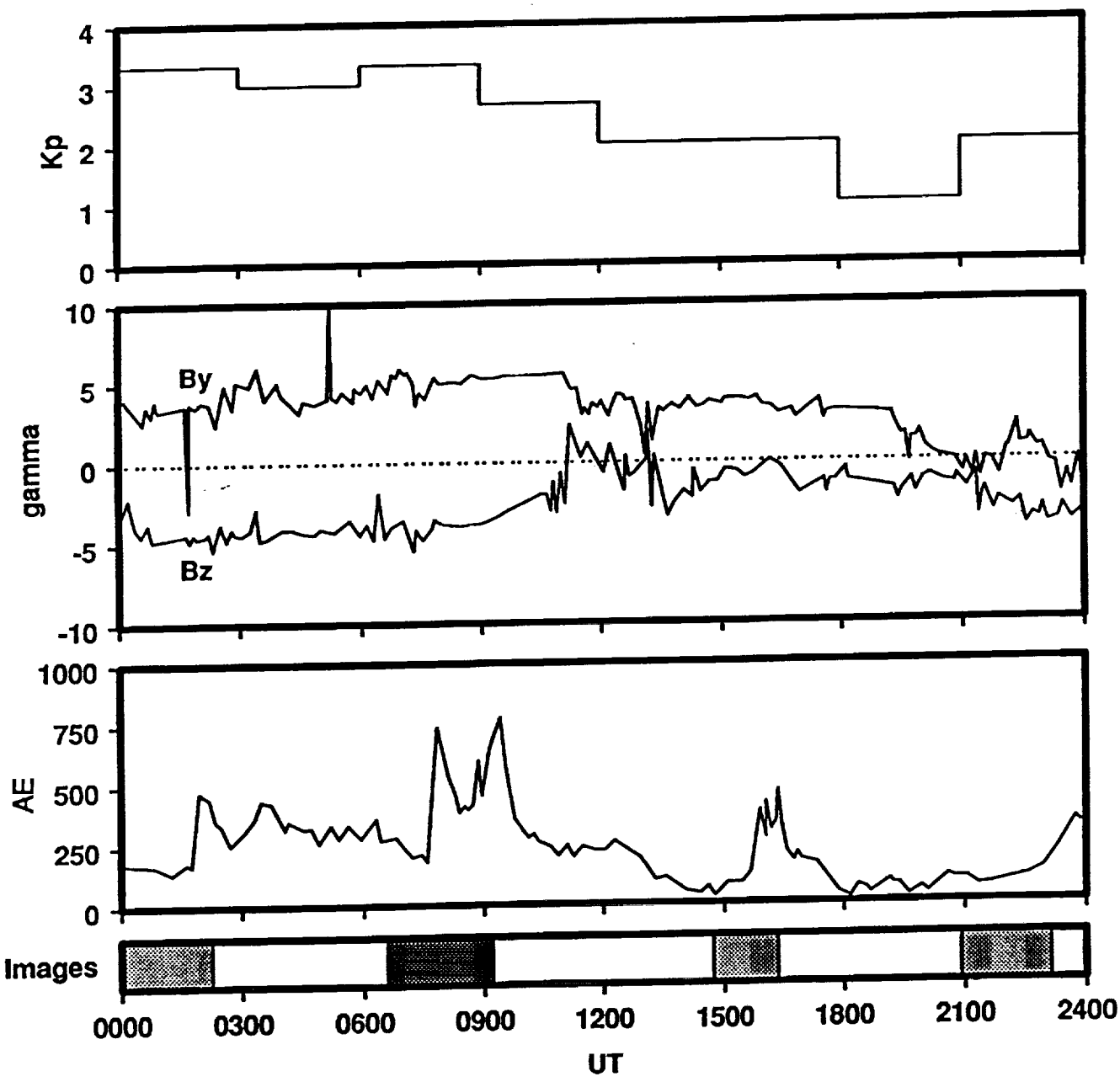
Kp
4
3
2
1
0
gamma
10
5
0
-5
-10
By
Bz
AE
1000
750
500
250
0
Images
0000
0300
0600
0900
1200
1500
1800
2100
2400
UT

Figure 1

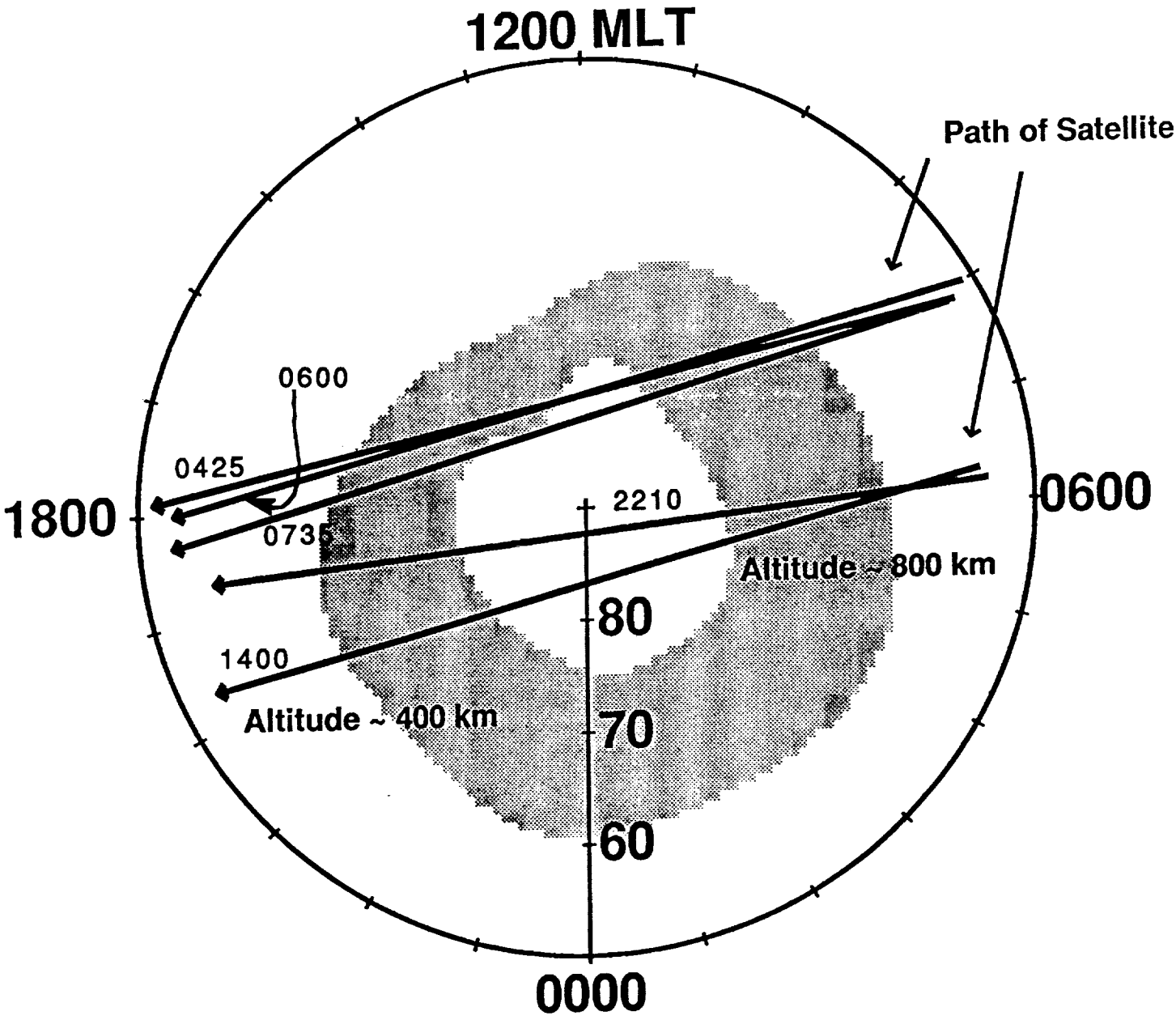
1200 MLT
Path of Satellite
0600
0425
1800
0600
2210
0735
Altitude ~ 800 km
80
1400
Altitude ~ 400 km
70
60
0000

Figure 2

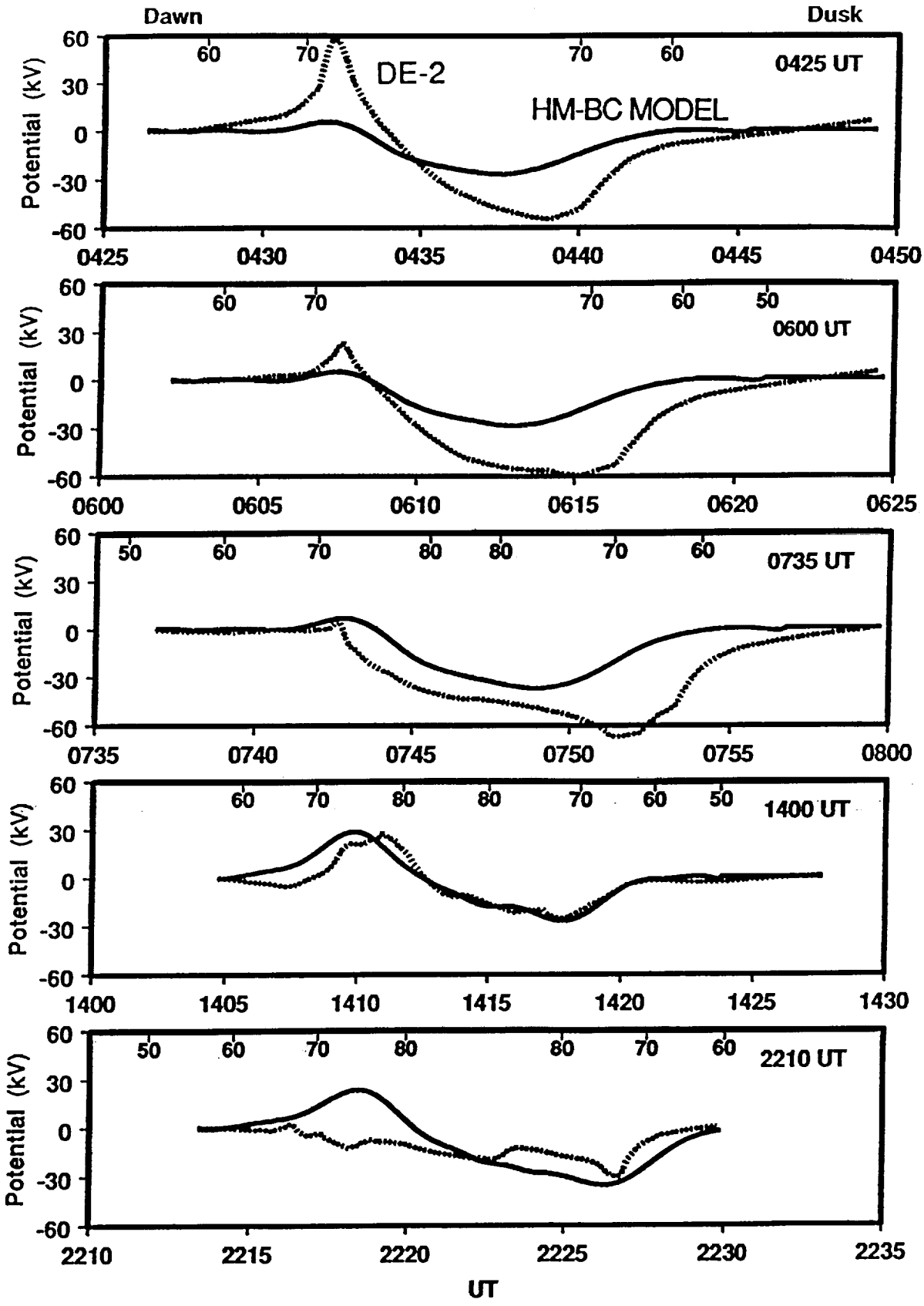
Dawn
Dusk
DE-2
HM-BC MODEL
0425 UT
0600 UT
0735 UT
1400 UT
2210 UT
Potential (kV)
UT

Figure 3

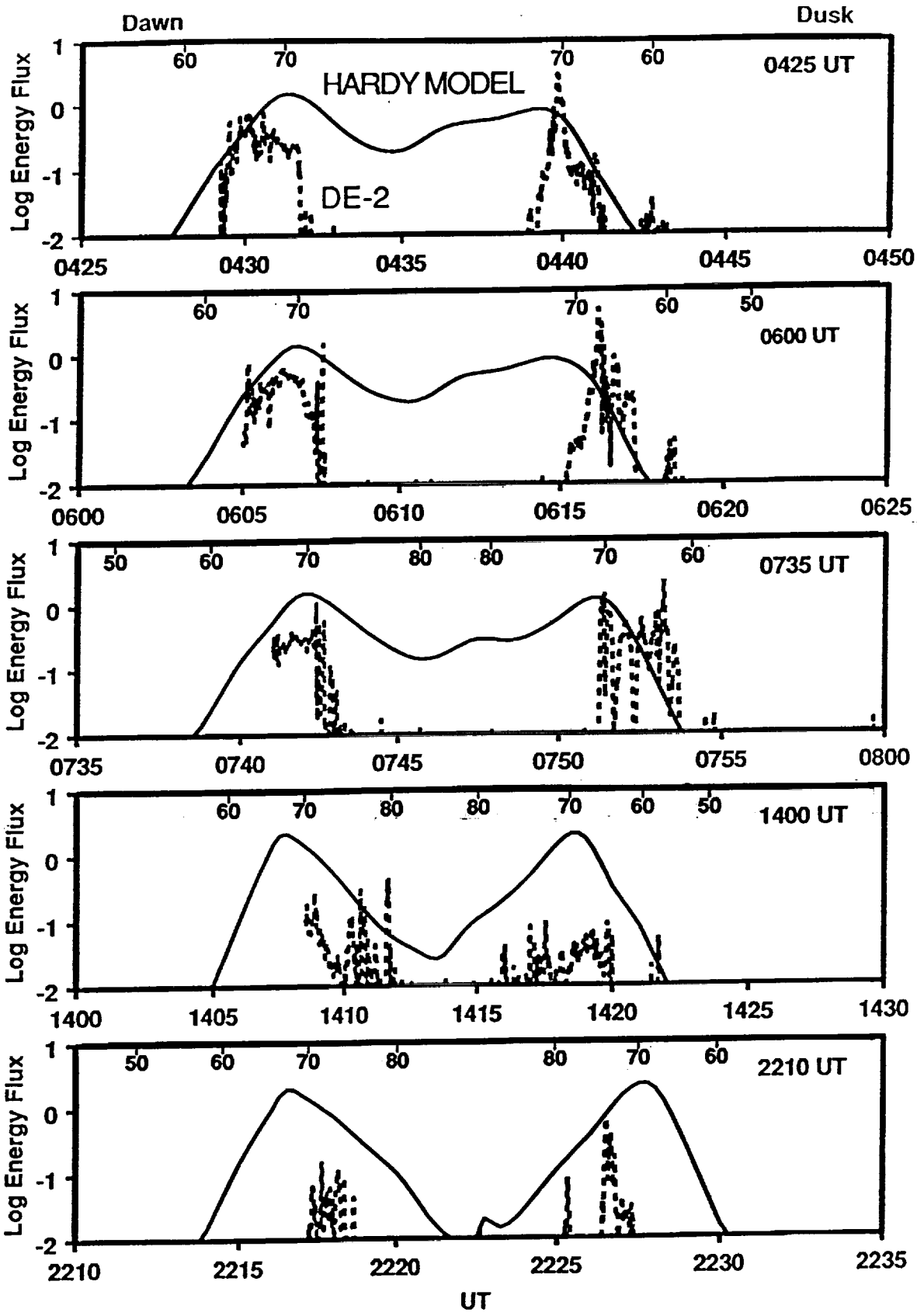
Dawn
Dusk
HARDY MODEL
DE-2
0425 UT
0600 UT
0735 UT
1400 UT
2210 UT
Log Energy Flux
UT

Figure 4

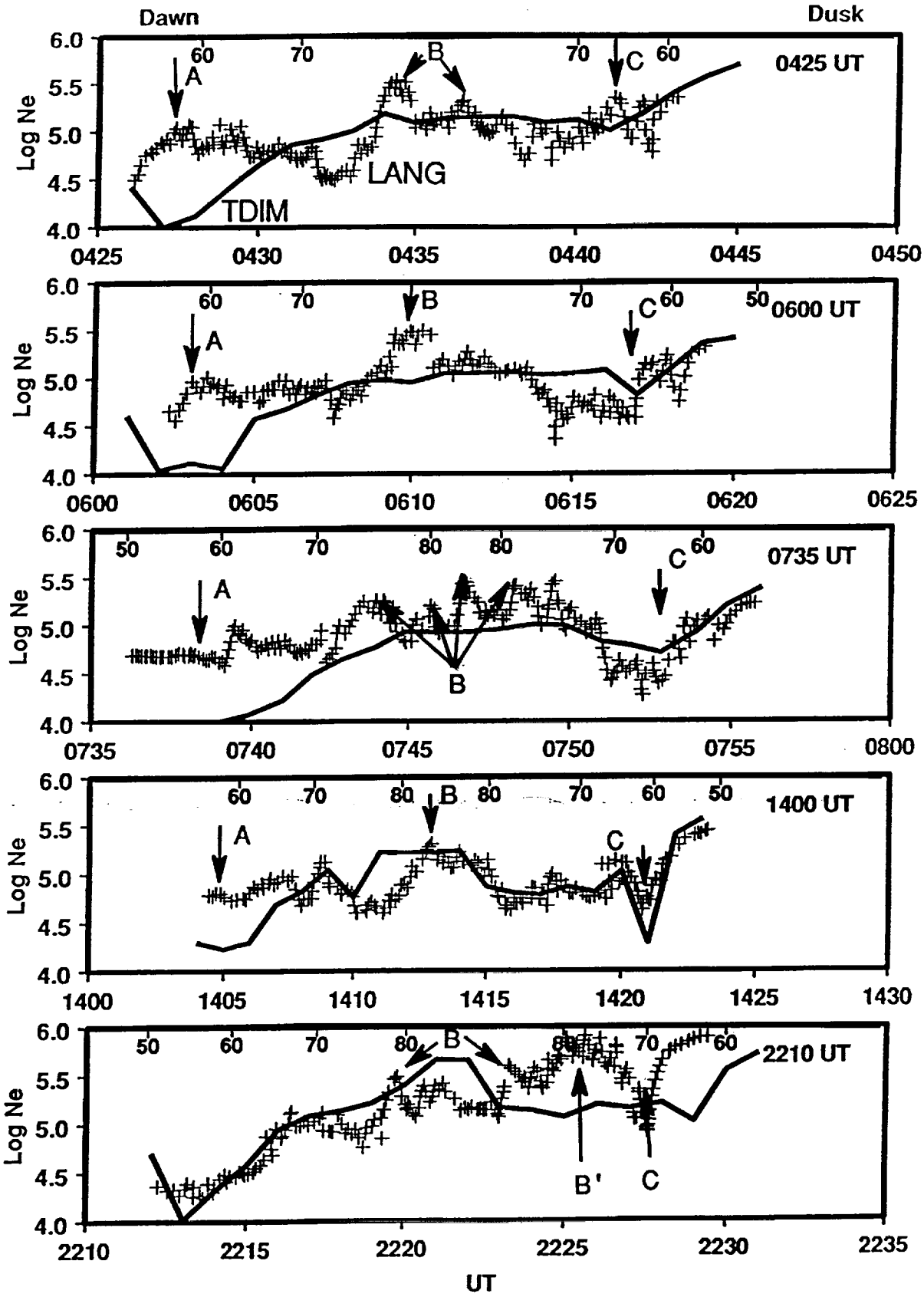
Dawn
Dusk
0425 UT
0600 UT
0735 UT
1400 UT
2210 UT
A
B
C
B'
LANG
TDIM
Log Ne
UT

Figure 5

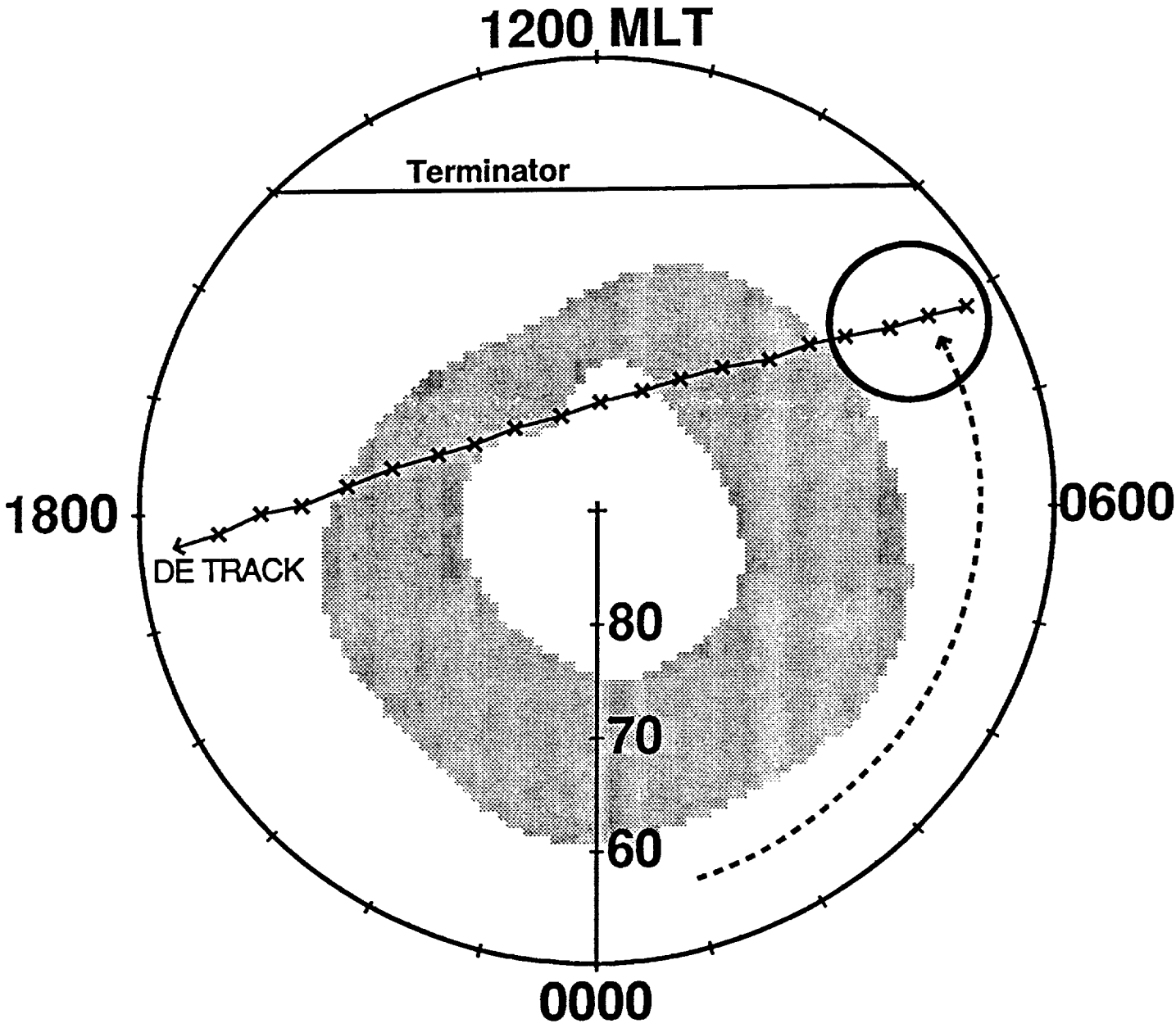

Figure 6

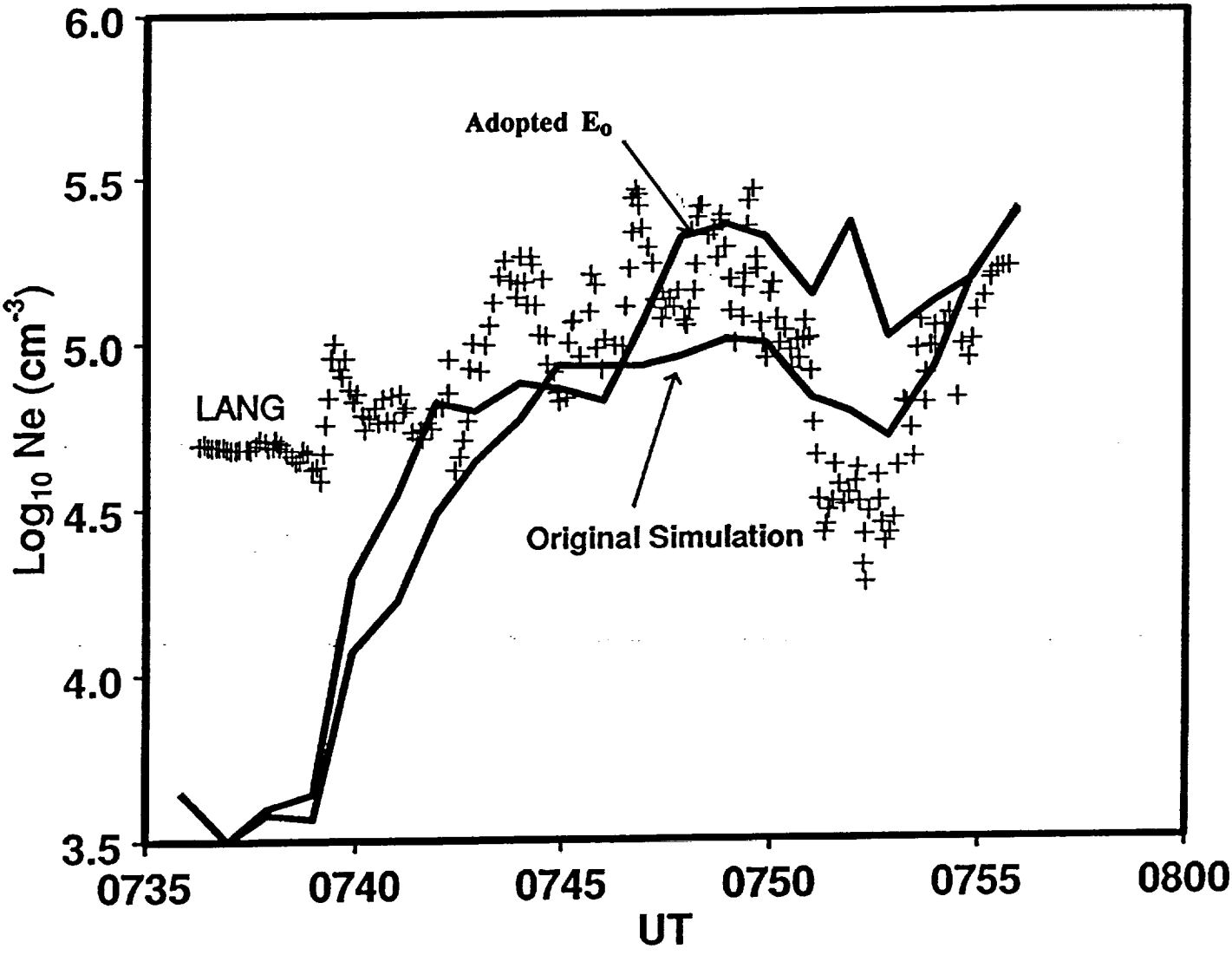
6.0
5.5
5.0
4.5
4.0
3.5
Log10 Ne (cm-3)
Adopted E0
LANG
Original Simulation
0735
0740
0745
0750
0755
0800
UT

Figure 7

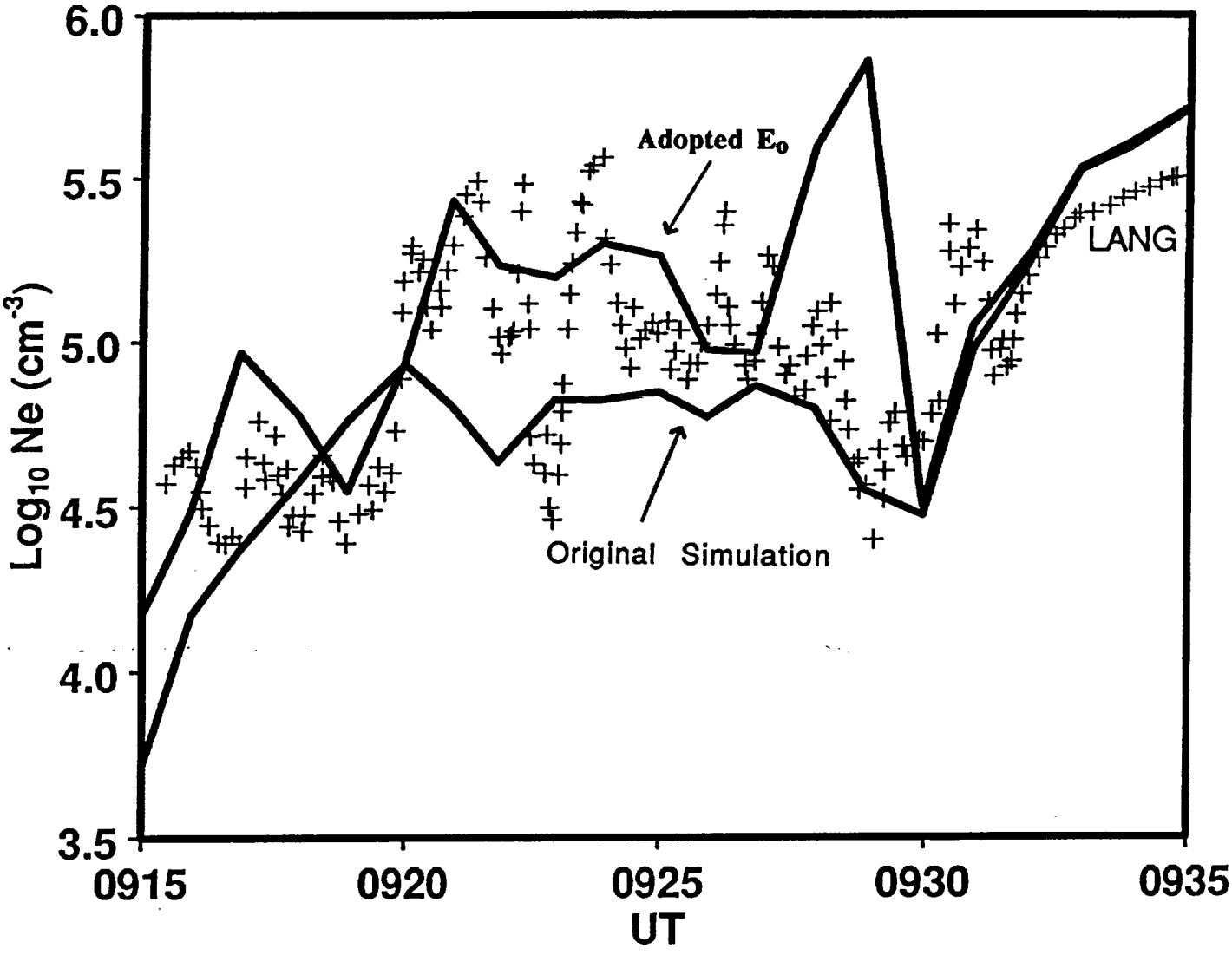
6.0
5.5
5.0
4.5
4.0
3.5
Log10 Ne (cm-3)
Adopted Eo
LANG
Original Simulation
0915
0920
0925
0930
0935
UT

Figure 8

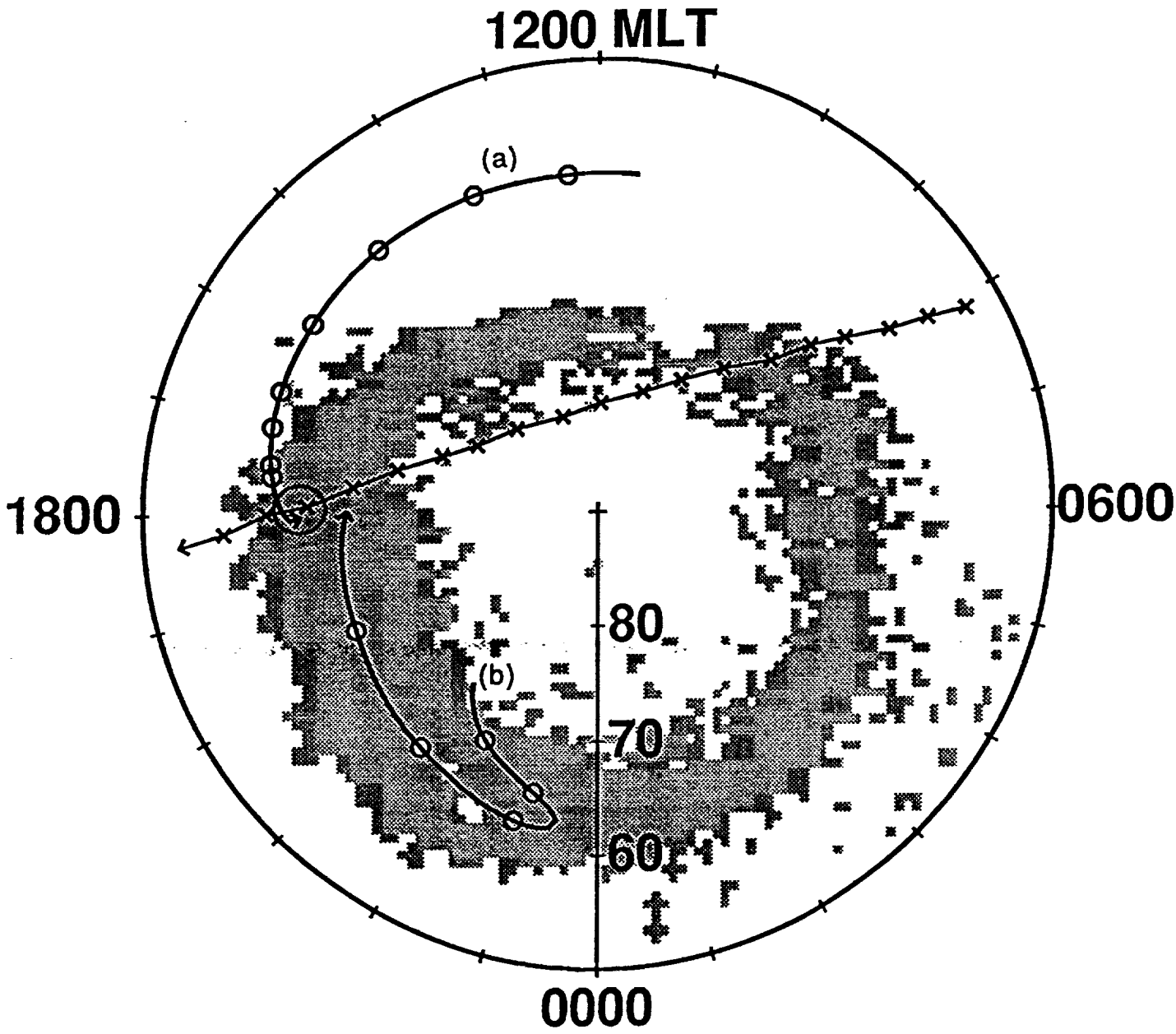

Figure 9

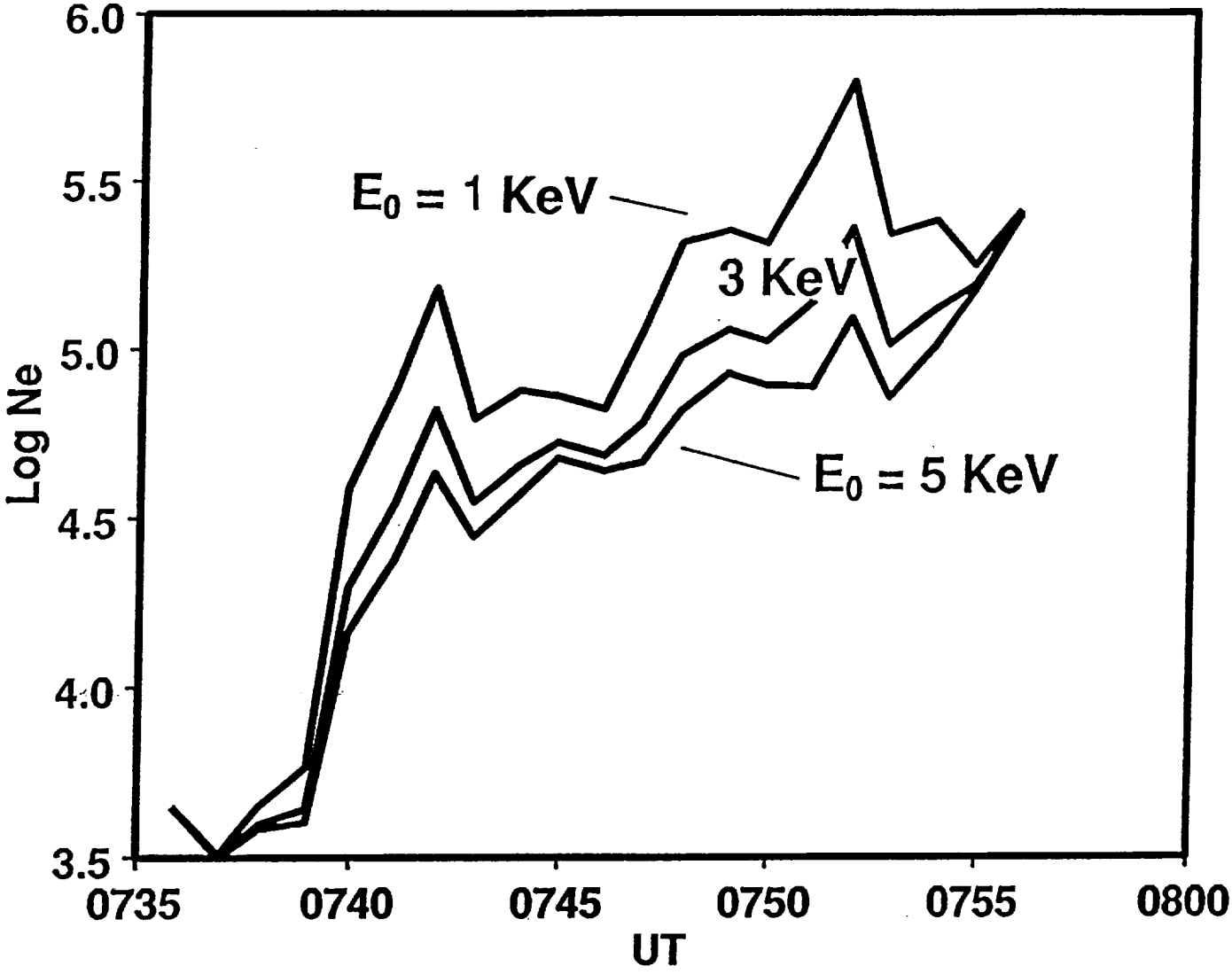
6.0
5.5
5.0
4.5
4.0
3.5
Log Ne
E_0 = 1 KeV
3 KeV
E_0 = 5 KeV
0735
0740
0745
0750
0755
0800
UT

Figure 10